



Advanced Topics to Distribution System Modelling & Analysis – Volt-Var Control, Distribution Resilience & Microgrid Dynamics and Control

[Lecture Hour = 9 hours]

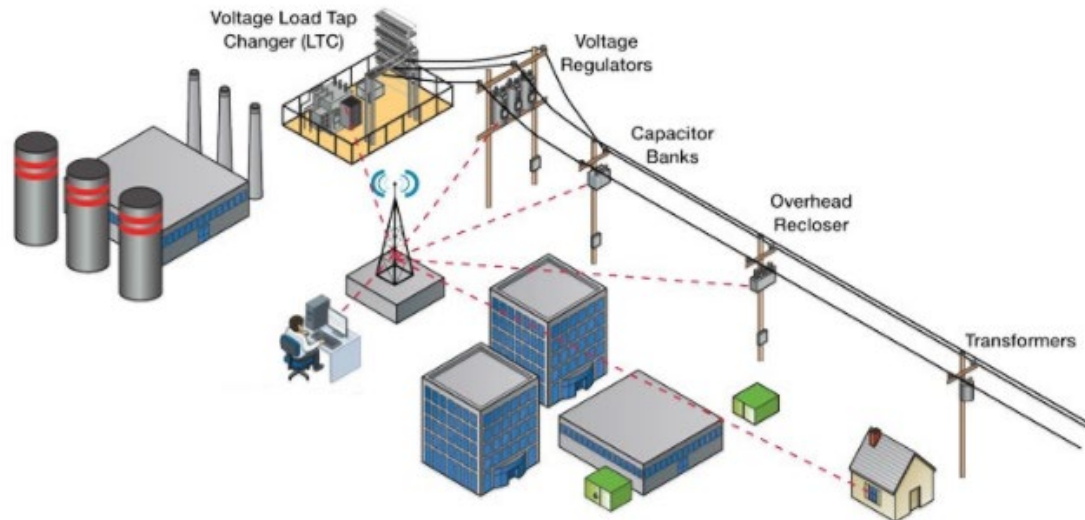
Karl M.H. LAI

Advanced Topics in Distribution System Modelling

- Conservative Voltage Reduction (CVR) and Volt-Var Optimization
 - Concept of VVC and VVC devices
 - Control Architecture of VVC
 - Decentralized (local) VVC
 - Centralized VVC
 - Hierarchical VVC
 - Voltage/VAR optimization (VVO)
 - Conservation voltage reduction (CVR)
 - Model predictive control (MPC)-based VVO (centralized, w/o PV inverter)
 - Multi-stage VVO (hierarchical, w/ PV inverter)
- Distribution System Resilience
- Microgrid – Dynamic Modelling and Control

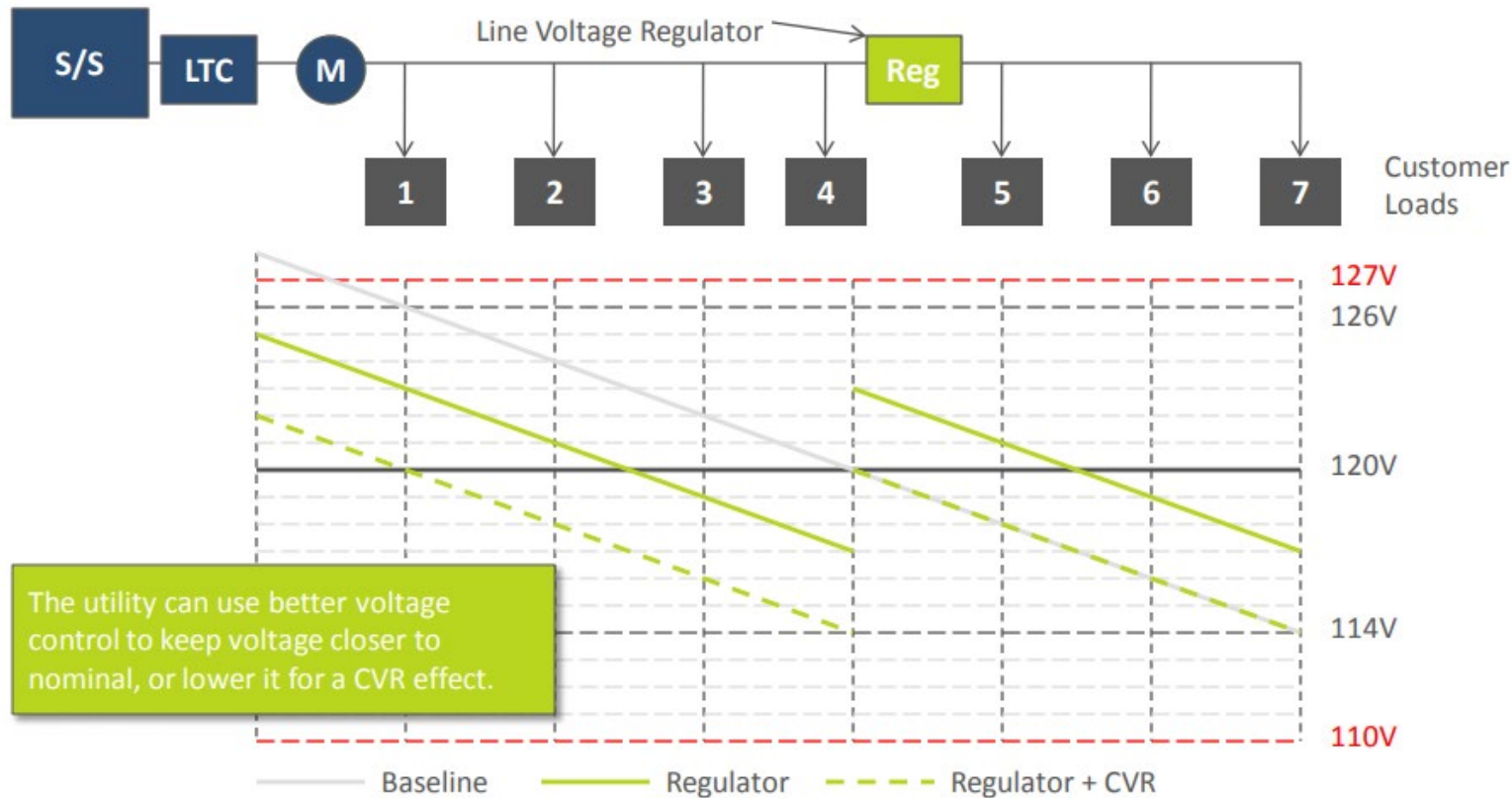
Concept of Volt-Var Control

- **Volt/VAR control** (VVC) refers to the process of managing voltage levels and reactive power (VAR) throughout the distribution systems.
- VVC can improve voltage profiles for all end-use customers and achieve multiple objectives, such as real power losses and voltage deviation.
- Conventionally, there are three devices for carrying out voltage management:
 - Substation Transformers with Load tap changer (LTC)
 - Line voltage regulators
 - Capacitor banks (CBs)



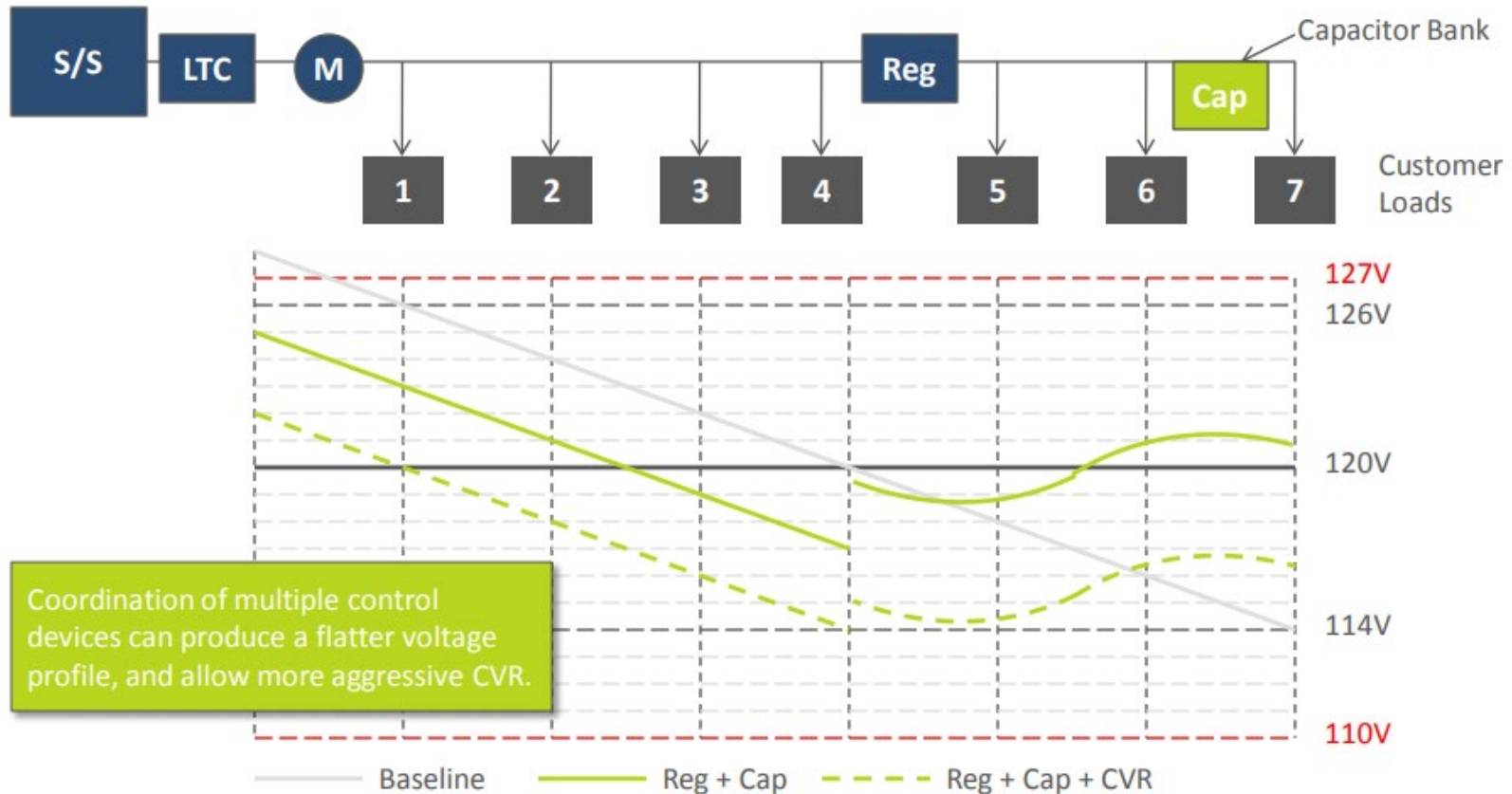
Voltage Regulation with Line Tap Changer (LTC)

- Line voltage drops from the **Line Tap Changer** *at the source* of the distribution line to customers farther out on the line.
- A **voltage regulator** can boost (raise) or buck (lower) voltage *at a point* on the distribution line and regulate down-line voltage.



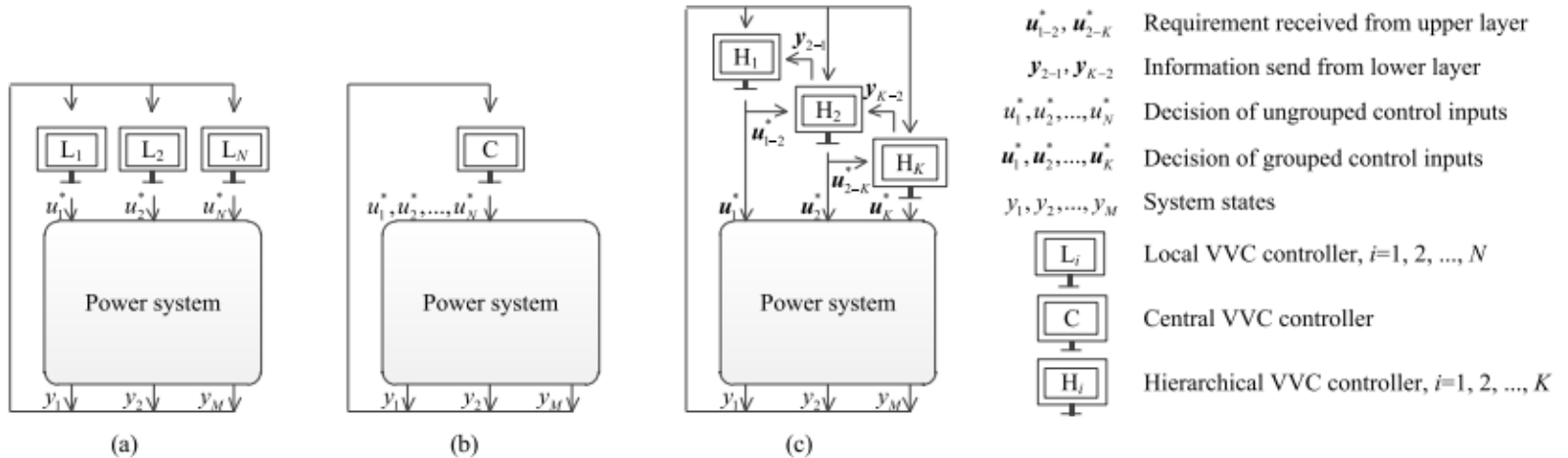
Coordinated LTC, Regulator and Capacitor Bank

- A **Capacitor Bank** can help regulation by compensating for the lagging power factor of load and the line itself



VVC and Smart Inverters

- Traditionally, distributed solar photovoltaics (PV) systems were installed with standard inverters that only output active power [kW].
- Recently, however, PV is increasingly be paired with smart inverters that can also *supply or absorb reactive power*.
 - With this ability to provide reactive power, distributed PV has the potential to support and actively **regulate local voltage and power factor** on the grid.
 - This local smart inverter control can be done through various smart inverter modes, which include fixed power factor configuration or autonomously controlling the reactive power output based on the local voltage.
- According to the control architecture, the VVC method can be classified into three categories:
 - Decentralized (local) VVC
 - Centralized VVC
 - Hierarchical VVC



Decentralized VVC

Local Volt/VAR controllers receive **local or partial information** of power system states;

Decide the control decisions of the local devices for VVC.

- For example, the control inputs can include voltage references of PV buses, reactive power output references of PQ buses and control instructions of reactive power compensators

It is worth mentioning that researchers are paying attention to **distributed VVC**. Similar to **decentralized VVC**, the control decisions are made by local volt/var controllers in distributed VVC.

* The difference between decentralized VVC and distributed VVC:

- each local VVC controller in **distributed VVC** can exchange information with the other local controllers,
- while the VVC controllers in **decentralized VVC** can only receive information.

Advantages

- Simple and easy to implement
- Does not require complicated computation and system-wide communication

Disadvantages

- Cannot consider the intermittent and fluctuating output of DERs for VVC from a system-wide perspective
- Hard to achieve an optimal control due to lack of full observation of system states and lack of information exchange between local controllers

Centralized VVC

- A central controller receives all the information of power system states.
- Then decides and send back the control inputs of all the devices for VVC in the system.

Advantages

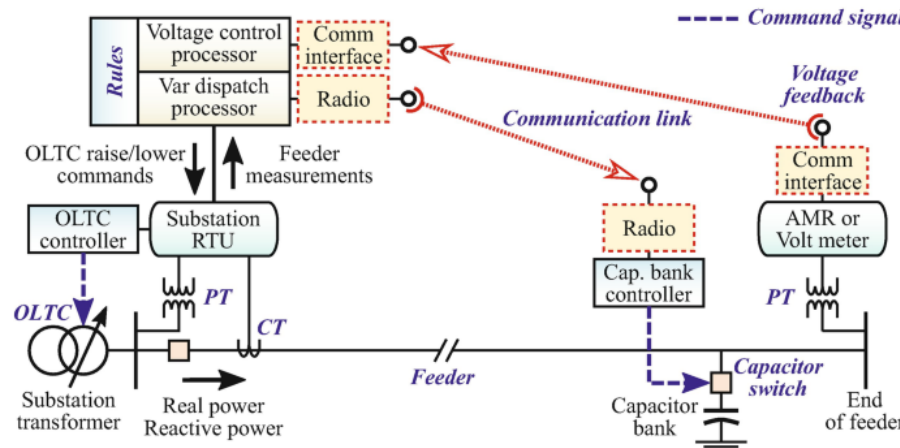
- Can achieve a **system-wide optimization**
- Can cope with various challenges presented by DERs to VVC from a system-wide perspective

Disadvantages

- Requires high capacity of computation and communication
- Inflexible to coordinate different device characteristics

Application

- System-wide optimal reactive power dispatch, when the computation and communication capacity in the power system is sufficient high
- The central controller can obtain whole information of system states and control all available VVC devices



Hierarchical VVC

- Multiple Volt/VAR controllers are organized in a hierarchical structure.
- All the controllers can receive partial or all the information of power system states.
- The controller at a lower layer complies with the decision made by the controller at the upper layer.

There are usually two ways to realize the hierarchical VVC :

- The controller at the lower layer adjusts its control inputs at a high frequency while the controller at the upper layer does it at a low frequency.
- The controller at the lower layer fulfills the requirements received from the controller at the upper layer and sends necessary information to the controller at the upper layer.

Advantages

- Has all advantage of centralized VVC
- Flexible to coordinate different device characteristic

Disadvantages

- Requires high capacity of computation and communication
- Complicated to design and implement

Challenge

- How to improve calculation efficiency for optimal reactive power dispatch in large-scale power system with uncertain DERs
- How to design the coordination of controllers at different layers

Conservation Voltage Reduction (CVR)

- It lowers distribution voltage levels to reduce peak demand and energy consumption.
- Nature of CVR
 - Load is sensitive to voltage
 - Load-to-voltage sensitivity varies
- The ZIP model is a load which is composed of constant impedance (Z), constant current (I) and constant power (P) elements.

Appliance	Z%	I%	P%
Induction Motor			
Oscillating Fan	73.32%	25.34%	1.34%
Display			
Magnavox TV	0.15%	82.66%	17.19%
Dell Liquid Display	-40.70%	46.29%	94.41%
Lighting			
Compact Fluorescent Light (13W)	40.85%	0.67%	58.48%
Compact Fluorescent Light (42W)	48.67%	-37.52%	88.85%

Conservation Voltage Reduction: Benefits

- Consumers can benefit from the **reduced energy consumption** from CVR. Utilities may lose revenues, which is a common problem for many demand response programs.
- The CVR benefits for utilities can be summarized as:
 - **Peak loading relief** of distribution systems
 - **Net loss reduction** considering both the transformers and distribution lines
 - Potential **incentives** and requirements from regulatory bodies (e.g., California Public Utilities Commission)
 - Combine with **system improvements** to achieve optimal Volt/VAR control
- CVR effects can be evaluated by CVR_f :

$$CVR_f = \frac{\% \text{ Load Change}}{\% \text{ Voltage Reduction}} = \frac{(P_{\text{CVR(off)}} - P_{\text{CVR(on)}})/P_{\text{CVR(off)}}}{(V_{\text{CVR(off)}} - V_{\text{CVR(on)}})/V_{\text{CVR(off)}}}$$

- The major challenges to quantify CVR effects is to distinguish the **changes in load and energy consumption due to voltage reduction** from other impact factor.
- CVR Assessment methods:
 - Comparison method: w/ and w/o CVR test on two similar feeder in the same period
 - Regression method: loads are modeled as (multivariate) regression function of impact factors (voltage, weather information, load consumptions of different days of the week and the month)
 - Synthesis method: aggregate load-to-voltage behaviors from load components or customer classes to estimate the CVR effects of a circuit
 - Simulation method : based on system modeling and power calculation w/ and w/o CVR test

Existing Methodologies for CVR Assessment

Methods	Summary	Positive Attributes	Negative Attributes
Comparison	Compare load consumption of a test feeder and a control group	Easy and straightforward	Dependent on control group, noise vulnerable
Regression	Estimate what load would have been without CVR	Clear physical meaning	Regression error, load model is linear
Simulation	Estimate what load would have been without CVR	Maybe highly precise (depends on model accuracy)	Precise load modeling is difficult, load model is time-invariant
Synthesis	Aggregate measured load behaviors	Quick estimation and forecast of CVR effect	Accurate load information is difficult to collect, load behaviors are time-invariant

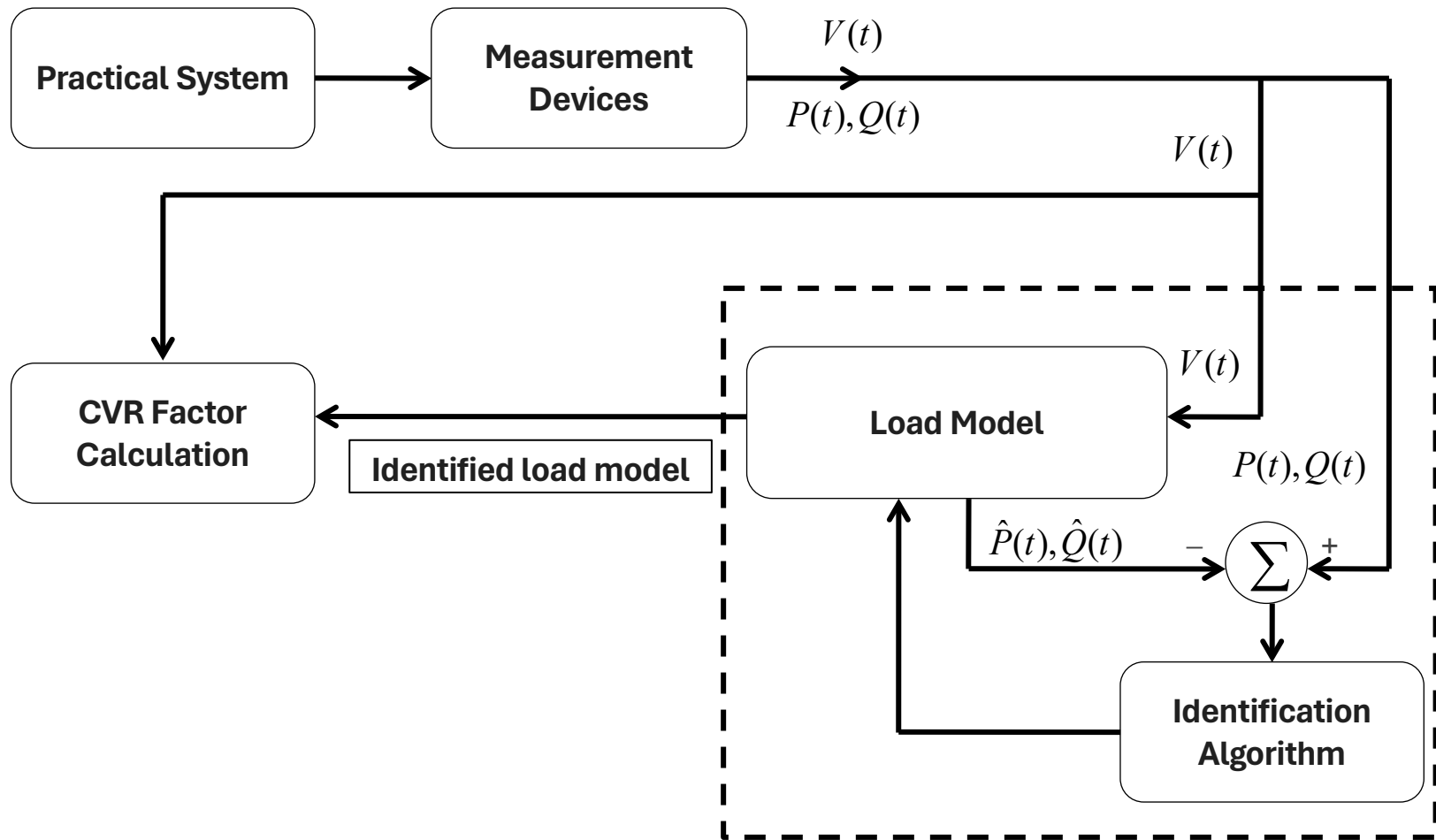
[4] Z. Wang and J. Wang, "Review on Implementation and Assessment of Conservation Voltage Reduction," *IEEE Transactions on Power Systems*, vol. 29, no. 3, pp. 1306-1315, May 2014.

CVR: Implementation

To implement CVR:

- Open-loop VVC (w/o voltage feedback): change LTC tap position, line drop compensation, voltage spread reduction, CB-based reduction and home voltage reduction.
- **Disadvantages of open-loop VVC**
 - the depth of voltage is limited
 - the control of all devices is not optimized (just based on local data)
 - cannot adapt to dynamic changes of distribution networks
- Closed-loop VVC: take advantage of various measurements to determine the best (optimal) VVC actions during certain time periods.
- **Advantages of closed-loop VVC**
 - optimal voltage reduction
 - optimal energy-saving effect
 - adaptive to dynamic system changes

Data-driven Assessment of CVR



Load Model Identification

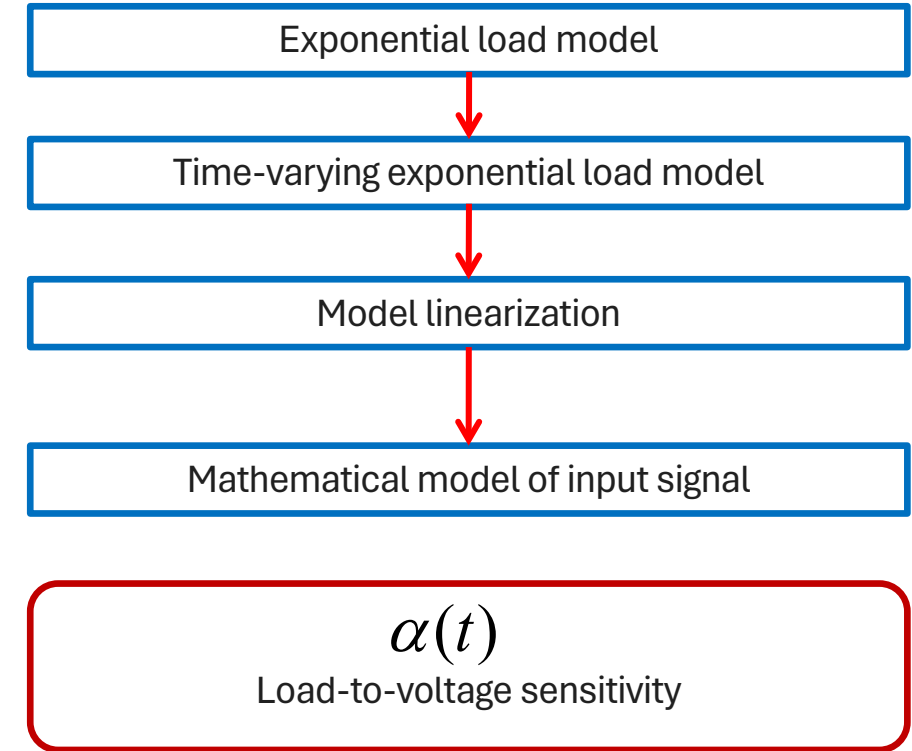
$$P = P_0 \left(\frac{V}{V_0} \right)^\alpha$$

$$P(t) = P_0(t) \left(\frac{V(t)}{V_0} \right)^{\alpha(t)}$$

$$\ln P(t) = \ln P_0(t) + \alpha(t) \ln V(t)$$

$$y_t = \varphi_t^T \theta_t + \varepsilon_t$$

$$\varphi_t = \begin{pmatrix} 1 \\ \ln V(t) \end{pmatrix}, \theta_t = \begin{pmatrix} \ln P_0(t) \\ \alpha(t) \end{pmatrix}$$



Load Model Identification

$$F_m = \sum_{k=0}^m \lambda^{m-k} (y_k - \Phi_k^T \Theta_k)^2, \quad \lambda \in (0.9, 1.0)$$

$$\hat{\Theta}_m = \arg_{\Theta} \min \sum_{k=0}^m \lambda^{m-k} (y_k - \Phi_k^T \Theta_k)^2$$

$$\hat{\Theta}_{m+1} = \hat{\Theta}_m + \mathbf{G}_m \left[y_m - \Phi_{m+1}^T \hat{\Theta}_m \right]$$

$$\mathbf{G}_m = \frac{\mathbf{R}_m \Phi_{m+1}}{1 + \Phi_{m+1}^T \mathbf{R}_m \Phi_{m+1}}$$

$$\mathbf{R}_{m+1} = \frac{\left[\mathbf{I} - \mathbf{G}_m \Phi_{m+1}^T \right] \mathbf{R}_m}{\lambda}$$

$$\mathbf{R}_0 = \text{diag}\{\beta_i\}$$

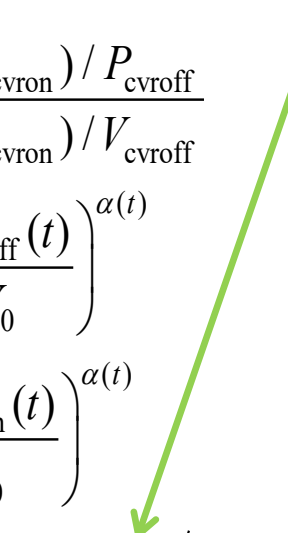
$$CVR_f = \frac{(P_{cvroff} - P_{cvron}) / P_{cvroff}}{(V_{cvroff} - V_{cvron}) / V_{cvroff}}$$

$$P_{cvroff} = P_0(t) \left(\frac{V_{cvroff}(t)}{V_0} \right)^{\alpha(t)}$$

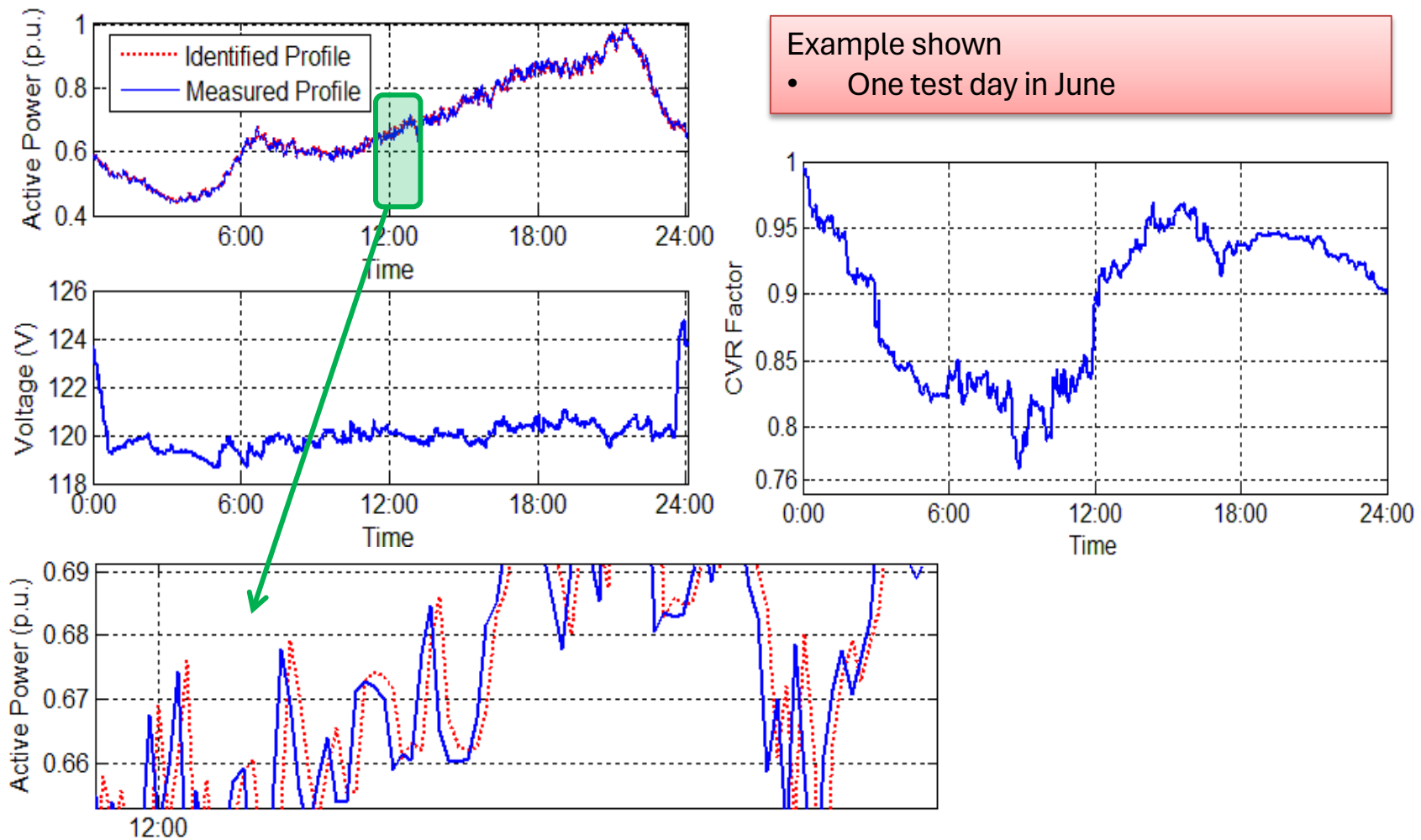
$$P_{cvron} = P_0(t) \left(\frac{V_{cvron}(t)}{V_0} \right)^{\alpha(t)}$$

$$CVR_f = \left(1 - \left(\frac{V_{cvron}(t)}{V_{cvroff}(t)} \right)^{\alpha(t)} \right) \left/ \left(1 - \left(\frac{V_{cvron}(t)}{V_{cvroff}(t)} \right) \right) \right.$$

$\hat{\alpha}(t)$



Data-driven Assessment of CVR



Topic: Rolling-Horizon VVO (centralized, w/o PV smart inverter)

- Ref. [7] proposes a model predictive control (MPC)-based VVO technique considering the integration of distributed generators and load-to-voltage sensitivities.
- The proposed model schedules optimal tap positions of LTC and switch status of CBs are obtained based on predictive output of wind turbines (WTs) and PV generators (PVs).
- The exponential load model is used to capture the various load behaviors (Compared with previous efforts on VVO which used constant-power load model).
- The uncertainties of **model predication errors** are considered in the proposed model.
- A scenario reduction technique is applied to enhance a tradeoff between the accuracy of the solution and the computational burden.
- Compared to constant-power load model, **exponential load model** (ELM) is more accurate in practice.
- In fact, the k_{pi} and k_{qi} are related with load compositions (for constant power load model, $k_{pi}=0$, $k_{qi} = 0$).

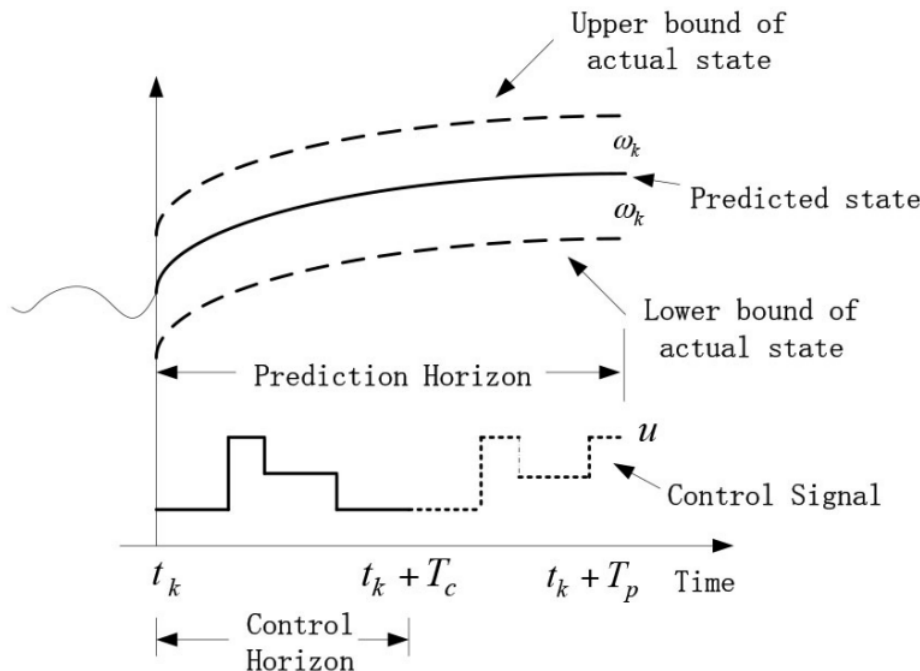
Load Type	k_p	k_q
Residential	1.04	4.19
Commercial	1.50	3.15
Industrial	0.18	6.00

$$p_i^l = P_i^b V_i^{k_{pi}}$$
$$q_i^l = Q_i^b V_i^{k_{qi}}.$$

Model Predictive Control (MPC)

MPC refers to algorithms that solve:

- A finite-horizon optimal control problem over the prediction horizon T_p
- The obtained control variables are applied to the system over control horizon T_c , where $T_c \leq T_p$
- At the end of the control horizon, the rest of the predicted control variable are discarded, and the entire procedure is repeated.



VVO as Stochastic MINLP

$$\min \mathbb{E} \left[\sum_{t=t_k}^{t_k+T_p} (\ell_t(\omega_t) + \Delta V_t(\omega_t)) \right]$$

The objective function minimizes

- (1) the expectation of **active power losses**;
- (2) **voltage deviation** along the feeder during the prediction horizon.

- The two objectives are equally weighted (Can be changed)
- ω_t is the prediction error

subject to

$$\begin{aligned} \Delta V_t(\omega_t) &= \max_i \{\Delta V_{i,t}(\omega_t)\}, \quad \Delta V_{i,t}(\omega_t) \\ &= |V_{i,t}(\omega_t) - V_{1,t}(\omega_t)| \end{aligned}$$

The maximum **voltage deviation** of all nodes.

$$\ell_t(\omega_t) = \sum_i r_i \frac{P_{i,t}^2(\omega_t) + Q_{i,t}^2(\omega_t)}{V_{1,t}^2(\omega_t)}, \quad \forall i \in B$$

Active losses of the distribution network

$$\begin{aligned} P_{i+1,t}(\omega_t) &= P_{i,t}(\omega_t) - p_{i+1,t}(\omega_t) \\ Q_{i+1,t}(\omega_t) &= Q_{i,t}(\omega_t) - q_{i+1,t}(\omega_t) \\ V_{i+1,t}(\omega_t) &= V_{i,t}(\omega_t) - \frac{r_i P_{i,t}(\omega_t) + x_i Q_{i,t}(\omega_t)}{V_{1,t}(\omega_t)} \end{aligned}$$

Linear form of the DistFlow equations

VVO as Stochastic MINLP

$$p_{i,t}(\omega_t) = p_{i,t}^l - p_{i,t}^g(\omega_t)$$

$$q_{i,t}(\omega_t) = q_{i,t}^l - q_{i,t}^g(\omega_t)$$

$$p_{i,t}^g(\omega_t) = P_{i,t}^{pred} + \omega_{i,t}$$

$$q_{i,t}^g = c_{i,t} Q_i^{cap}$$

$$V_{1,t} = TAP_t V_s$$

$$p_{i,t}^l = (P_{i,t}^{b,pred} + \omega_t) V_{i,t}^{k_{pi}}(\omega_t)$$

$$q_{i,t}^l = (Q_{i,t}^{b,pred} + \omega_t) V_{i,t}^{k_{qi}}(\omega_t)$$

$$1 - \varepsilon \leq V_{i,t}(\omega_t) \leq 1 + \varepsilon$$

$$\sum_{t=t_k}^{t_k+T_p-T_c} |c_{i,t+T_c} - c_{i,t}| \leq CAP^{\max}$$

$$\sum_{t=t_k}^{t_k+T_p-T_c} |TAP_{t+T_c} - TAP_t| \leq TAP^{\max}.$$

The outputs of DG unit and capacitors are represented as **negative loads**.

It assumes outputs of DG units equal the predicted value plus the predicted values plus the predicted errors ω . ω belongs to an uncertainty set, which may vary with predicted values.

Cap Banks output. $c_{i,t}$ represents the **on/off status** of the capacitor at node i during the time interval t .

V_s represents the primary voltage of the transformer at the substation, which is assumed to be 1.0. p.u.. The secondary voltage is modeled as a function of the primary voltage.

The exponential load models are used to represents active and reactive load consumption.

$P_{i,t}^{b,pred}, Q_{i,t}^{b,pred}$ change with a load profile which can be obtained by using short-term load forecasting techniques.

It indicates the voltage of each node should be within a certain range for proper operation of the distribution circuit, ε is usually set to be 0.05.

The max number of daily switching operations of LTC and CBs are shown.

Prediction errors

- Errors always exist in prediction models.
- Beta distribution is used to calculate the predication errors for WTs and PVs. The beta function can be defined by two shape parameters α and β , which models the occurrence of real power values x when a certain prediction value, $P_{i,t}^{pred}$ has been forecasted:

$$f_{P_{i,t}^{pred}}(x) = x^{\alpha-1}(1-x)^{\beta-1}.$$

$$\frac{P_{i,t}^{pred}}{S_{base}} = \frac{\alpha_{i,t}}{\alpha_{i,t} + \beta_{i,t}}$$

$$\sigma_{i,t}^2 = \frac{\alpha_{i,t}\beta_{i,t}}{(\alpha_{i,t} + \beta_{i,t})^2(\alpha_{i,t} + \beta_{i,t} + 1)}. \quad \sigma_{i,t} = 0.2 \times \frac{P_{i,t}^{pred}}{P_i^{cap}} + 0.21.$$

- A normal distribution is used to represent the forecasting uncertainty of load consumption:
 - The mean value of the normal distribution is forecasted load
 - The standard deviation is set to be 2% of the expected load
- All above distributions and parameters settings can be changed according to the available information of a system.

Expected Value Problem

- It is necessary to show how much improvement can be achieved if the stochastic prediction errors are considered in MPC.
- The random error ω is replaced by its expected value $\bar{\omega}_t = E(\omega_t)$, and then the expected value problem (EV), which is a deterministic optimization can be defined as:

$$EV = \min \sum_{t=t_k}^{t_k+T_p} (\ell_t(\bar{\omega}_t) + \lambda(\bar{\omega}_t))$$

- Define the expected value solution as \bar{x} . The expected results of using the EV solution can be represented as

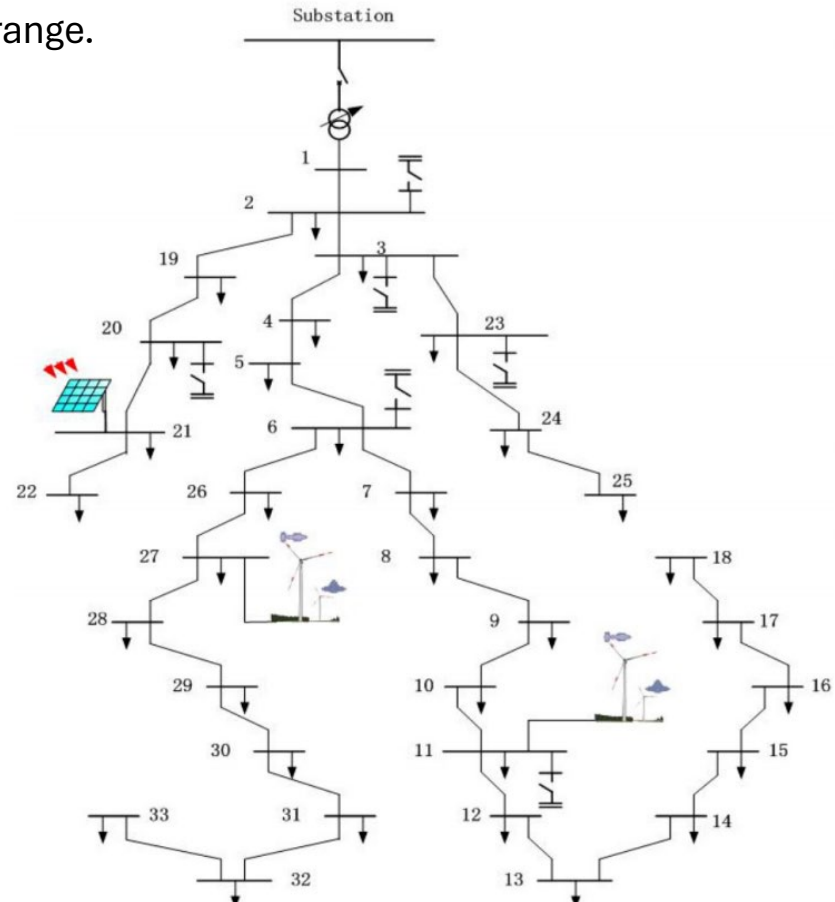
$$EEV = \frac{1}{N'} \sum_{h=1}^{N'} (\ell_t(\bar{x}, \omega^h) + \lambda(\bar{x}, \omega^h))$$

- EEV measures the performance of \bar{x} . The N' is the number of scenario.
- It can compare EEV and the objective value of the proposed MPC-VVO to see how the stochastic programming outperforms the deterministic programming.

Case Study

The proposed methodology has been examined on the modified 33-bus radial distribution network.

- Two WTs and one PV
- Different types of loads
- The substation transformer is with $\pm 10\%$ tap range.
- Switched capacitors are installed at nodes 2, 3, 6, 11, 21 and 23 (30 kVAR).
- Prediction horizon $T_p = 6$ h
- Control horizon $T_c = 15$ min
- 100 generated scenarios
- 15 scenarios after reduction



Case Study

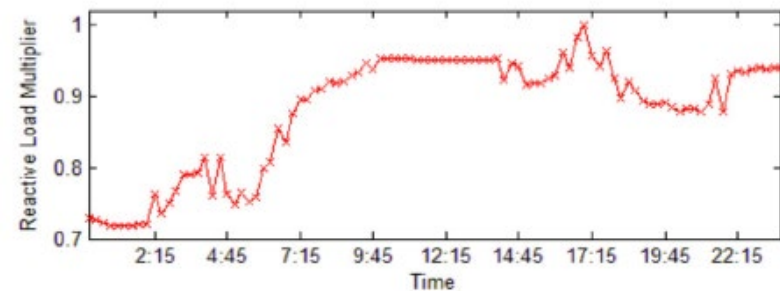
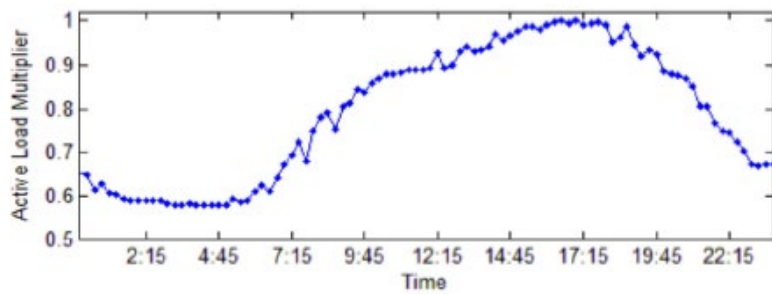
- All loads in the case study are represented by ELM, the load consumption of node i at time t can be represented as

$$p_{i,t}^l = P_i^b M_t^p V_{i,t}^{k_{pi}}$$
$$q_{i,t}^l = Q_i^b M_t^q V_{i,t}^{k_{qi}}.$$

- The value of basic components P_i^b and Q_i^b can be found in the paper, the exponents of each type of load.

Type	Residential	Commercial	Industrial
Node number	2, 3, 4, 5, 6, 7, 8, 9, 12, 13, 14, 15	10, 11, 16, 17 19, 20, 21, 22	18, 23, 24, 25

- The multipliers M_t^p and M_t^q (same for all nodes) are used to make the load profile change with time.



[8] M. E. Baran and F. F. Wu, "Network reconfiguration in distribution systems for loss reduction and load balancing," *IEEE Trans. Power Del.*, vol. 4, no. 2, pp. 1401–1407, Apr. 1989.

Numerical Results

Different results of LTCs and CB for EXL model and CP model:

- EXL: exponential model
- CP: constant power model

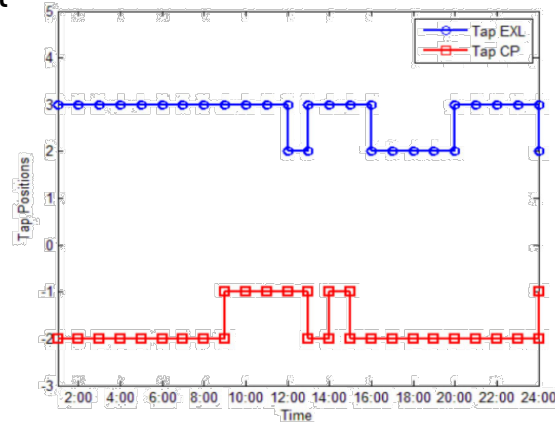


Fig.6 Tap positions with EXL and CP

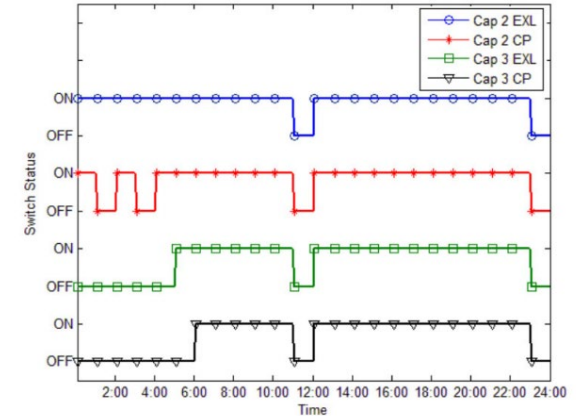


Fig.7 Switch status of CB2 and CB3 with EXL and CP

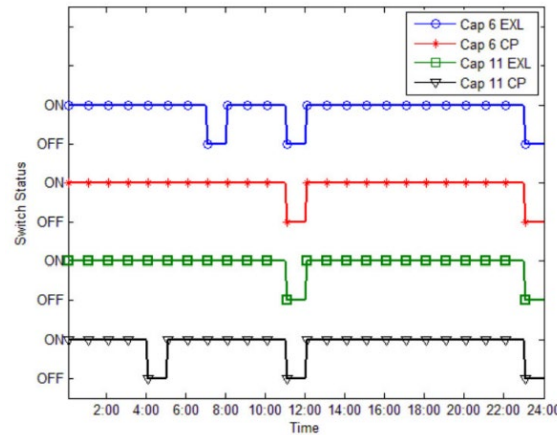


Fig.8 Switch status of CB6 and CB11 with EXL and CP

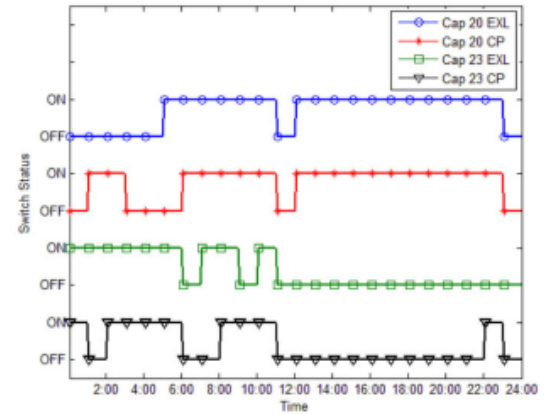


Fig.9 Switch status of CB20 and CB23 with EXL and CP

Numerical Results

- Fig. 10 shows the voltages of all nodes for different cases. Base represents the voltages with DGs and ELM, but without OLTC and CBs.
- Compared to base case, the proposed MPC-based VVO can largely improve the voltage profile.
- The optimal voltage levels with CP model are relatively higher than those with ELM.
 - The reason is that losses are proportional to the square of the current, and the current of a constant-power load is inversely proportional to the voltage.

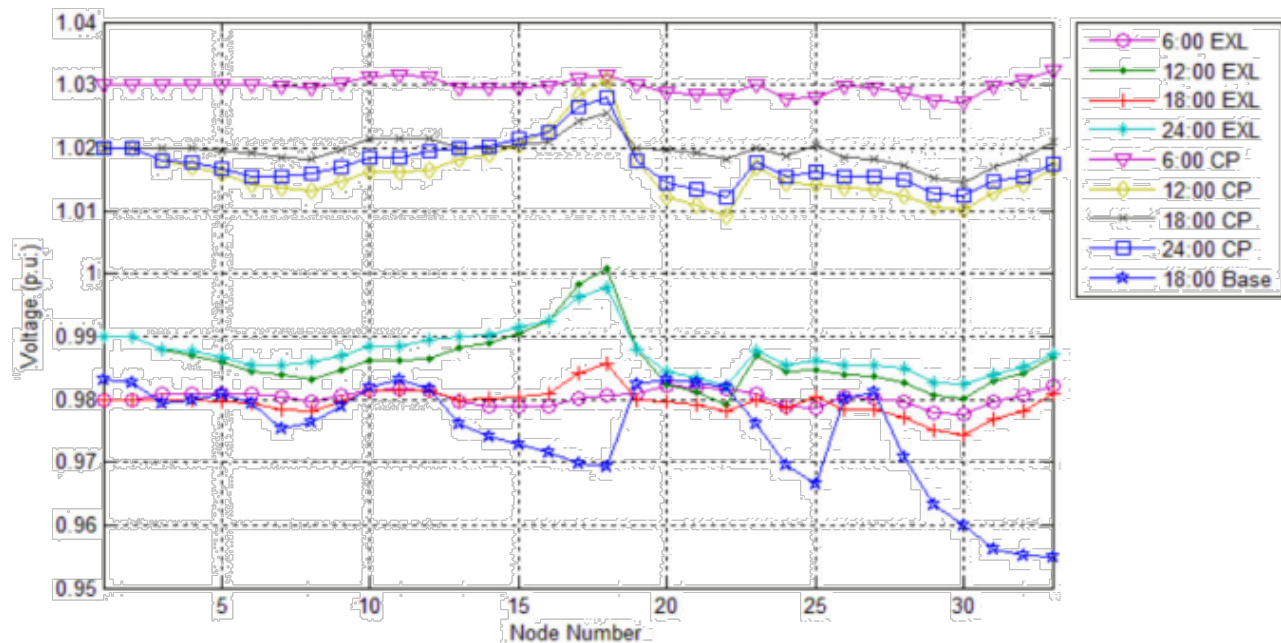


Fig.10 Voltage profiles of EXL, CP and Base cases

Numerical Results

- Fig. 11 shows the active power losses and maximum voltage deviation of VVO with ELM, CP, EEV and base case.
- Compared to base case, the proposed MPC-based VVO can
 - reduce the maximum voltage deviation by 65% and power losses by 77%.
- Compared to EEV (deterministic model), the proposed MPC-based VVO can
 - reduce the maximum voltage deviation by 49% and power losses by 72%.

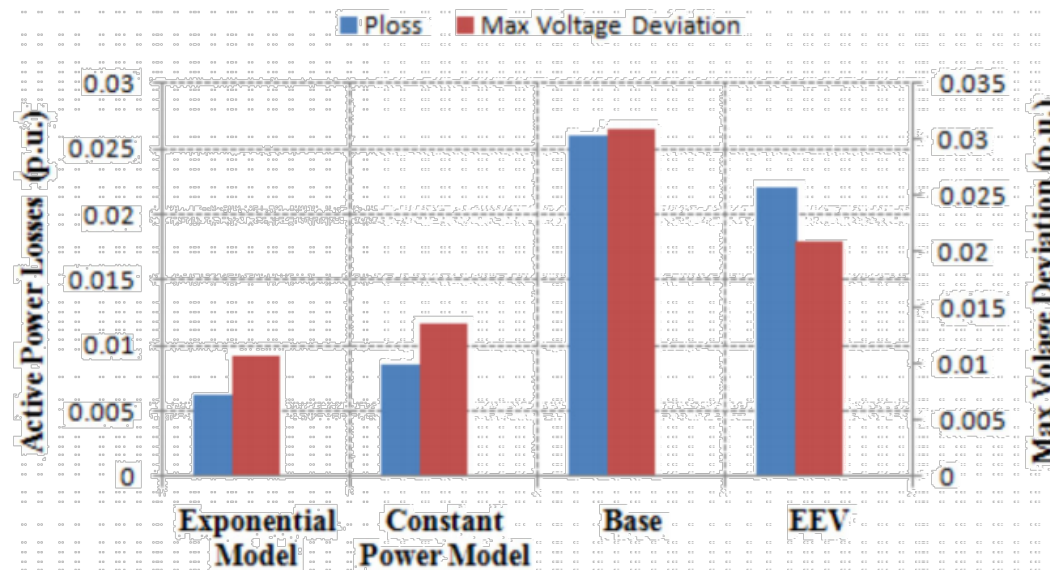


Fig.11 Active power losses and max voltage deviations

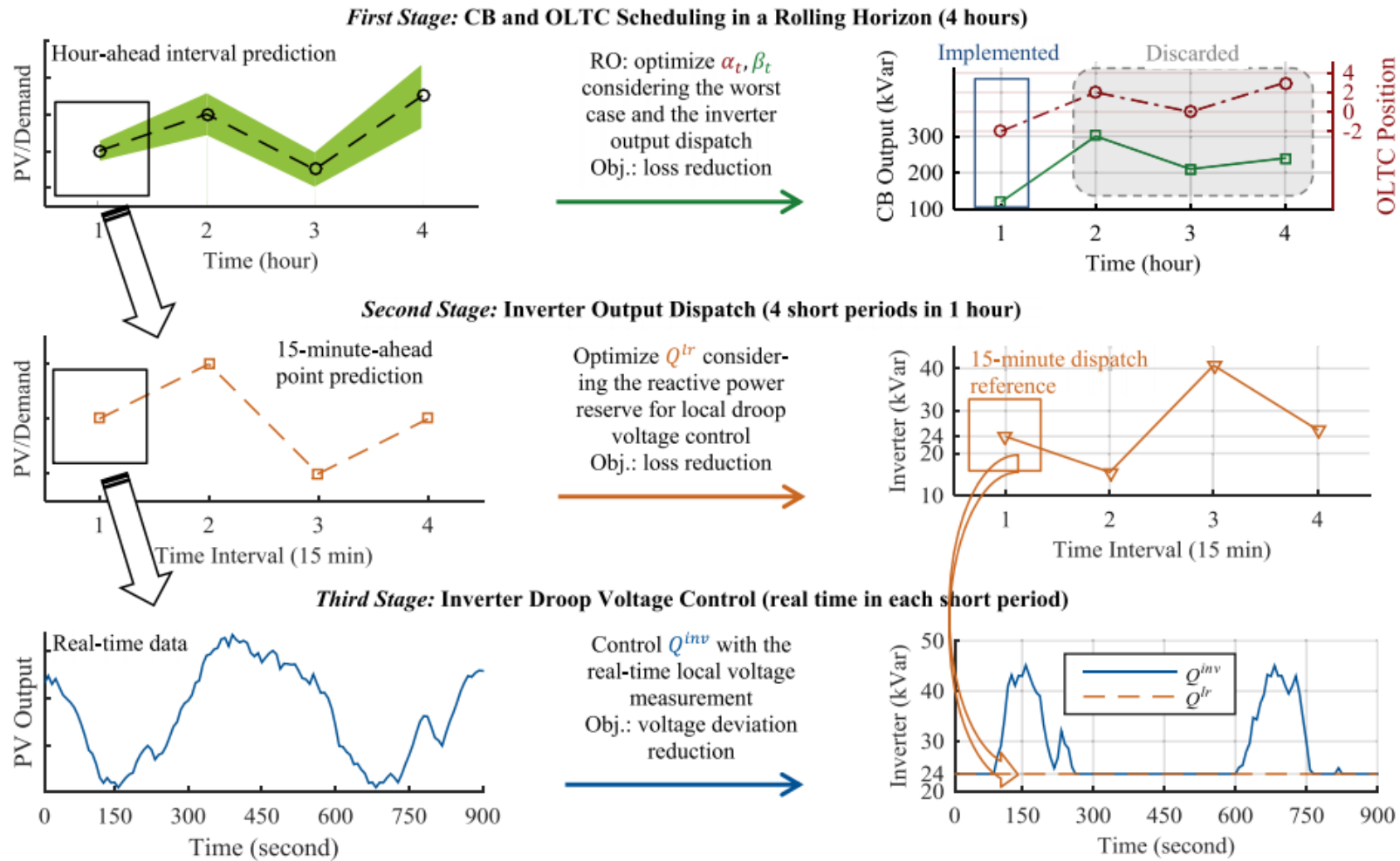
Multi-stage VVO (hierarchical, with PV smart inverters)

- Ref. [8] proposes a novel three-stage robust inverter-based VVC (TRI-VVC) approach for high PV penetrated distribution networks.
- Coordinating three different control stage from centralized VVC to local VVC to reduce energy loss and mitigate voltage deviation.
 - In the first stage, CBs and LTC are scheduled hourly in a rolling horizon.
 - In the second stage, PV inverters are dispatched in a short time-window.
 - In the third stage, PV inverters respond to real-time voltage violation through local droop controllers.
- To address the uncertain PV output and load demand, a robust optimization model is proposed to optimize the first two stages while taking into account the droop voltage control support from the third stage.

[8] C. Zhang, Y. Xu, Z. Dong and J. Ravishankar, "Three-Stage Robust Inverter-Based Voltage/Var Control for Distribution Networks With High-Level PV," in *IEEE Transactions on Smart Grid*, vol. 10, no. 1, pp. 782-793, Jan. 2019.

TRI-VVC

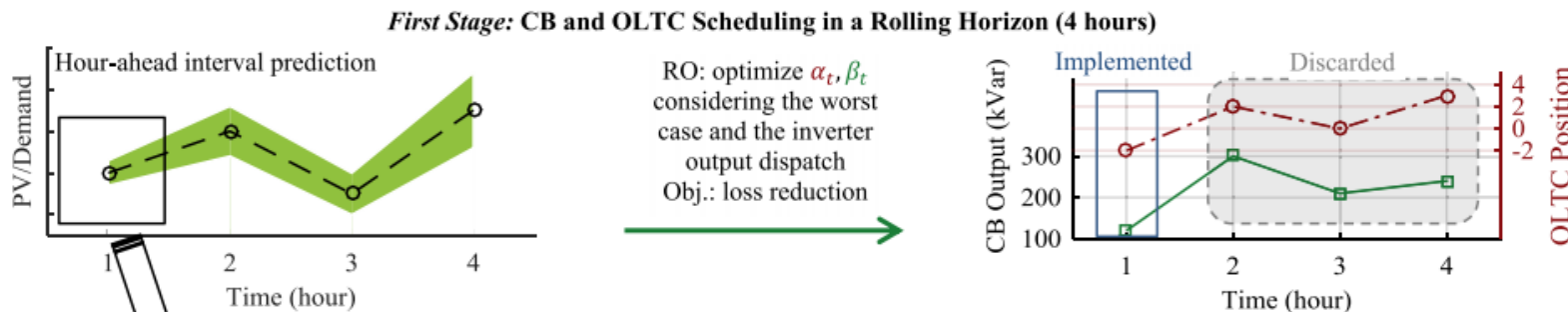
- The TRI-VVC aims at robustly minimizing network energy losses and meanwhile maintaining secure voltages under fast and uncertain PV generation and load demand variations.



First Stage: CB and OLTC scheduling in rolling horizons (1-hour)

The first stage aims at optimally scheduling CBs and an OLTC.

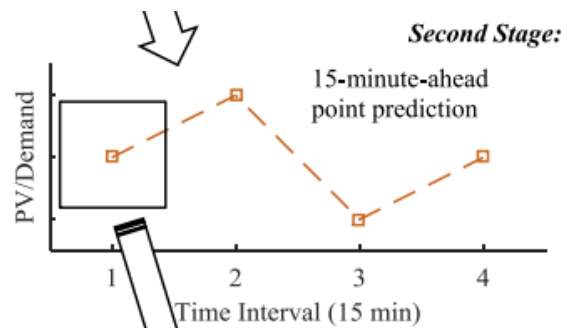
- The PV generation and load demand are predicted over a finite prediction horizon T (4 hours).
- The hourly CB outputs and OLTC position are optimized for the whole horizon to minimize the energy loss while satisfying the voltage constraints.
- Only the decisions (CBs and OLTC) of the first hour are implemented. The optimization procedure is rolled to benefit from more accurate PV output and load forecasting in coming future with shorter leading-time.
- The inverter dispatch is optimized as a compensation operation under the worst case (PV output and demand) in the first stage. The inverter dispatch is optimized again in the second stage according to uncertainty realization.



Second Stage: Inverter output dispatch (15-min)

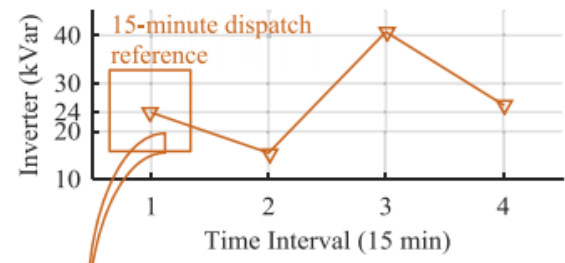
In the second stage, the PV inverters are dispatched to reduce network energy in a loss in a shorter period, e.g., 15-min, as a recourse action for the first stage decision after the uncertainties are realized.

- More accurate 15-min ahead predictions of PV generation and demand are used.
- The inverter reactive power output is optimized and implemented for each 15-min period within the current hour.
- The optimized inverter output is also set as the reference point for the third stage.



Second Stage: Inverter Output Dispatch (4 short periods in 1 hour)

Optimize Q^{tr} considering the reactive power reserve for local droop voltage control
Obj.: loss reduction

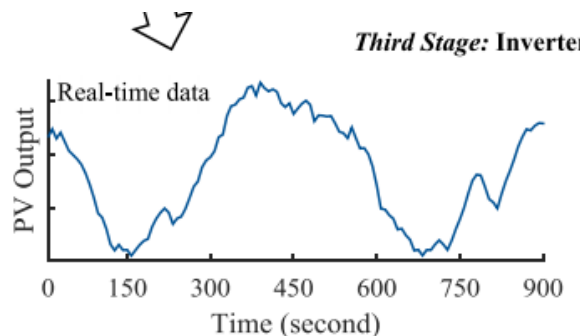


Third Stage: Inverter droop voltage control (real-time)

The first two stages minimize the loss while satisfying the voltage constraints under the uncertainties in 1-hour to 15-min periods. However, within each 15-min period, the PV output can still dramatically vary under special conditions (transient cloud movements), where the voltage limits may be violated.

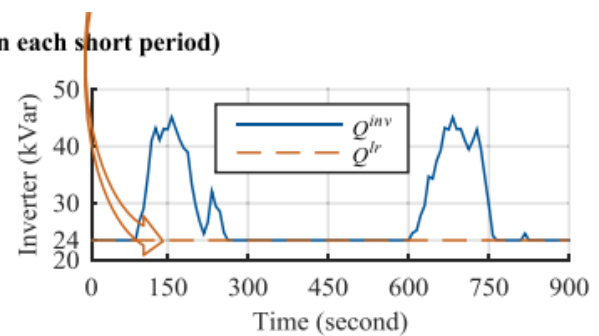
Thus, the third stage provides real-time (1-sec) reactive support for the possible voltage violations. A droop controller is designed as:

- If a real-time local voltage is out of the allowed operational limits due to significant PV output changes, the inverters generate or consume reactive power linearly with the voltage changes.
- If the voltage is still within the allowed limits, the inverter output is kept to the value optimized from the second stage.



Third Stage: Inverter Droop Voltage Control (real time in each short period)

Control Q^{inv} with the
real-time local voltage
measurement
Obj.: voltage deviation
reduction



Mathematics Formulation

- The proposed TRI-VVC is formulated as the following optimization model:

$$\min \quad \sum_{t \in T} \sum_{i \in N} P_{i,t}^{loss} \tau$$

} Objective function is to minimize the total energy loss in the current prediction horizon T .
 τ is the time length of the first stage (hour)

$$\text{s.t. } \alpha_{i,j,t} \in \{0, 1\}, \forall i, j, t \\ \beta_t \in \{-10, -9, \dots, -1, 0, 1, \dots, 9, 10\}, \forall t$$

} $\alpha_{i,j,t}$ is the binary on/off decision of j th unit of the CB at node i during period t .
 β_t is the integer position of the LTC during period t .

$$\sum_{t \in T} |\alpha_{i,j,t} - \alpha_{i,j,t-1}| \leq CB_{i,j}^{max}, \forall i, j$$

} Allowed maximal changing time for the CB switch for the current T .

$$\sum_{t \in T} |\beta_t - \beta_{t-1}| \leq OLTC^{max} \\ |\beta_t - \beta_{t-1}| \leq OLTC_t^{max}, \forall t$$

} Allowable maximal times for the LTC position changes during the whole horizon T and each period t .

$$Q_{i,t}^{disp} = Q_{i,t}^{max} - Q_{i,t}^{res}, \forall i, t \\ -Q_{i,t}^{disp} \leq Q_{i,t}^{lr} \leq Q_{i,t}^{disp}, \forall i, t$$

} It calculated the reactive power dispatch capacity of the inverter in the second stage $Q_{i,t}^{disp}$.
Then, the dispatch range of the inverter reactive power output $Q_{i,t}^{lr}$ is defined.

$$\underline{P/Q}_{i,t}^{PV/D} \leq P/Q_{i,t}^{PV/D} \leq \overline{P/Q}_{i,t}^{PV/D}, \forall i, t$$

} PV output and load demand $P/Q_{i,t}^{PV/D}$ can vary within the predicted lower and upper bound.

Mathematics Formulation

$$Q_{i,t}^{CB} = Q_{unit}^{CB} \sum_{j \in M} \alpha_{i,j,t}, \quad \forall i, t$$

} CB reactive power output $Q_{i,t}^{CB}$ with on/off decision $\alpha_{i,j,t}$.

$$V_{1,t} = V_0 + \beta_t V^{Tap}, \quad \forall t$$

} Substation voltage $V_{1,t}$ with LTC position β_t .

$$\underline{V}_i \leq V_{i,t} \leq \overline{V}_i, \quad \forall i, t$$

} The voltage magnitude of each node $V_{i,t}$ must be kept within the allowed deviation range.

$$-P_i^{cap} \leq P_{i,t} \leq P_i^{cap}, \quad \forall i, t$$

} The active power flow $P_{i,t}$ is limited with the line capacity.

$$\begin{aligned} P_{i+1} &= P_i - P_i^{loss} + P_{i+1}^{G(PV)} - P_{i+1}^D - P_{i+1}^{lat}, \quad \forall i \\ Q_{i+1} &= Q_i - Q_i^{loss} + Q_{i+1}^{G(CB/lr)} - Q_{i+1}^D - Q_{i+1}^{lat}, \quad \forall i \\ V_{i+1} &= V_i - \frac{R_i P_i + X_i Q_i}{V_0}, \quad \forall i, \end{aligned}$$

} Fully linearized Dist-Flow model (will be introduced in the future):
Active, reactive power flow and voltage relationships for two neighboring buses.

$$\begin{aligned} P_i^{loss} &= \sum_{k \in K_i} a_{i,k} (P_{i,k} - P_{i,k}^*) + \sum_{l \in L_i} b_{i,l} (Q_{i,l} - Q_{i,l}^*) \\ Q_i^{loss} &= \sum_{k \in K_i} c_{i,k} (P_{i,k} - P_{i,k}^*) + \sum_{l \in L_i} d_{i,l} (Q_{i,l} - Q_{i,l}^*) \end{aligned}$$

} Linear calculation for the complex power losses.

$$P_i = \sum_{k \in K_i} (P_{i,k} + P_{i,k}^*), \quad Q_i = \sum_{l \in L_i} (Q_{i,l} + Q_{i,l}^*), \quad \forall i$$

} Divide the complex power flow into pieces.

Mathematics Formulation

$$\begin{aligned} 0 \leq P_{i,k} &\leq P_i^{(k)} - P_i^{(k-1)}, \quad \forall i, k \\ P_i^{(k-1)} - P_i^{(k)} &\leq P_{i,k}^* \leq 0, \quad \forall i, k \\ 0 \leq Q_{i,l} &\leq Q_i^{(l)} - Q_i^{(l-1)}, \quad \forall i, l \\ Q_i^{(l-1)} - Q_i^{(l)} &\leq Q_{i,l}^* \leq 0, \quad \forall i, l \end{aligned}$$



Each piecewise power flow variable can vary only within its corresponding interval.

$P_{i,k}^*$ and $Q_{i,k}^*$ are the negative piecewise power flow variable and they are utilized to calculate the power loss when the power flow is in the reverse direction.

$$\begin{aligned} f_i(x) &= \frac{R_i}{V_i^2}x^2, \quad g_i(x) = \frac{X_i}{V_i^2}x^2, \quad \forall i \\ a_{ik} &= \frac{f_i(P_i^{(k)}) - f_i(P_i^{(k-1)})}{P_i^{(k)} - P_i^{(k-1)}}, \quad \forall i, k \\ b_{il} &= \frac{f_i(Q_i^{(l)}) - f_i(Q_i^{(l-1)})}{Q_i^{(l)} - Q_i^{(l-1)}}, \quad \forall i, l \\ c_{ik} &= \frac{g_i(P_i^{(k)}) - g_i(P_i^{(k-1)})}{P_i^{(k)} - P_i^{(k-1)}}, \quad \forall i, k \\ d_{il} &= \frac{g_i(Q_i^{(l)}) - g_i(Q_i^{(l-1)})}{Q_i^{(l)} - Q_i^{(l-1)}}, \quad \forall i, l \end{aligned}$$



The calculation of all the linear equation slopes.

Robust Optimization

- The **robust optimization** (RO) first searches for the worst case of uncertainty realization then optimizes the objective under the worst case.
- Compared to the conventional **stochastic optimization**, the RO has three major advantages:
 - It does not need a probability distribution function or scenario-based data to model the uncertainty.
 - It achieves a robust solution according to the *worst case* instead of a solution based on the **optimal expectation**.
 - RO can achieve high computational efficiency, since it utilizes uncertainty sets to model uncertainties instead of many scenarios which are utilized in stochastic optimization.
- The RO model for the proposed TRI-VVC strategy can be formulated in the following compact matrix form

$$\begin{aligned}
 & \min_{x} \max_{u} \min_{y} \quad a^T y \\
 \text{s.t.} \quad & Bx \geq c \\
 & Dx + Ey \leq f \\
 & Gx + Hy + Iu = j \\
 & u \in U
 \end{aligned}
 \quad \left. \right\}$$

$$\min_{\alpha, \beta} \sum_{t \in T} \sum_{i \in N} P_{i,t}^{loss} \tau \quad \longrightarrow \quad \min_{\alpha, \beta} \max_{P^{PV}, P^D, Q^D} \min_{Q^{inv}, P, Q, V} \sum_{t \in T} \sum_{i \in N} P_{i,t}^{loss} \tau.$$

Robust Optimization

- The CBs status α and the LTC position β are the first stage decision variable which are “here-and-now” decision variable.
- The inverter output Q^{lr} is the “wait-and-see” decision variable of the second stage.
- The maximization in this “min-max-min” form is to search for the worst case of the uncertainty where the largest energy loss would occur, i.e., the uncertainty variables are optimized to some certain values leading to the highest energy loss.

In this paper, a balanced three-phase 33-bus radial distribution network with CBs, an OLTC and PVs installed is used in the case study.

- The power flow of this system is assumed as balanced three-phase flow.
- Each CB has 10 capacitor units of 30 kVAR.
- In the test, $V_0 = 1$ p.u., $V^{Tap} = 0.005$ p.u., the allowed operational voltage range $[\underline{V}_i, \overline{V}_i] = [0.95, 1.05]$.
- The critical voltage range used in the PV inverter droop control $[\underline{V}^{cri}, \overline{V}^{cri}] = [0.94, 1.06]$.

Case Study

- The proposed TRI-VVC is applied for 24 hours. The 24-hour rolling horizon predictions of the PV output and the load demand are shown as below.

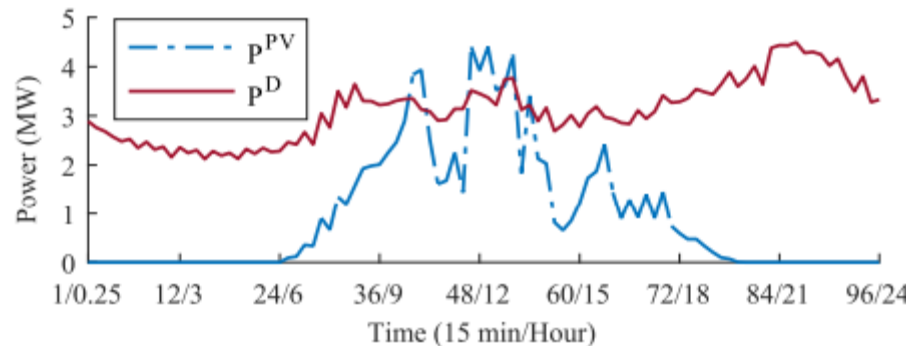


Fig.13 24-hour PV output and load demand profile

- The 24-hour simulation results are shown.

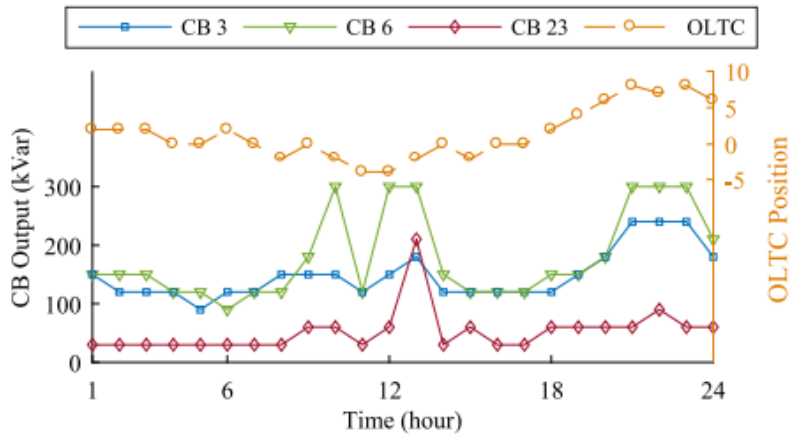


Fig.14 24-hour first stage decisions

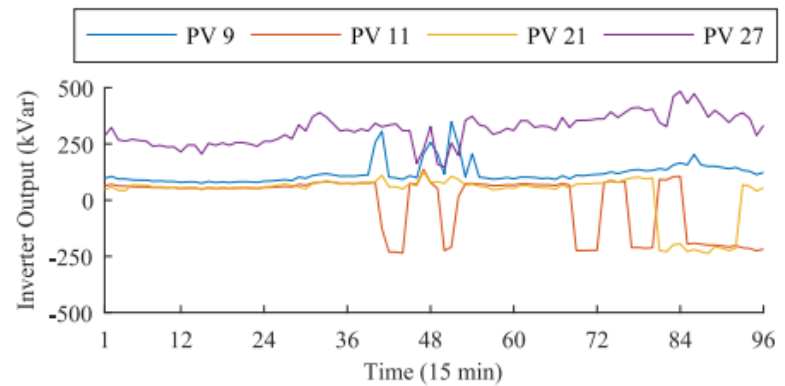


Fig.15 24-hour second stage decisions

Case Study

- The proposed TRI-VVC strategy is compared with a conventional single-stage centralized VVC (SSC-VVC) strategy.
- * In this conventional method, the operating decisions of the CBs, the OLTC and the inverters are optimized together with rolling point predictions where only mean values are predicted.

Strategy	SSC-VVC	TRI-VVC
Daily Voltage Violation Rate (%)	100	0
15-minute Voltage Violation Rate (%)	10.80	0
Voltage Absolute Deviation (p.u.)	0.0194	0.0171
Daily Energy Loss (MWh)	4.048	4.013

- The TRI-VVC strategy can achieve effectively robust solutions against the uncertainties to avoid voltage violation while carrying out relatively low energy loss.

Summary

- VVC helps the operator mitigate dangerously low or high voltage conditions by suggesting required action plans for all VVC devices.
- VVO optimally manages voltage levels and reactive power to achieve more efficient grid operation by reducing system losses, peak demand or energy consumption or a combination of multi-objectives.
- CVR reduces customer voltages along a distribution circuit to reduce electricity demand and energy consumption.

Advanced Topics in Distribution System Modelling

- Conservative Voltage Reduction (CVR) and Volt- Var Optimization
- Distribution System Resilience
 - Definition and Metrics for Power System Resilience and Reliability
 - Resilience Enhancement
 - Distribution System – Repair and Restoration
 - Resilience Oriented Design (ROD) Optimization
- Microgrid – Dynamic Modelling and Control

Definitions

Resilience	The ability to prepare for and adapt to changing conditions and withstand and recover rapidly from disruptions.
Reliability	The ability of the system to satisfy the customer demand within accepted standards and in the amount desired.

	Resilience	Reliability
Events Considered	Low Probability, High Consequence Hazards	High Probability, Low Consequence Hazards
Risk-based?	Yes	No
Binary or continuous?	Resilience is considered a continuum, confidence is specified	Operationally, the system is reliable or not. Confidence is unspecified
Measurement focus	Focus is on measuring impact to humans	Focus is on measuring the impact to the system

Reliability Metrics

SAIFI - System Average Interruption Frequency Index

Average frequency of sustained interruptions per customer:

$$= \frac{\text{Number of interrupted customers}}{\text{Total number of customers}}$$

SAIDI - System Average Interruption Duration Index

Customer minutes of interruption or customer hours :

$$= \frac{\text{Sum of all customer interruption durations}}{\text{Total number of customers}}$$

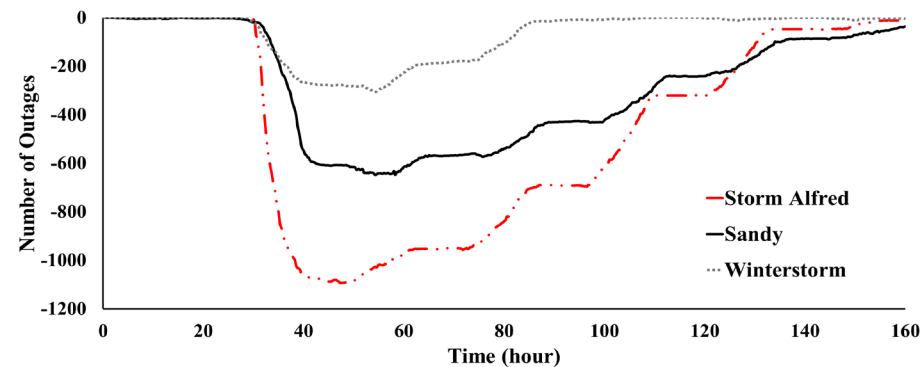
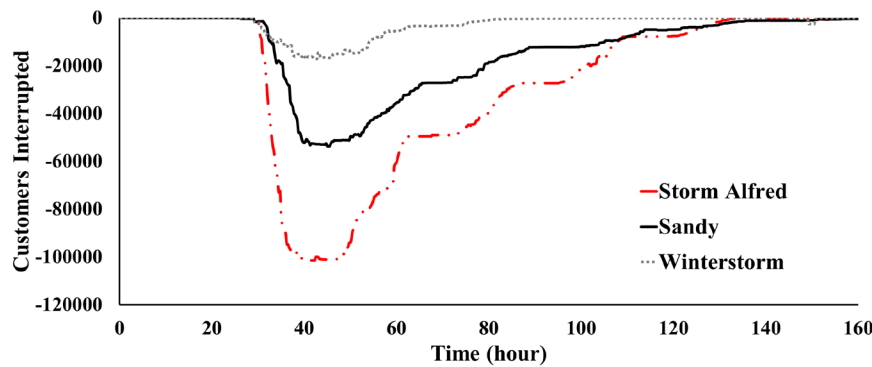
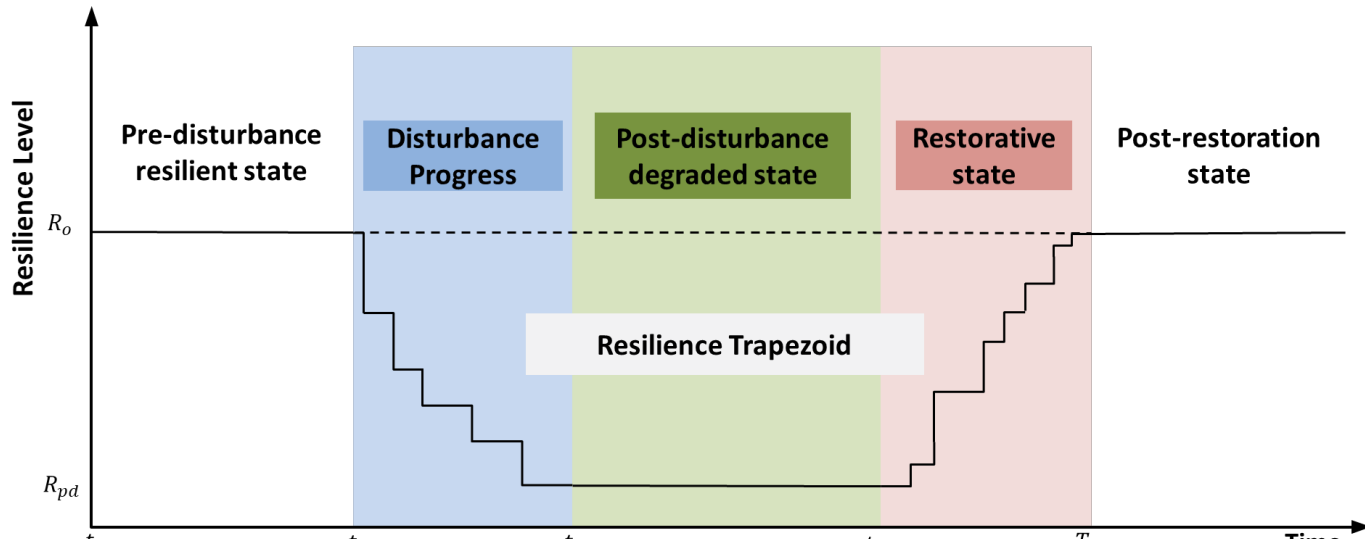
CAIDI - Customer Average Interruption Duration Index

Average time needed to restore service to the average customer: $\frac{\text{SAIDI}}{\text{SAIFI}}$

Why reliability metrics cannot be directly applied to resilience?

- 1) Undervalue the impact of large-scale events and focus on normal operating conditions;
 - 2) High standard deviation.
-
- Many utilities exclude major events from SAIFI and SAIDI.
 - There is a need to design new metrics for resilience.

Resilience Curve



Metric for Resilience

Metric	Equation	Description
Storm Average Interruption Frequency Index (STAIFI)	$\frac{\text{Total Number of Customers Interrupted}}{\text{Total Number of Customers Served}}$	<ul style="list-style-type: none">• STAIFI and STAIDI exhibit too much uncertainty because of their high standard deviation.• The metrics are static and do not represent the dynamic evolution of damage and recovery processes.
Storm Average Interruption Duration Index (STAIDI)	$\frac{\text{Total Customer Storm Interruption Minutes}}{\text{Total Number of Customers Served}}$	<ul style="list-style-type: none">• Insufficient representation of the physical aspect of grids.• Difficult to estimate due to the uncertainties in the recovery process.
Estimated Time of Restoration (ETR)	$\text{Time of Outage} + \text{Estimated Recovery Time}$	<ul style="list-style-type: none">• Fails to provide a clear indication of the network's ability to withstand weather events.

Metric for Resilience

Metric	Equation	Description
Speed of degradation	$\frac{R_{pd} - R_0}{t_{ee} - t_{oe}}$	<ul style="list-style-type: none"> This metric indicates how fast the resilience drops after an extreme event. It can be used to measure the network's ability to withstand the event, but not for recovery.
Amount of degradation	$R_0 - R_{pd}$	<ul style="list-style-type: none"> The metric measures the initial impact of the extreme event.
Duration of the post-disturbance degraded state	$t_r - t_{ee}$	<ul style="list-style-type: none"> Indicates the quality of the initial immediate response after the event. This metric highly depends on the fault location, isolation and service restoration (FLISR) technologies being used.
Speed of network recovery	$\frac{R_0 - R_{pd}}{T - t_r}$	<ul style="list-style-type: none"> The metric measures the quality of the response from the utility. It includes the speed of damage assessment, repair process and crew management, and power restoration operation.
Area of the resilience trapezoid	$\int_{t_{oe}}^T R(t) dt$	<ul style="list-style-type: none"> This metric gives an overall indicator of the system performance.

Metric for Resilience

- Measure resilience at the network-level involving both infrastructure and services (Wei 2013)
- Combine the **infrastructure** and **service** resilience metrics (Ji 2017)

$$R(t) = 1 - \frac{1}{C_0} E\{C(t; d)\}$$

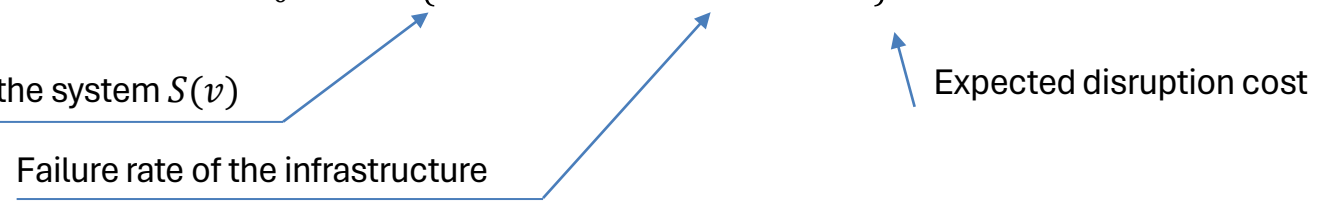
d : a threshold on tolerable delays for recovery
 C_0 : is a normalization factor

$$E\{C(t; d)\} = \int_0^{t-d} E_{S(v)} \left\{ \lambda_i^f(v|S(v)) E\{G_i(v, t)|S(v)\} \right\} dv$$

Expected state of the system $S(v)$

Failure rate of the infrastructure

Expected disruption cost



- This metric does not include weather variables. An open issue is how to derive resilience metrics combining weather with the infrastructure and services.

Resilience Enhancement

Phases	Actions
Long-term planning	<ul style="list-style-type: none">• Infrastructure hardening• Vegetation management• Adding distributed energy resources (DER)• Implementing smart grid technologies<ul style="list-style-type: none">• Automated switching devices and sensors• Smart meters for situational awareness
Short-term pre-event preparation	<ul style="list-style-type: none">• Weather forecast and damage prediction• Pre-position crews• Pre-allocate equipment and fuels• Pre-position mobile energy sources
Post-event restoration	<ul style="list-style-type: none">• Automatic fault isolation and service restoration• Improved damaged assessment<ul style="list-style-type: none">• Damage location prediction• Smart meters• Drones• Optimizing repair scheduling and crew routing• Dynamic network reconfiguration• Use of DERs, demand response, and microgrids for restoration

Research on Resilience

- Resilience: The ability to prepare for and adapt to changing conditions and withstand and recover rapidly from disruptions.

- A tri-stage robust optimization model
- A two-stage stochastic optimization model
- S. Ma, S. Li, Z. Wang, F. Qiu, Resilience-Oriented Distribution System Design with Decision-Dependent Uncertainty, *IEEE Trans. Power Syst.*, 2018.
- S. Ma, L. Su, Z. Wang, F. Qiu, Resilience Enhancement of Distribution Grids Against Extreme Weather Events, " *IEEE Trans. Power Syst.*, 2018.
- S. Ma, B. Chen, Z. Wang, Resilience enhancement strategy for distribution systems under extreme weather events, *IEEE Trans. Smart Grid*, 2016.

- Co-optimize distribution grid operation and crew repair
- A. Arif, Z. Wang, J. Wang, C. Chen, "Repair and resource scheduling in unbalanced distribution systems using neighborhood search," *IEEE Trans. Smart Grid*, accepted, 2019.
- A. Arif, S. Ma, Z. Wang, J. Wang, S. M. Ryan, C. Chen, "Optimizing service restoration in distribution systems with uncertain repair time and demand," *IEEE Trans. Power Syst.*, vol. 33, no. 6, pp. 6828-6838, Nov. 2018.
- A. Arif, Z. Wang, J. Wang, C. Chen, "Power distribution system outage management with co-optimization of repairs, reconfiguration, and DG dispatch," *IEEE Trans. Smart Grid*, vol. 9, no. 5, pp. 4109-4118, Sept. 2018.

Planning

- Tree trimming
- DERs
- Automatic Switches
- Hardening
- Microgrids

Preparation

- Weather forecasting
- Outage modelling and prediction
- Crew and equipment allocation

Damage Assessment

- Fault location
- UAVs
- Repair time prediction

Repair & Restoration

- Fault isolation and service restoration
- Dispatch repair crews and repair scheduling
- Microgrid formation

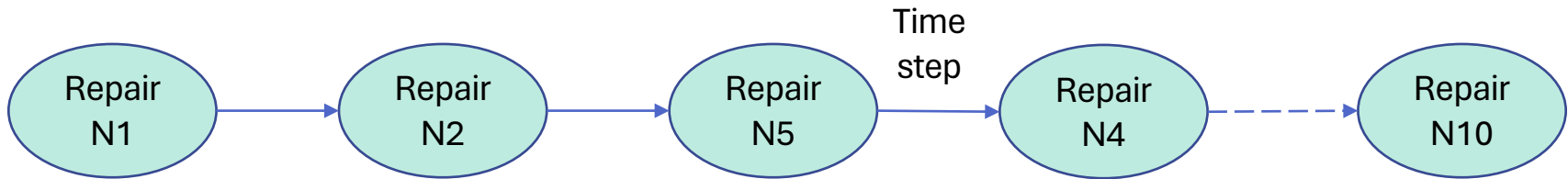
- A. Arif, Z. Wang, C. Chen, B. Chen, A stochastic multi-commodity logistic model for disaster preparation in distribution systems, *IEEE Trans. Smart Grid*, accepted, 2019.

- A. Arif, Z. Wang, "Distribution network outage data analysis and repair time prediction using deep learning," *IEEE Int Conf. Probabilistic Methods Appl. Power Syst.*, Boise, ID, 2018.

Review: Repair and Restoration

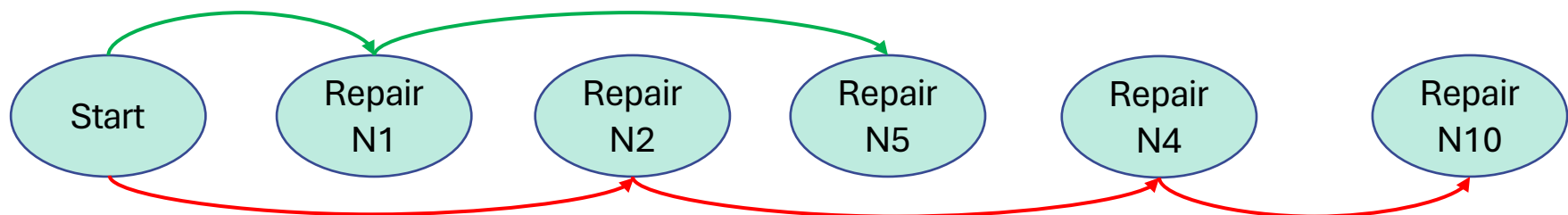
How do utilities schedule the repairs?

- Define priorities for the damaged components → dispatch the crews according to the priorities
- 2-Step approach for transmission systems (Pascal Van Hentenryck and Carlton Coffrin 2015):
- Restoration Ordering Problem: assume only one component can be repaired at each time steps
(Solved using MILP)



Routing: solve a routing problem with precedence constraints

- Solved using Constraint Programming
- Precedence constraint



Problem Statement

What is missing?

- An optimization strategy for disaster preparation that selects staging areas and allocates crews and equipment while considering the system's components
- A co-optimization method that jointly optimizes crew routing and distribution system operation
- Solution algorithms for solving these difficult problems

Pre-event preparation

- Choose staging locations
- Mobilize available crews and request assistance if necessary
- Obtain and allocate equipment

Post-event repair and restoration

- Coordinate tree and line crews
- Manage equipment
- Isolate damaged components
- Operate the distribution system



Summary

- Develop a two-stage stochastic program
- Use fragility models to generate scenarios
- Uncertainties: damaged components, equipment, and repair times

Objective

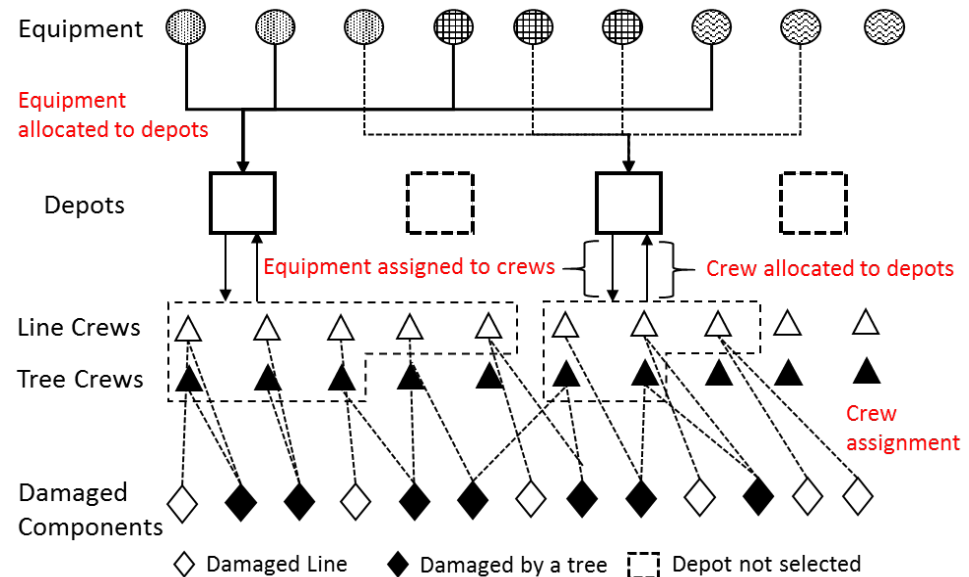
- Minimize preparation costs and penalty over unmet demand and late repairs

First-stage

- Depot selection
- Crew and equipment allocation

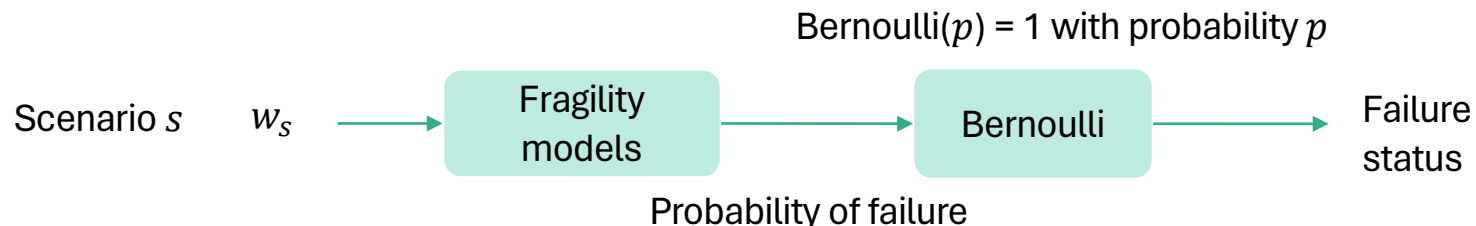
Second-stage

- Assign crews to damaged components

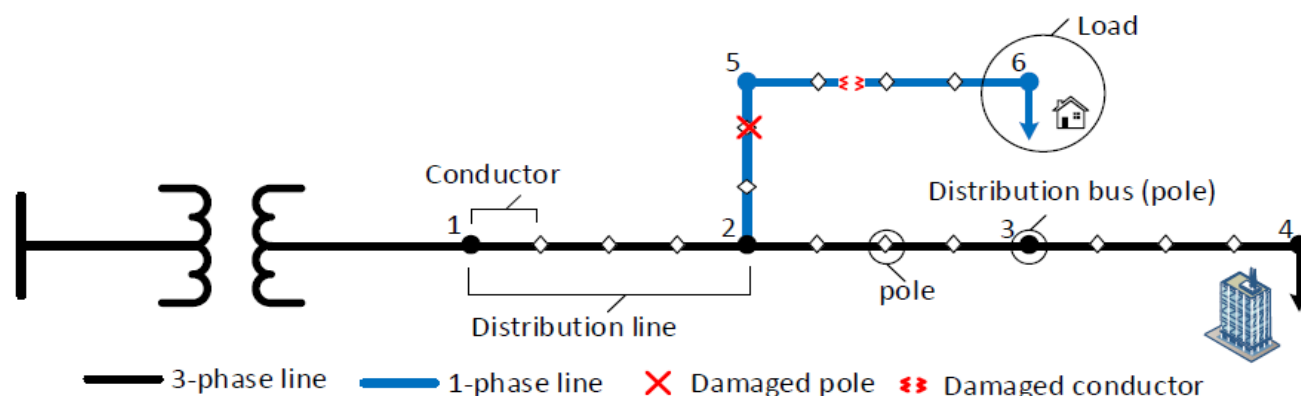


Scenario Generation (1/2)

- Assuming a hurricane is forecasted
- We generate wind speeds using lognormal distribution and hurricane model (Javanbakht 2018, Kaplan 1995)



- Fragility models to (Ouyang 2014):
 - Calculate the probability of failure of each pole
 - Calculate probability of failure of each conductor
 - Probability of wind induced damage
 - Probability of damage due to fallen trees



Scenario Generation (2/2)

- Calculate required equipment (poles, transformers, conductors)
- Estimate the repair times using normal distributions (Ouyang 2014)
- Identify critical components
 - Solve a MILP to identify minimum number of lines to repair
 - Minimize number of lines to be repaired while serving all critical loads
 - Status of the line: u_k
 - Status of the load: y_i

$$\min \sum_{k \in \Omega_{DL}(s)} u_k$$

$$\text{subject to } y_i = 1, \forall i \in \Omega_{CD}$$

subject to power operation constraints

- **First-stage objective:** minimize the costs of equipment transportation, ordering equipment and external crews, and staging depots

$$\min \sum_{\forall d, e, \tau} \mathcal{P}_{d,e,\tau}^{TE} E_{d,e,\tau} + \sum_{\forall d, \tau} \mathcal{P}_{\tau}^{EI} EI_{d,\tau} + \sum_{\forall d} (\mathcal{P}^{EC}(LI_d + \mathcal{T}I_d) + \mathcal{P}_d^D \nu_d)$$

- **Second-stage objective:**

- Minimize the costs associated with the crews. The costs of crews include labor, food, and accommodation
- Minimize penalty costs of unmet equipment demand and time it takes to repair all components

$$\min \sum_{\forall s} \Pr(s) \left(\sum_{\forall c} \mathcal{P}_c^H H_{c,s} + \sum_{\forall d, \tau} \mathcal{P}_{\tau}^{LF} \mathcal{E}_{d,\tau,s} + \mathcal{P}^R (\mathcal{L}_s^T + \mathcal{L}_s^L) \right)$$

Constraints

First-stage constraints

- Select depots
- Transfer existing equipment/crews between depots
- Acquire new equipment/crews
- Depot capacity constraint

Second-stage constraints

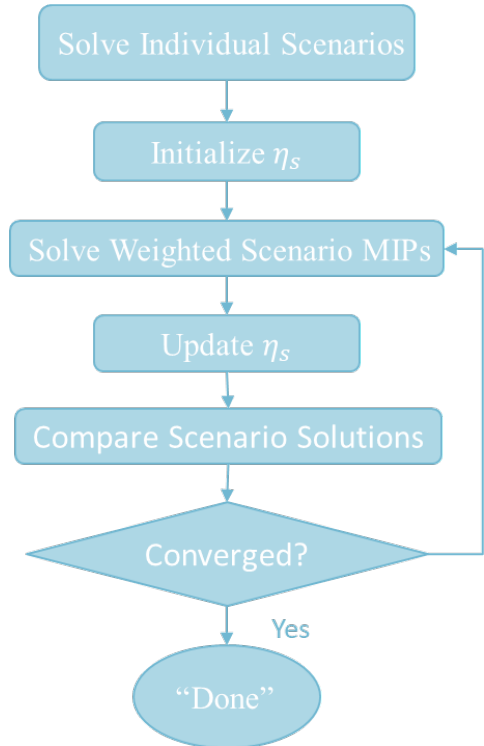
- Crews are assigned to repair damaged the components
- The assignment is constrained by the distance
- Calculate working hours
- Assign equipment to the crews
- We must have enough equipment for critical components
- Calculate unmet equipment demand

Solution Methods

- The Extensive Form (EF)
 - Write down the full variable and constraint set for all scenarios
 - Attempt to solve with a commercial MIP solver
 - Best solution, but often does not work due to memory or time limits

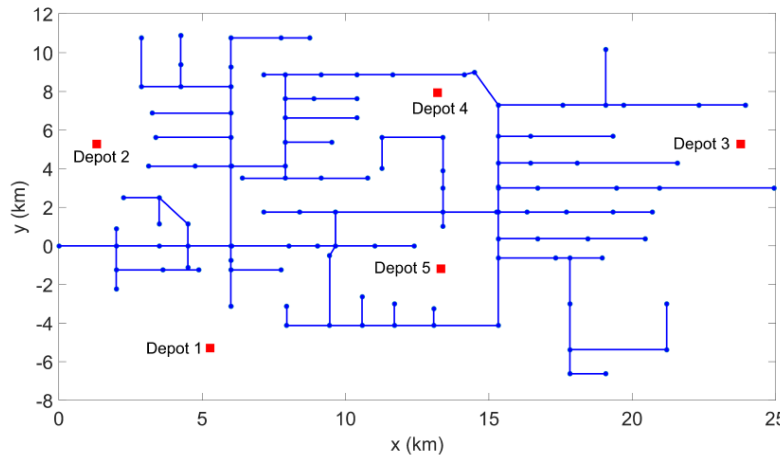
- **Progressive hedging**

- Scenario-based decomposition
- Pros: parallelizable
- Cons: heuristic
- Algorithm:
 1. Solve each scenario independently
 2. Find the average first-stage solution $\bar{x} = \sum_{\forall s} \Pr(s) x_s$
 3. Calculate penalty factor $\eta_s = \rho(x_s - \bar{x})$
 4. Augment the penalty factor to the stochastic model and solve
 5. If $\sum_{\forall s} \Pr(s) ||x_s - \bar{x}|| > \epsilon$ go to 2
- The algorithm terminates once all first-stage decisions x_s converge to a common \bar{x}
- The PH algorithm may experience slow convergence
- We fix some of the first-stage variables (depot selection and crew allocation) if they converge to the same values after some number of iterations



Results (1/2)

- IEEE 123-bus system
- Proposed method (SCRAP) is compared with:
 - Deterministic allocation (DA)
 - Robust stochastic optimization method (RSO) (Bozorgi-Amiri 2013)
- Main difference is in the number of equipment acquired
- The deterministic solution did not consider some of the extreme cases
- RSO favors a solution that would perform better with worst-case scenarios



PRE-EVENT PREPARATION RESULTS

	SCRAP		DA		RSO	
Staged Depots	1	4	1	4	1	4
Line Crews	6	4	6	4	6	4
Tree Crews	2	1	2	1	2	1
Equipment	1	10	6	10	0	15
	2	16	13	13	6	26
	3	3	0	3	0	3
	4	6	2	7	1	6
	5	3.8 km	2 km	2.5 km	1.5 km	5 km
Costs	\$146,766		\$117,443		\$183,371	

Results (2/2)

- The wait-and-see (WS) solution is calculated to provide a lower bound
- We calculate the objective value of the stochastic model for each method by using the first-stage decisions of the different methods

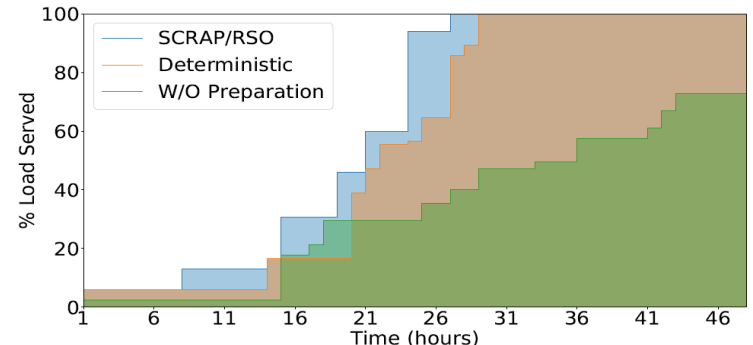
Method	Objective Value	Computation Time
WS	\$513,170	N/A
SCRAP-EF	\$549,554	300 min
SCRAP-PH	\$551,585	106 min
RSO	\$608,683	335 min
ED	\$714,602	2 min

Restoration Phase

- To assess the devised preparation plan, we solve the repair and restoration problem with and without preparation
- A new random damage scenario is generated on the IEEE 123-bus system
- The stochastic and robust models have enough equipment, however, RSO has a large surplus

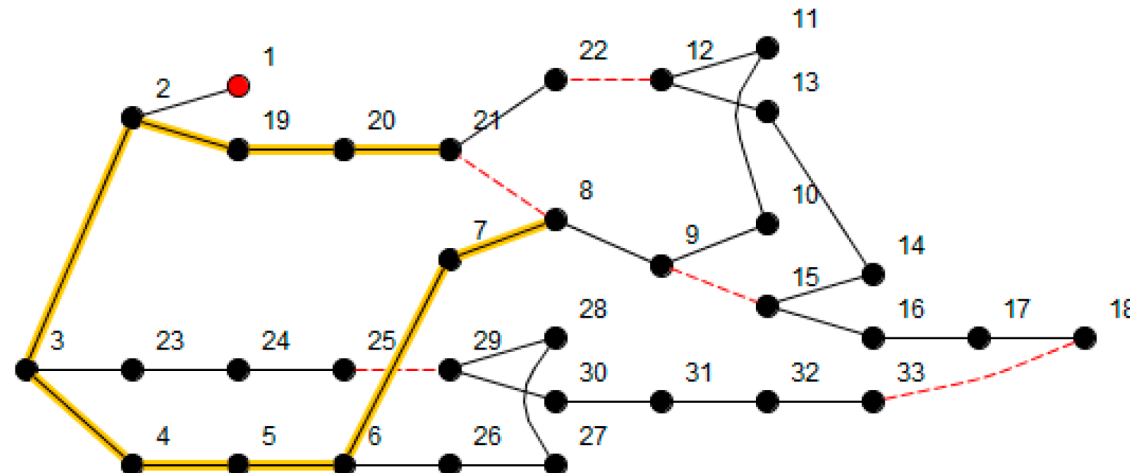
REPAIR AND RESTORATION PERFORMANCE AFTER THE EVENT		
Preparation	Equipment	Load served (kWh)
SCRAP	{+3,+11,+3,+6,+0.32 km}	80,136 kWh
RSO	{+10,+23,+3,+7,+3.7 km}	80,136 kWh
DA	{-3,+1,+3,+6,-0.34 km}	77,448 kWh
W/O Preparation	{-3,-3,+3,+6,-0.34 km}	46,667 kWh

“-”: shortage; “+”: surplus; the load served is for the first 48 hours
 Equipment: {Poles for 3-phase lines, Poles for single-phase lines,
 3-phase transformers, single-phase transformers, conductor}



Distribution System Restoration

- **Reconfiguration:** optimal reconfiguration of the distribution network with the objective of maximizing the served loads.
- **Reconfiguration and DG dispatch:** optimal reconfiguration of the distribution network and DG operation.
- **Networked Microgrids:** optimal operation of interconnected individual microgrids with defined boundaries.
- **Microgrid formation:** optimal operation of microgrids with dynamic boundaries.
- **Repair Scheduling:** repair scheduling of distribution systems' assets without considering network operations.



Review: Repair and Restoration (1/3)

MILP for transmission system repair and restoration (Arab 2015)

Assumptions

- Neglect travel time
- Crews are immediately present at the damaged components
- No specific crew assignments

Model

- Transmission system operation
- Repair schedule

The diagram illustrates the relationship between two tables: Repair status and Operation status, both spanning four transmission lines (Line 1 to Line 4). A blue bracket labeled "Repair time" spans the first three columns of both tables. A blue arrow points from the "Repair status" table to the "Operation status" table, indicating a dependency where the repair of damaged components (red cells) enables the restoration of transmission lines (red cells with value 1).

Repair status

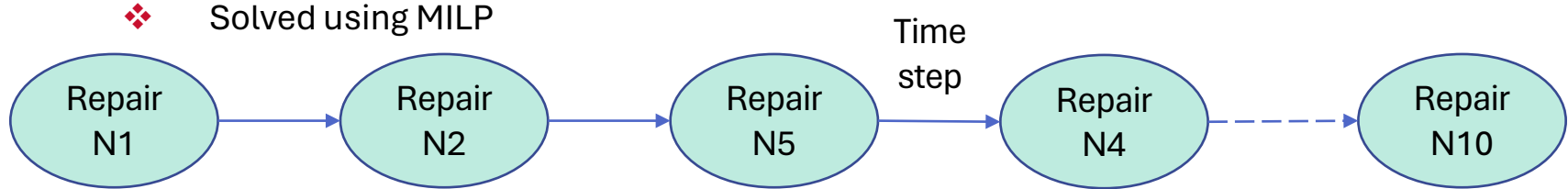
	Repair status						
	Repair time						
	1	1	1	0	0	0	0
Line 1	1	1	1	0	0	0	0
Line 2	1	1	1	1	0	0	0
Line 3	0	0	0	1	1	0	0
Line 4	0	0	0	0	1	1	0

Operation status

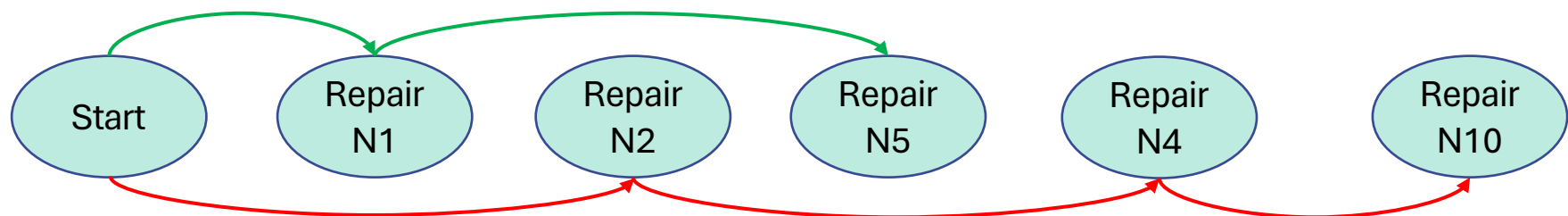
	Operation status						
	Repair time						
	0	0	0	1	1	1	1
Line 1	0	0	0	1	1	1	1
Line 2	0	0	0	0	1	1	1
Line 3	0	0	0	0	0	1	1
Line 4	0	0	0	0	0	0	1

Review: Repair and Restoration (2/3)

- ❖ A project by Los Alamos National Lab and National ICT Australia (NICTA), Australian National University.
- ❖ 2-Step approach for transmission systems (Pascal Van Hentenryck and Carlton Coffrin 2015):
 1. Restoration Ordering Problem: assume only one component can be repaired at each time step
 - ❖ Solved using MILP



2. Routing: solve a routing problem with precedence constraints
 - ❖ Solved using Constraint Programming
 - ❖ Precedence constraint



Review: Repair and Restoration (3/3)

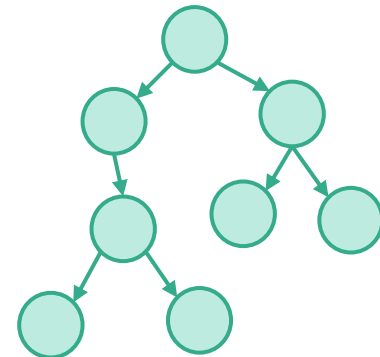
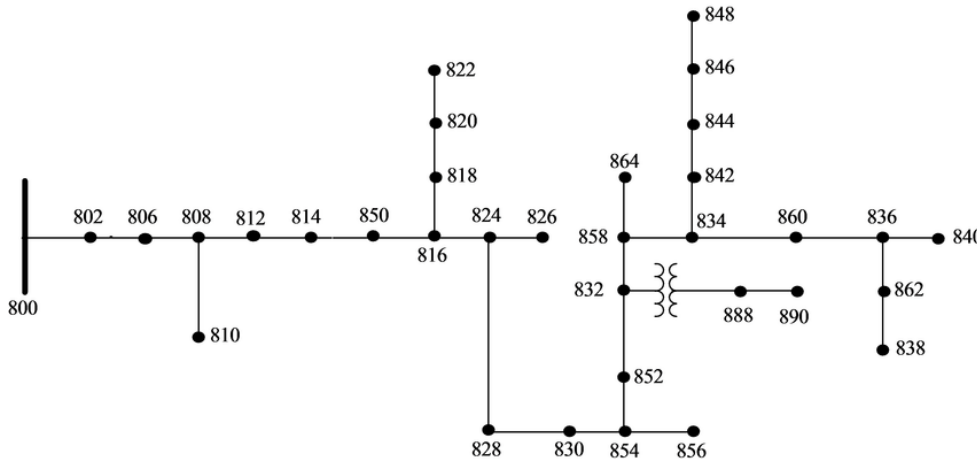
❖ Yushi Tan and Daniel S. Kirschen , University of Washington, 2017 (preprint).

- Assumptions

- Network is radial without switches.
- Power only from substation.
- Travel time is neglected.
- Power operation constraints are neglected.

- Method

- Solve scheduling problem (LP) to minimize the total weighted completion time under with “outtree” precedence constraint
 - obtain priority list
- Whenever a crew is free, select among the remaining candidate lines the one with the highest priority.

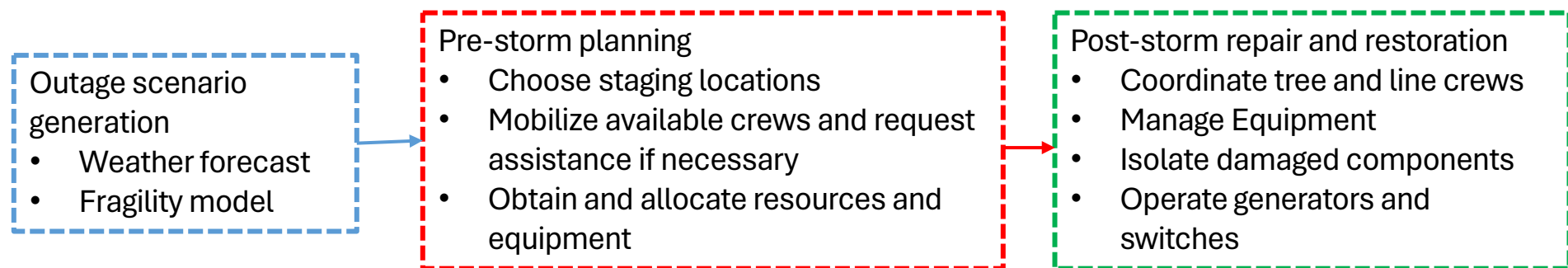


Research Objectives

- What is missing?
 - A co-optimization method that jointly optimizes crew routing and distribution system operation.
 - Modeling fault isolation and tree/obstacle removal before repairing the lines.
 - A preparation strategy before repair and restoration to ensure a fast response.

Objectives

1. Proactive response: develop a stochastic program to pre-stage and prepare human resources and equipment before extreme weather events.
2. Develop MILP and stochastic mixed integer linear program (SMIP) models to co-optimize repair scheduling and the recovery operation of distribution systems.
3. Design solution algorithms for solving the above problems.



Contributions

- A novel mathematical model for jointly optimizing the repair crew routing and distribution network restoration is developed. The model can improve utilities' response to extreme events.
- A mathematical formulation is developed for fault isolation and service restoration. Isolation has been neglected in distribution system restoration studies that use mathematical programming.
- Development of efficient algorithms for solving the co-optimization problem.
 - Cluster-based decomposition
 - Priority-based decomposition
 - Hybrid mathematical programming and search algorithm

Mathematical Model

Distribution system repair and restoration problem (DSRRP)

Assumption:

Damage assessment has been conducted: the locations are known and the repair time is estimated.

Objective

- Minimize cost of shedding loads and switching operation

$$\min \sum_{\forall t} \left(\sum_{\forall \varphi} \sum_{\forall i} (1 - y_{i,t}) \rho_i^D P_{i,\varphi,t}^D + \rho^{SW} \sum_{k \in \Omega_{SW}} \gamma_{k,t} \right)$$

Constraints

- Distribution system operations
 - Power flow
 - Cold-load pickup
 - Voltage constraints
 - Reconfiguration and fault isolation constraints
- Crew routing
 - Path-flow constraints
 - Start/end location
 - A damaged line is repaired by one crew
 - Arrival (repair start) time
 - Tree removal before line repair
 - Equipment constraints

Distribution System Constraints

1. Generator limits
2. Line limits
3. Node balance
4. Kirchhoff voltage law
5. Voltage regulators

- 1 $\boxed{0 \leq P_{i,\varphi,t}^G \leq P_i^{G_{max}}, \forall i, \varphi, t}$
- 1 $\boxed{0 \leq Q_{i,\varphi,t}^G \leq Q_i^{G_{max}}, \forall i, \varphi, t}$
- 2 $\boxed{-u_{k,t}p_{k,\varphi}P_k^{K_{max}} \leq P_{k,\varphi,t}^K \leq u_{k,t}p_{k,\varphi}P_k^{K_{max}}, \forall k, \varphi, t}$
- 2 $\boxed{-u_{k,t}p_{k,\varphi}Q_k^{K_{max}} \leq Q_{k,\varphi,t}^K \leq u_{k,t}p_{k,\varphi}Q_k^{K_{max}}, \forall k, \varphi, t}$
- 3 $\boxed{\sum_{\forall k \in K(.,i)} P_{k,\varphi,t}^K + P_{i,\varphi,t}^G = \sum_{\forall k \in K(i,.)} P_{k,\varphi,t}^K + P_{i,\varphi,t}^L, \forall i, \varphi, t}$
- 3 $\boxed{\sum_{\forall k \in K(.,i)} Q_{k,\varphi,t}^K + Q_{i,\varphi,t}^G = \sum_{\forall k \in K(i,.)} Q_{k,\varphi,t}^K + Q_{i,\varphi,t}^L, \forall i, \varphi, t}$
- 4 $\boxed{U_{j,t} - U_{i,t} + \bar{Z}_k S_k^* + \bar{Z}_k^* S_k \leq (2 - u_{k,t} - p_k)M, \forall k \in \Omega_L \setminus \Omega_V, t}$
- 4 $\boxed{U_{j,t} - U_{i,t} + \bar{Z}_k S_k^* + \bar{Z}_k^* S_k \geq -(2 - u_{k,t} - p_k)M, \forall k \in \Omega_L \setminus \Omega_V, t}$
- 5 $\boxed{-(2 - u_{k,t} - p_k)M \leq a_k^2 U_{j,t} - U_{i,t}, \forall k \in \Omega_V, t}$
- 5 $\boxed{a_k^2 U_{j,t} - U_{i,t} \leq (2 - u_{k,t} - p_k)M, \forall k \in \Omega_V, t}$

u : status of the line

p_k : for line k with phases a, c ,

$$p_k = [1, 0, 1]$$

$$U = V^2$$

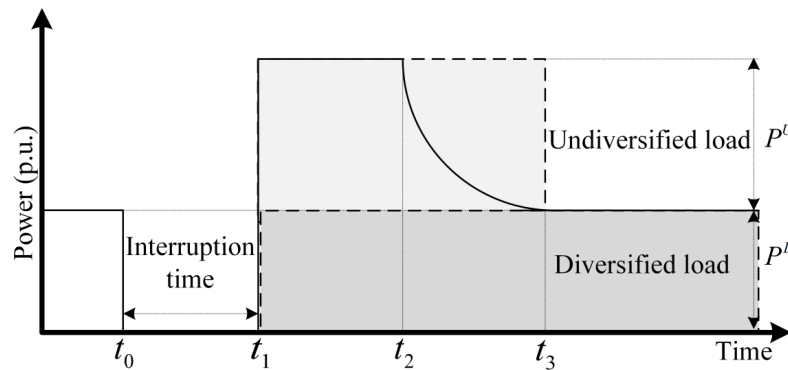
a_k : the ratio between the primary and secondary winding for each phase

Cold-Load Pickup

- Cold load pickup (CLPU) is the well-known problem defined as excessive inrush current drawn by loads when the distribution circuits are re-energized after extended outages.
- The typical behaviour of CLPU can be represented using a delayed exponentially decaying function.
- We use two blocks to provide a conservative approach and guarantee the supply-load balance (Liu, PSERC 2009).

$$P_{i,\varphi,t}^L = y_{i,t} P_{i,\varphi,t}^D + (y_{i,t} - y_{i,\max(t-\lambda,0)}) P_{i,\varphi,t}^U, \quad \forall i, \varphi, t$$

$$Q_{i,\varphi,t}^L = y_{i,t} Q_{i,\varphi,t}^D + (y_{i,t} - y_{i,\max(t-\lambda,0)}) Q_{i,\varphi,t}^U, \quad \forall i, \varphi, t$$



- λ : number of time steps required for the load to return to normal condition.
- If a load goes from a de-energized state $y = 0$, to an energized state $y = 1$, it will go back to normal condition after λ .

Voltage Regulator

Voltage regulator with variable tap setting

Voltage on the secondary side = $a \times$ voltage on the primary

The standard voltage regulator provides $\pm 10\%$ adjustment in thirty-two 0.625 % steps

$$a = [1 + 0.00625 \times \text{Tap}] \rightarrow U_j = [1 + 0.00625 \times \text{Tap}]^2 U_i$$

Tap = -16, -15, ..., 16

Define variable $\tau \in \{0,1\}^{33}$, where $\tau_1 = 1 \rightarrow \text{Tap} = -16$

$$\mathbf{r} = a^2 = [0.8100, 0.8213, \dots, 1.2100]$$

Exact linear constraints

$$-M(1 - \tau_p) + r_p U_i \leq U_j \leq r_p U_i + M(1 - \tau_p), \forall \text{ voltage regulators}, p \in \{1..33\}$$

Example: if a^2 is desired to be 0.81, then $\tau_p = 1$, if $p = 1$

$$0.81 U_i \leq U_j \leq 0.81 U_i$$

Simplified constraint

$$0.81 U_i \leq U_j \leq 1.21 U_i$$

Reconfiguration

1. Radiality constraints (for radial networks)

$$\sum_{k \in \Omega_{K(l)}} u_{k,t} \leq |\Omega_{K(l)}| - 1, \forall l, t$$

2. Count switching operations

$$\gamma_{k,t} \geq u_{k,t} - u_{k,t-1}, \forall k \in \Omega_{SW}, t$$

$$\gamma_{k,t} \geq u_{k,t-1} - u_{k,t}, \forall k \in \Omega_{SW}, t$$

3. Fault Isolation:

- Force the voltage to be zero on damaged lines
- The voltage propagates through KVL until a CB/switch stops the propagation

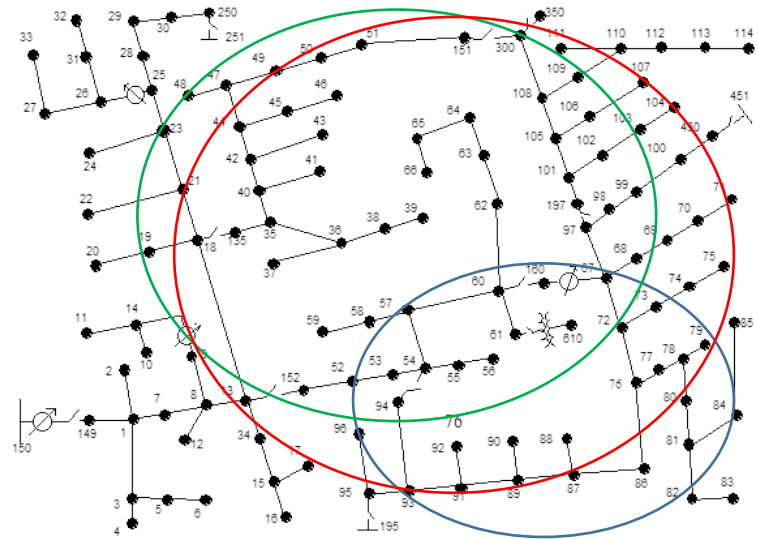
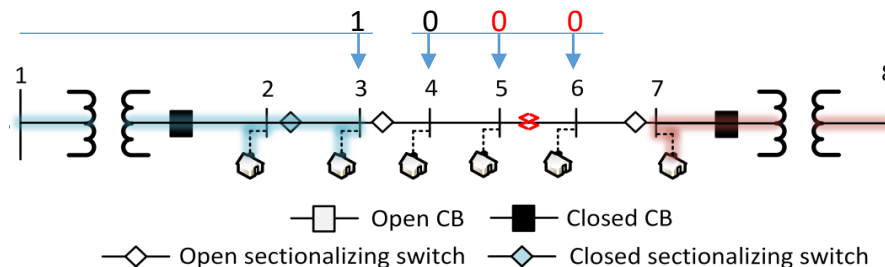
χ : outage status of bus
 $\Omega_{K(l)}$: set of lines in loop l
 Ω_{DK} : set of damaged lines
 γ : Binary parameter
 equals one if a switch changes its status

$$2u_{k,t} \geq \chi_{i,t} + \chi_{j,t}, \forall k \in \Omega_{DK}, t$$

$$\chi_{i,t} U_{min} \leq U_{i,t} \leq \chi_{i,t} U_{max}, \forall i, t$$

$$\chi_{i,t} \geq y_{i,t}, \forall i, t$$

$$u_{k,t} = 1, \forall k \notin \{\Omega_{SW} \cup \Omega_{DK}\}, t$$



Crew Routing (1/2)

- Vehicle routing problem (VRP)
 - Starting and ending locations
 - Path-flow constraint
 - A damaged component is visited only once by a line crew and a tree crew (if required)

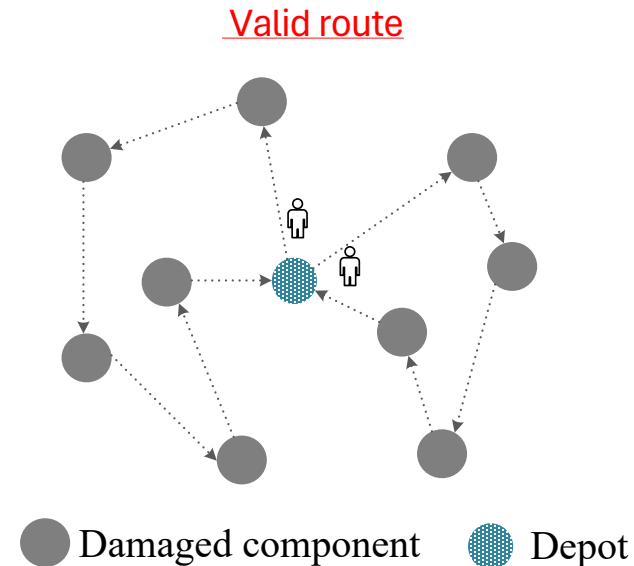
$$\sum_{\forall m \in N} x_{\phi_c^0, m, c} = 1, \forall c$$

$$\sum_{\forall m \in N} x_{m, \phi_c^1, c} = 1, \forall c$$

$$\sum_{\forall n \in N \setminus \{m\}} x_{m, n, c} - \sum_{\forall n \in N \setminus \{m\}} x_{n, m, c} = 0, \forall c, m \in N \setminus \{\phi_c^0, \phi_c^1\}$$

$$\sum_{\forall c \in C^L} \sum_{\forall m \in N \setminus \{n\}} x_{m, n, c} = 1, \forall n \in \Omega_{DK}$$

$$\sum_{\forall c \in C^T} \sum_{\forall m \in N \setminus \{n\}} x_{m, n, c} = 1, \forall n \in \Omega_{DT}$$



x : binary var equals 1 if crew travels the path

$\phi^{0/1}$: start/return location time

N : set of nodes

Ω_{DT} : set of lines damaged by trees

$C^{L/T}$: set of line/tree crews

Crew Routing (2/2)

1. Calculate arrival time $Arrival_n = Arrival_m + Travel_{mn} + Repair_m$
2. Tree crews must finish before the line crews start repairing
3. Set arrival time = 0 (empty) if a crew does not visit a component
4. Crews must have enough equipment to repair the components
5. Each crew has a capacity
6. Equipment are used/picked up as the crews travel between components
 - Equipment on hand = equipment at previous location – equipment used
7. The equipment is taken from the depot/warehouse

1
$$\alpha_{m,c} + \mathcal{T}_{m,c} + tr_{m,n} - (1 - x_{m,n,c}) M \leq \alpha_{n,c}$$

$$\forall m \in N \setminus \{\phi_c^1\}, n \in N \setminus \{\phi_c^0, m\}, c$$

2
$$\sum_{c \in C^L} \alpha_{m,c} \geq \sum_{c \in C^T} \alpha_{m,c} + \mathcal{T}_{m,c} \sum_{\forall n \in N} x_{m,n,c}, \forall m \in \Omega_{DT}$$

3
$$0 \leq \alpha_{m,c} \leq M \sum_{n \in N} x_{n,m,c}, \forall m \in N \setminus \{\phi_c^0, \phi_c^1\}, c$$

α : arrival time
 T : repair time
 tr : travel time
 Res^C : number of resources a crew takes from a depot
 Res^D : number of resources in the depot
 Cap^r : capacity required to carry an equipment
 Cap^C : capacity of the crew
 E : number of resources a crew has at location
 R : required resources to repair a damaged component

4
$$\sum_{\forall n \in N} x_{n,m,c} \mathcal{R}_{m,r} \leq E_{c,m,r}, \forall m, r, c \in C^L$$

5
$$\sum_{\forall r} Cap_r^R E_{c,m,r} \leq Cap_c^C, \forall m, c \in C^L$$

$- M(1 - x_{m,n,c}) \leq E_{c,m,r} - \mathcal{R}_{m,r} - E_{c,n,r} \leq M(1 - x_{m,n,c}),$
 $\forall m \in N \setminus \{\phi_c^1\}, n \in N \setminus \{\phi_c^0, m\}, c \in C^L, r$

6
$$- M(1 - x_{w,n,c}) \leq E_{c,w,r} + Res_{c,w,r}^C - E_{c,n,r} \leq M(1 - x_{w,n,c}),$$

 $\forall w, n \in N \setminus \{\phi_c^0, \phi_c^1, w\}, c \in C^L, r$

$- M(1 - x_{\phi_c^0, n, c}) \leq Res_{c, \phi_c^0, r}^C - E_{c, n, r} \leq M(1 - x_{\phi_c^0, n, c}), \forall n \in N \setminus \{\phi_c^0\}, c \in C^L, r$

7
$$Res_{w,r}^D \geq \sum_{\forall c \in C^L, \phi_c^0 = w} Res_{c, \phi_c^0, r}^C + \sum_{\forall c \in C^L} Res_{c, w, r}^C, \forall w, r$$

Connecting Operation and Routing

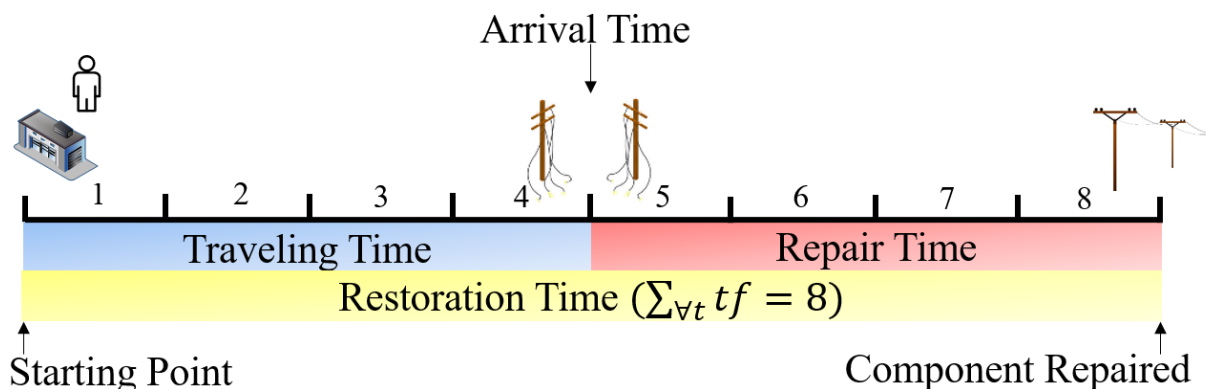
When can we operate the component?

1. Define binary variable f which equals 1 once the line is repaired
2. Calculate the restoration time (Arrival time + Repair time)
3. Set the status of the line ($u_{k,t}$) to 1 once the line is repaired

$$\sum_{\forall t} f_{m,t} = 1 , \forall m \in \Omega_D$$

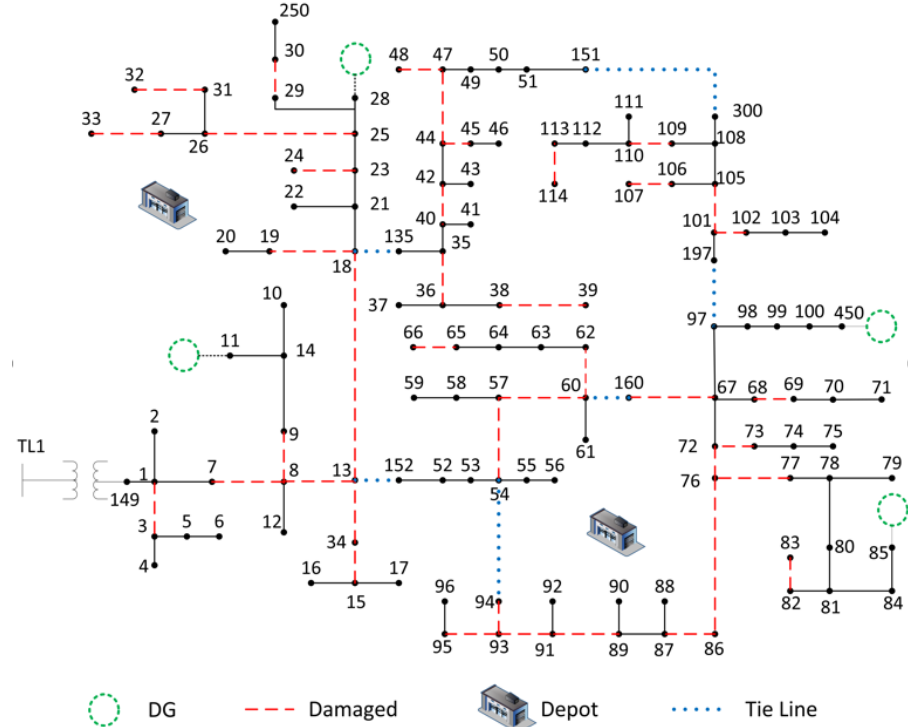
$$\sum_{\forall t} t f_{m,t} \geq \sum_{\forall c} (\alpha_{m,c} + T_{m,c} \sum_{\forall n \in N} x_{m,n,c}), \forall m \in \Omega_D$$

$$u_{m,t} = \sum_{\tau=1}^t f_{m,\tau} , \forall m \in \Omega_{DL}, t$$



Challenges

- VRP is NP-hard, obtaining the optimal solution for large cases is very challenging.
- VRP is commonly solved using heuristic methods.
- Combining VRP with distribution system operation highly increases the complexity.
- Large number of damages:
 - Routing becomes extremely difficult
- E.g. 30 damaged components and 10 crews:
$$x_{m,n,c} \rightarrow 30 \times 30 \times 10 = 9000 \text{ integer variables for routing only}$$
- Computation time is critical!



Proposed Solution Algorithms

- Direct method
 - Use commercial solvers (e.g., CPLEX, GUROBI) to solve the mathematical model
- Priority-based
- Cluster-based (C-DSRRP)
- Assignment-based (A-DSRRP)
- A-DSRRP → Neighborhood Search

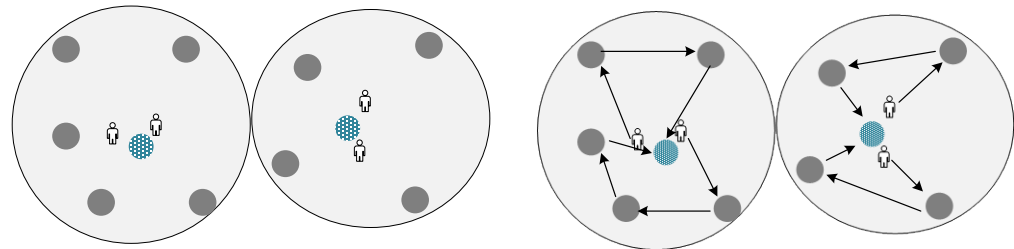
Priority-based

- The goal of this method is to mimic the approach used in practice
- Define the priority of the lines
 1. Repair lines connected to high-priority customers.
Weight factor $W_1 = 10$
 2. Repair 3-phase lines.
Weight factor $W_2 = 5$
 3. Repair single phase lines and individual customers.
Weight factor $W_3 = 1$
- Identify the lines that must be repaired to restore high-priority customers.
 - $\text{Min } \{(\text{number of lines to repair}) | \text{s.t. operation constraints}\}$
- Solve the crew routing problem
 - $\text{Min } \{(\sum_{\forall p} \sum_{k \in L_p} \sum_{c \in C^L} W_p \alpha_{c,k}) | \text{s.t. routing constraints}\}$

L_p :set of lines to repair with priority p

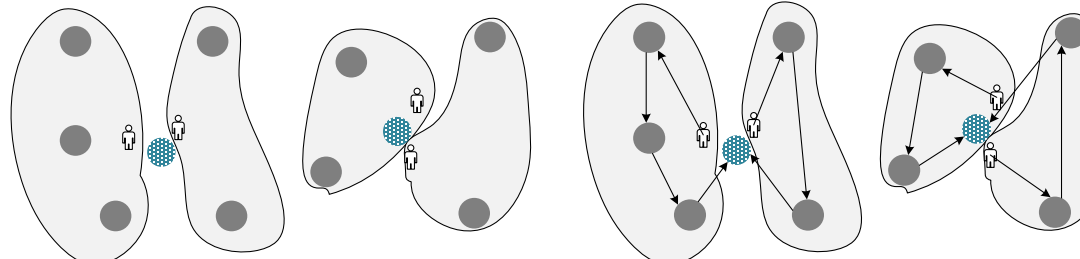
Cluster-based

- Cluster the damaged components to depots.
 - $\min \{(\text{distance between depots and components}) | \text{s.t. resource constraint}\}$
 - C-DSRRP
 - Solve DSRRP with the crews routed based on the clusters.
- VRP problem → Multi-VRP subproblems



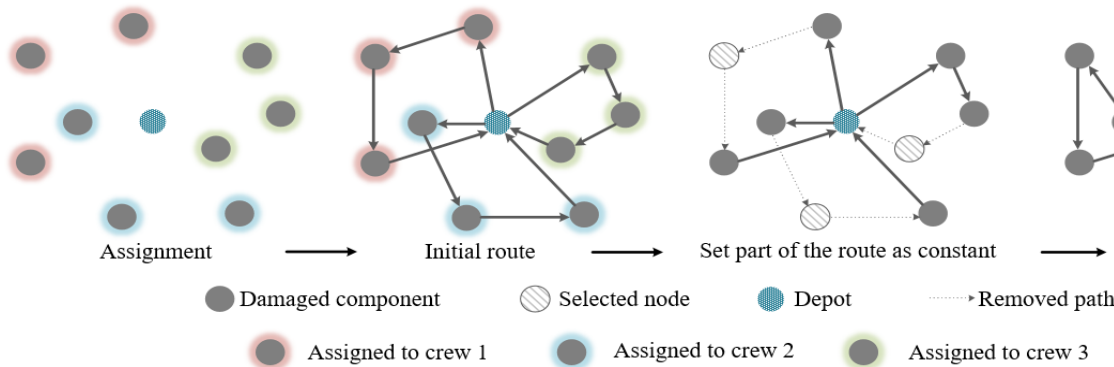
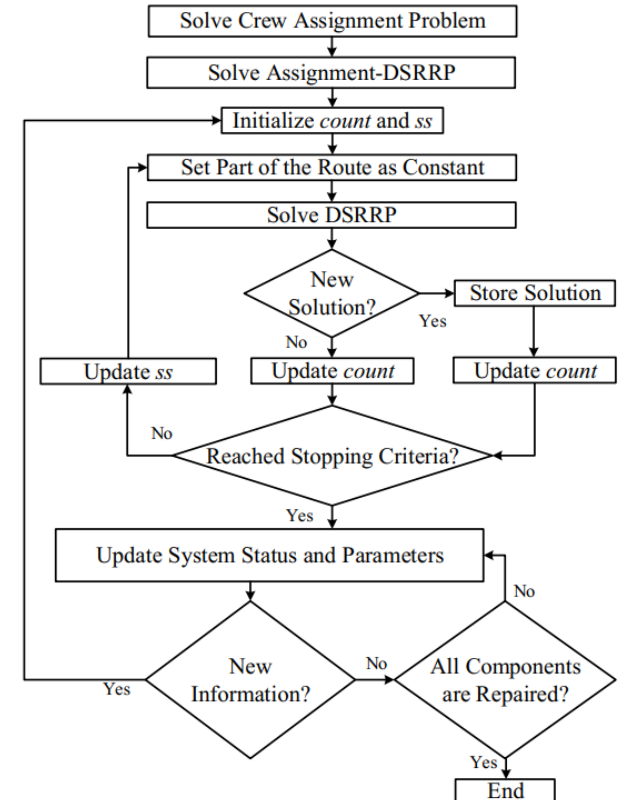
Assignment-based

- Assign the damaged components to crews.
 - $\min \{(\text{distances between components that are assigned to the crews}) | \text{s.t. resource constraint and assignment constraints}\}$
 - A-DSRRP
 - Solve DSRRP with the crews routed based on the assignments.
- VRP problem → Multi-TSP subproblems



Reoptimization (A-DSRRP → Large Neighborhood Search)

1. Select ss nodes (damaged components)
2. Remove part of the route connected to the selected components
3. Set rest of the route to be constant
4. Solve the optimization problem DSRRP (with *warm start* and limit 120 s)
5. Repeat until we reach the stopping criteria (increase ss after $count$ iterations without change)
6. Update the route once new information is obtained

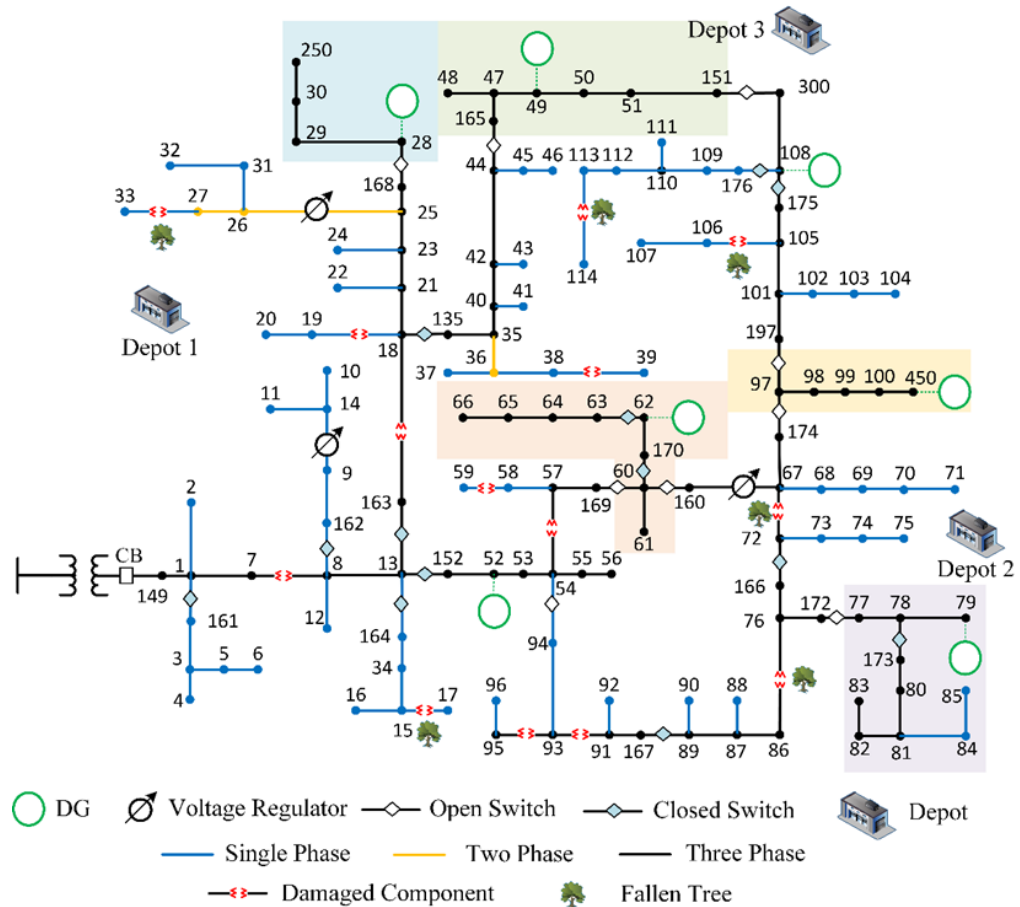


Algorithm

- Use assignment-based approach
- Subproblem I:
 - Assign the damaged components to the crews
 - Consider uncertainty of the repair times
 - Solve using the extensive-form
- Subproblem II
 - Solve stochastic DSRRP with the crews dispatched to the assigned damaged components
 - Use Progressive Hedging to solve the stochastic DSRRP model

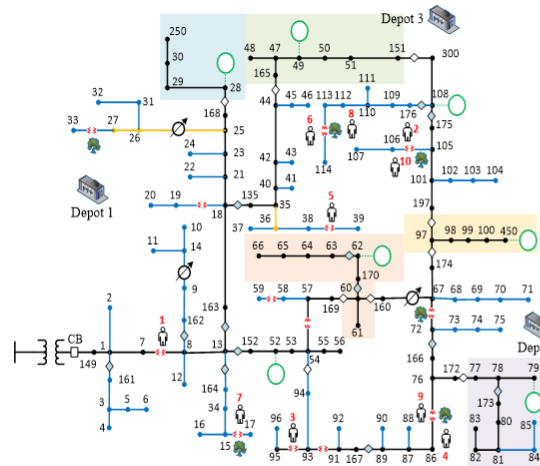
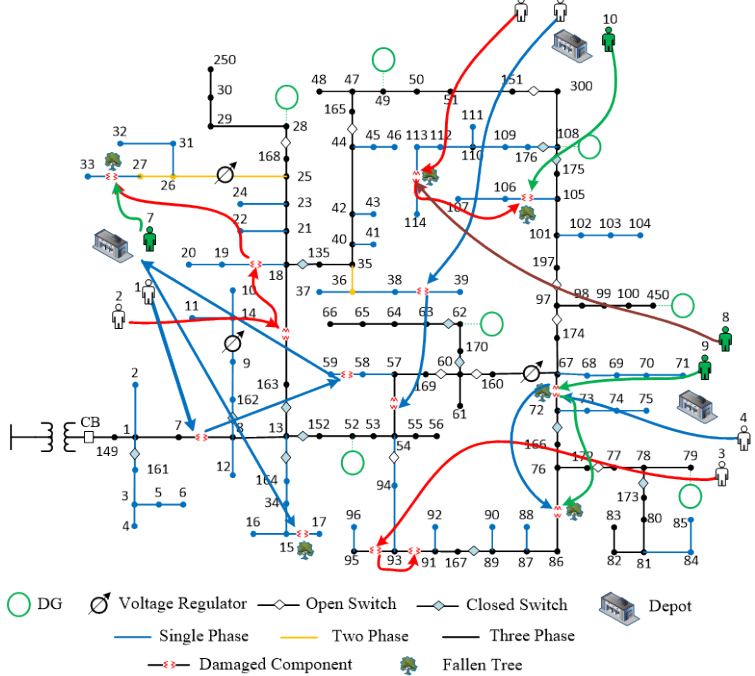
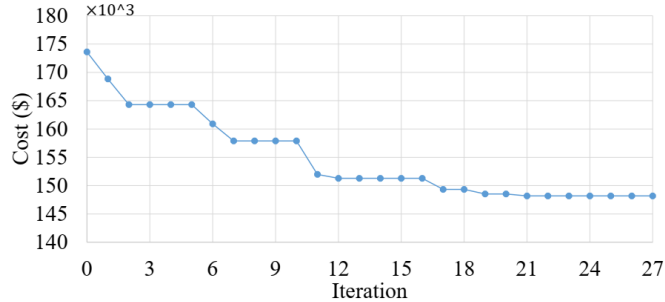
Test Case

- Modified IEEE 123-bus distribution feeder.
- 7 dispatchable DGs and 18 new switches are installed.
- Loads at buses 30, 48, 49, 53, 65, and 76 are critical loads.
- 3 depots, 6 line crews, and 4 tree crews.
- 14 damaged lines.
- Repair times
 - Intensity of the damage is represented by the repair time.
 - Repair time is generated using a truncated lognormal distribution (Z. Zhu 2012).
- Time limit 3600 seconds (Van Hentenryck 2011).
- Solved using AMPL-CPLEX.

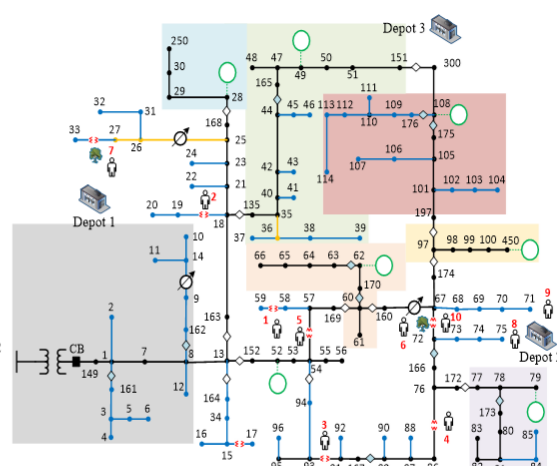


Simulation Results: Re-optimization

- Objective: \$148,185
- Energy served = 62,436 kWh
- All loads are served after 9 hours
- Iterations: 27
- Computation time: 3120 seconds



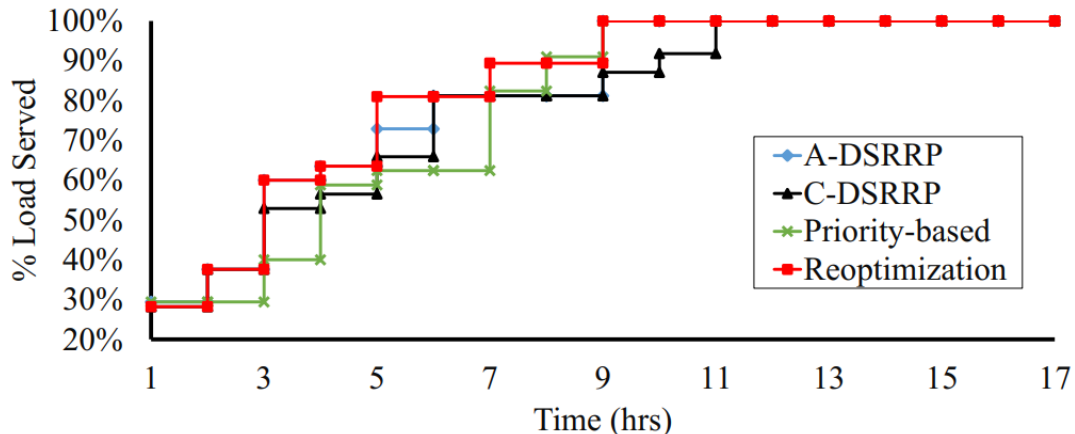
After 2 hours



After 4 hours

Results: Solution Comparison

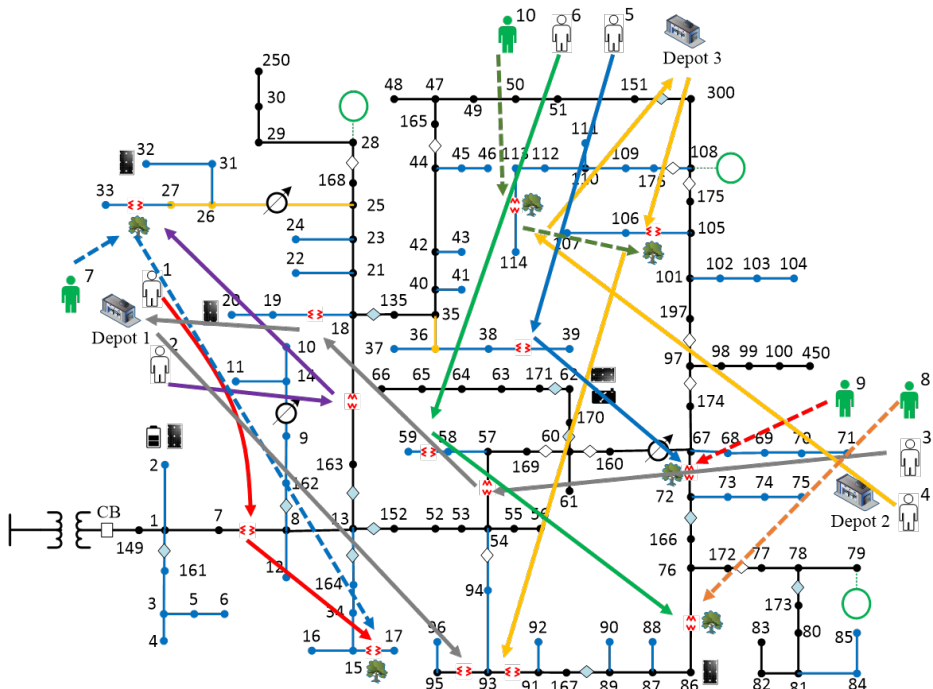
- Optimal solution is obtained by using the Re-optimization solution to warm-start CPLEX and solve the complete method



Test	Damage	Reoptimization			Priority-based		
		Obj.	% Gap	Comp. Time	Obj.	% Gap	Comp. Time
1	15 Lines	\$158,023	0.00%	660 s	\$162,734	2.98%	464 s
2	20 Lines	\$248,986	2.53%	762 s	\$279,197	14.97%	392 s
3	25 Lines	\$388,760	2.27%	782 s	\$467,278	22.93%	520 s

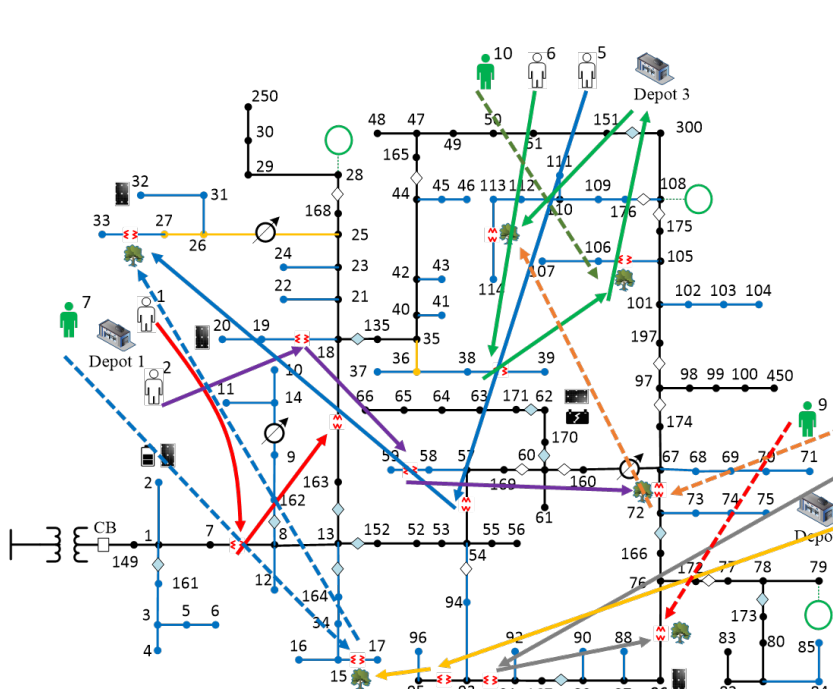
Results: Route Comparison

Reoptimization (optimal) route



○ DG ○ Voltage Regulator ◊ Open Switch ◆ Closed Switch ■ Depot
— Single Phase — Two Phase — Three Phase — Damaged Component
◐ Fallen Tree ◐ On-grid PV ◐ Hybrid system ◐ Grid-forming PV+BESS

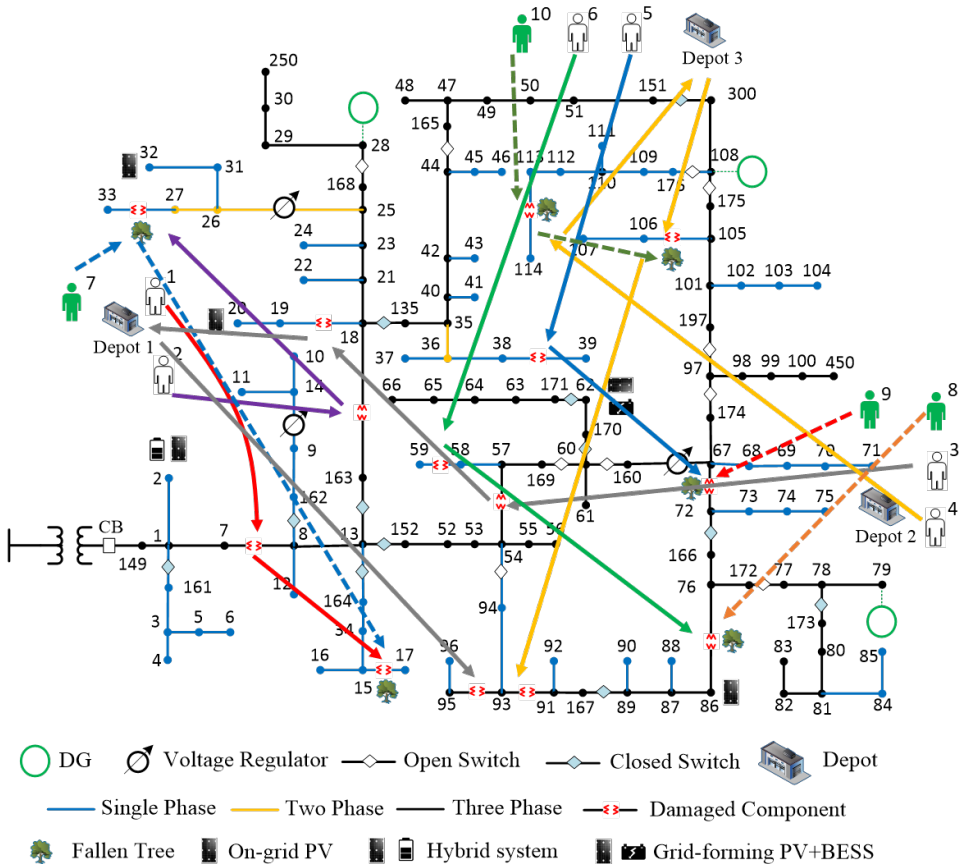
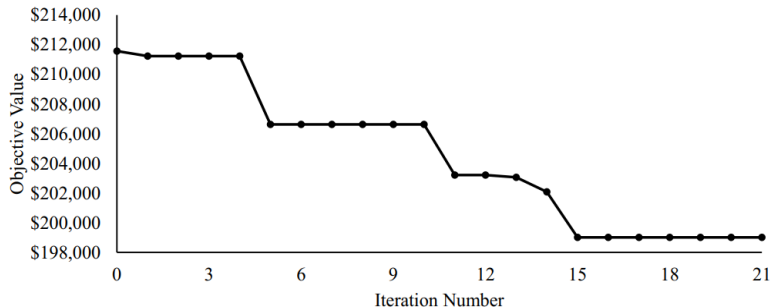
Priority-based route



○ DG ○ Voltage Regulator ◊ Open Switch ◆ Closed Switch ■ Depot
— Single Phase — Two Phase — Three Phase — Damaged Component
◐ Fallen Tree ◐ On-grid PV ◐ Hybrid system ◐ Grid-forming PV+BESS

Results: Re-optimization

- Objective value: \$199,210
- Iterations: 21
- Computation time: 694 seconds



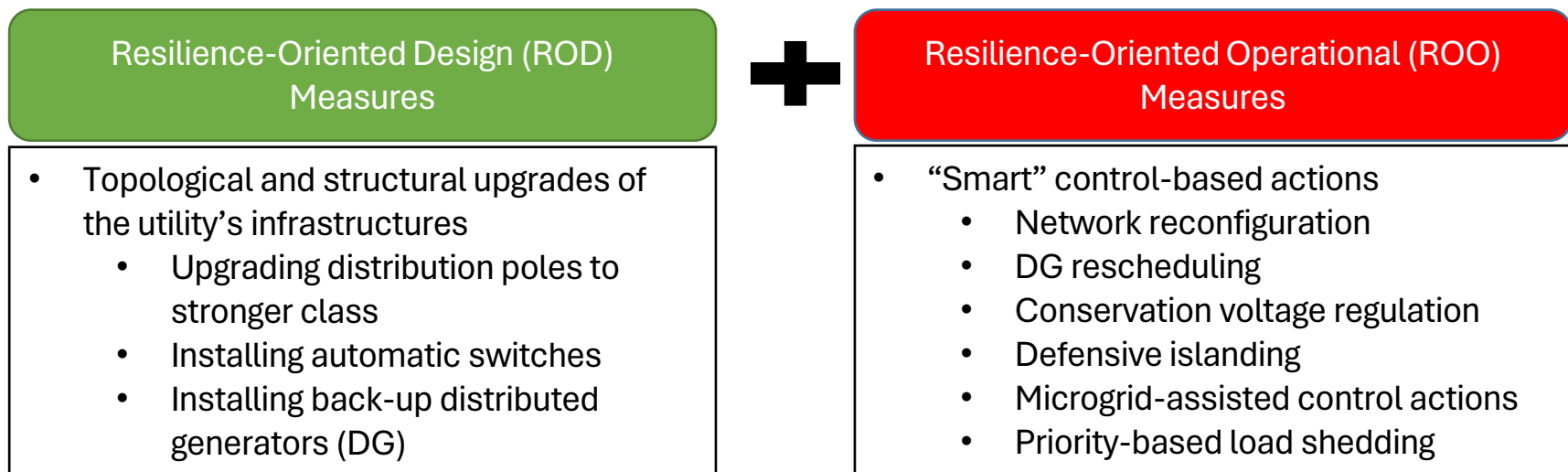
- To show the importance of DGs and automatic switches, we vary the number of DGs and switches for the 14 damage case
- The best performance is obtained with the highest number of DGs and switches, as expected
- Switches are needed so that the DGs reach their full potential

Conclusions

- Effective preparation procedures can ensure that enough equipment is present for repairing the damaged components in the network and facilitate a faster restoration process
- Co-optimizing repair and recovery operation leads to better results compared to solving the two problems separately
- Efficient repair schedule along with DGs and controllable switches limit the outage size and can decrease the restoration time
- Advanced solution algorithms are required for solving the co-optimization problem due to its complexity
- A dynamic approach where the deterministic solution is periodically updated can achieve better solutions than stochastic programming

Introduction: The Resilience Enhancement Measures

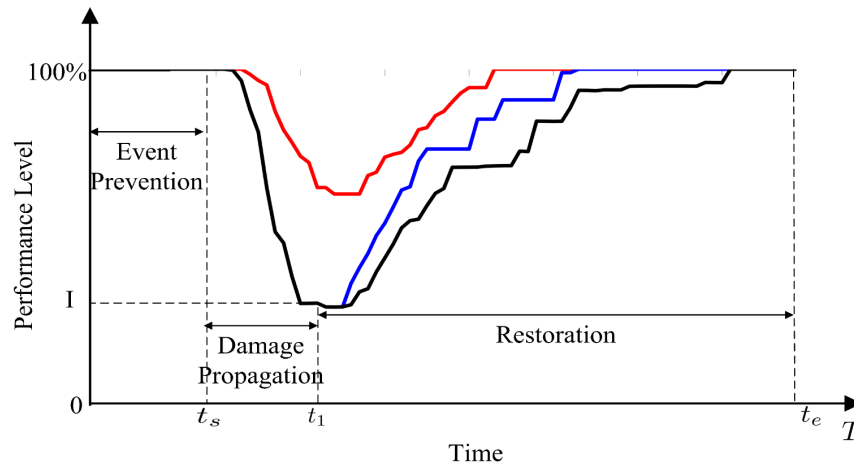
- Two resilience goals of distribution systems [7]:
 - System adaptation (to reduce the impact of future events)
 - System survivability (to maintain an adequate functionality during and after the event)
- Resilience enhancement measures:



Introduction: The Big Picture

A resilient distribution system

- **Planning:** pole hardening, and DG and switch installation
- **Operation:** co-optimization of repair scheduling and restoration operation



How to optimally apply ROD measures to prevent distribution system from extensive damages caused by extreme weather events

- Some *spatial-temporal correlations* exist among ROD decisions, extreme weather events, and system operations
 - Occurrence, intensity and traveling path of events are *uncertain*
 - Physical infrastructure damage status are affected by both extreme weather event and ROD decisions
 - ROD decisions affect system recovery and the associated outage/repair costs

Introduction: The Big Picture

How to optimally apply ROD measures to prevent distribution system from extensive damages caused by extreme weather events

- A *time-varying interaction* exists between structural damages and electric outage propagation
→ Difficult to capture the entire *failure-recovery-cost process* of distribution systems during and after an extreme weather event.

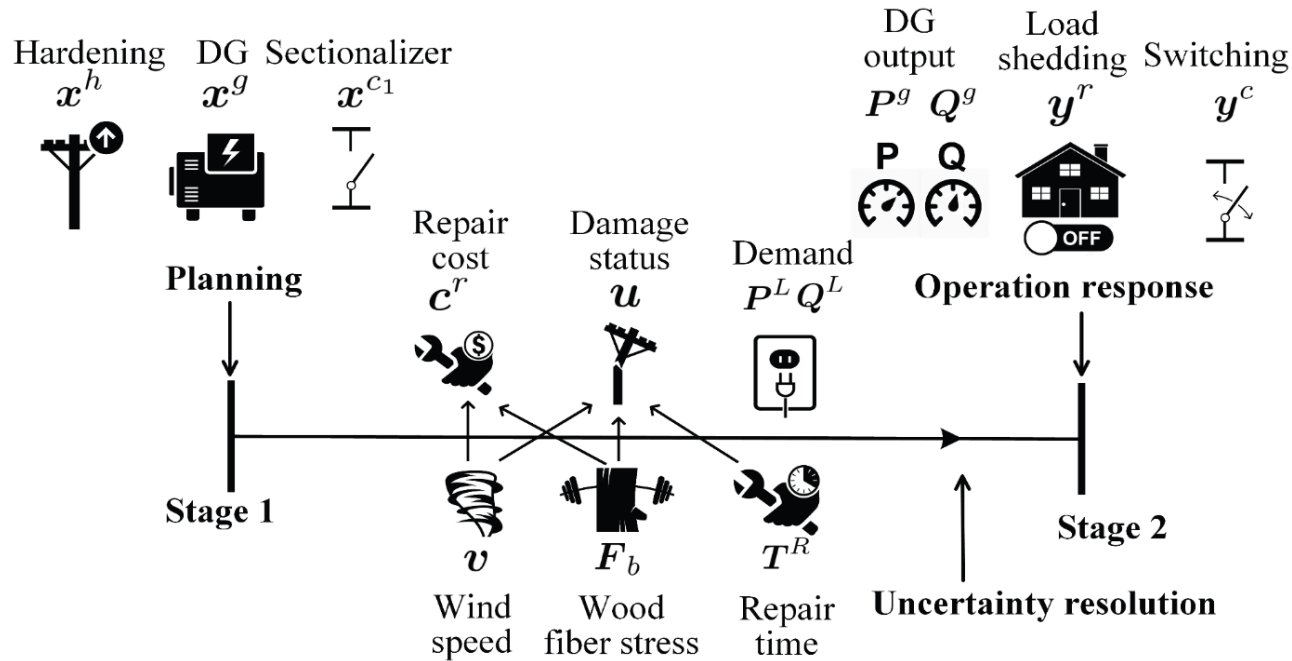
Uncertainty Consideration	Measures	Model/Algorithm
• Use a polyhedral set to represent damage uncertainty	• line hardening	• Robust optimization/column-and-constraint generation algorithm
• Use failure probabilities of distribution lines to represent damage uncertainty set	• Pole hardening • Vegetation management • Combination of both	• Tri-level robust optimization/greedy algorithm
• Use failure probabilities of overhead lines and underground gas pipelines to generate line damage uncertainty set	• Line hardening	• Tri-level robust optimization/column-and-constraint generation algorithm
• Use fragility model to generate line damage uncertainty	• Line hardening • DG placement • Switch Installation	• Two-stage stochastic program/a scenario-based variable neighborhood decomposition search algorithm
• Use fragility model to generate line damage uncertainty	• Line hardening • DG placement • Switch Installation	• Two-stage stochastic program/Progressive hedging algorithm
• Model repair time uncertainty		
• Consider load demand uncertainty		

Research Objective

- Develop a new modeling and solution methodology for the ROD of distribution systems against wind-induced extreme weather events
 - Develop a hybrid stochastic process with a deterministic causal structure to describe the spatio-temporal correlations of ROD decisions and uncertainties
 - Formulate a two-stage stochastic mixed-integer linear program (SMILP) to capture the impacts of ROD decisions and uncertainties on system's responses to extreme weather events
 - Design solution algorithm for solving the above problems.
- Model a hybrid independent stochastic process with a deterministic causal structure to capture the spatiotemporal correlation among the various uncertainties and ROD decisions
 - avoid establishing the high-dimension joint distribution of uncertain variables
 - model the evolving impacts of extreme weather events on physical infrastructures
- Propose a two-stage SMILP to optimally implement multiple ROD measures considering various uncertainties, thus increasing the infrastructure strength and enabling self-healing operations
 - captures the entire failure-recovery process
 - the self-healing operation in the second stage can mimic the outage propagation with minimum service interruption
- Develop a customized DD algorithm to balance optimality and solution efficiency

Overview

- ROD problem is modeled as a two-stage stochastic decision process:
 - Planner makes ROD decisions
 - The operation uncertainties are resolved during the extreme weather event
 - Operator makes the recourse decisions



First-Stage Decisions

- Hardening poles:
 - Strengthening vulnerable components
 - Consider 6 pole types
 - Pole stress
- Installing Backup DGs
 - Increasing adequacy of power supply
- Adding sectionalizers
 - Increasing topological flexibility
 - Can be added at both ends of a line

Uncertainty Modelling

- Consider three groups of random variables that have direct impacts on the evolution of the system operation state
 - Line damage status
 - Repair costs
 - Load demands

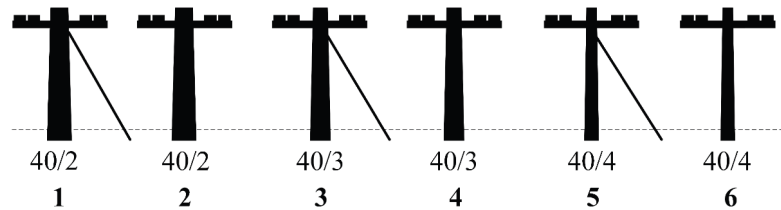


Fig.1. Pole types

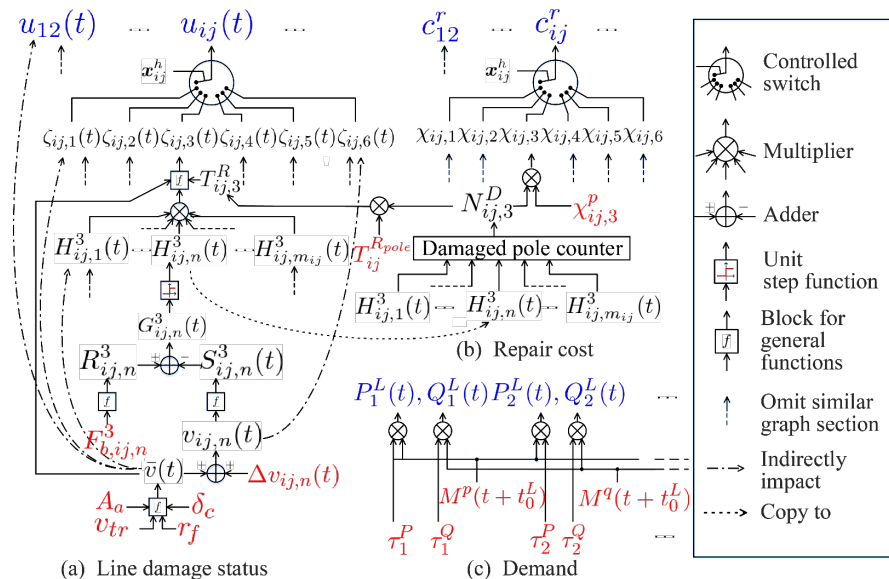
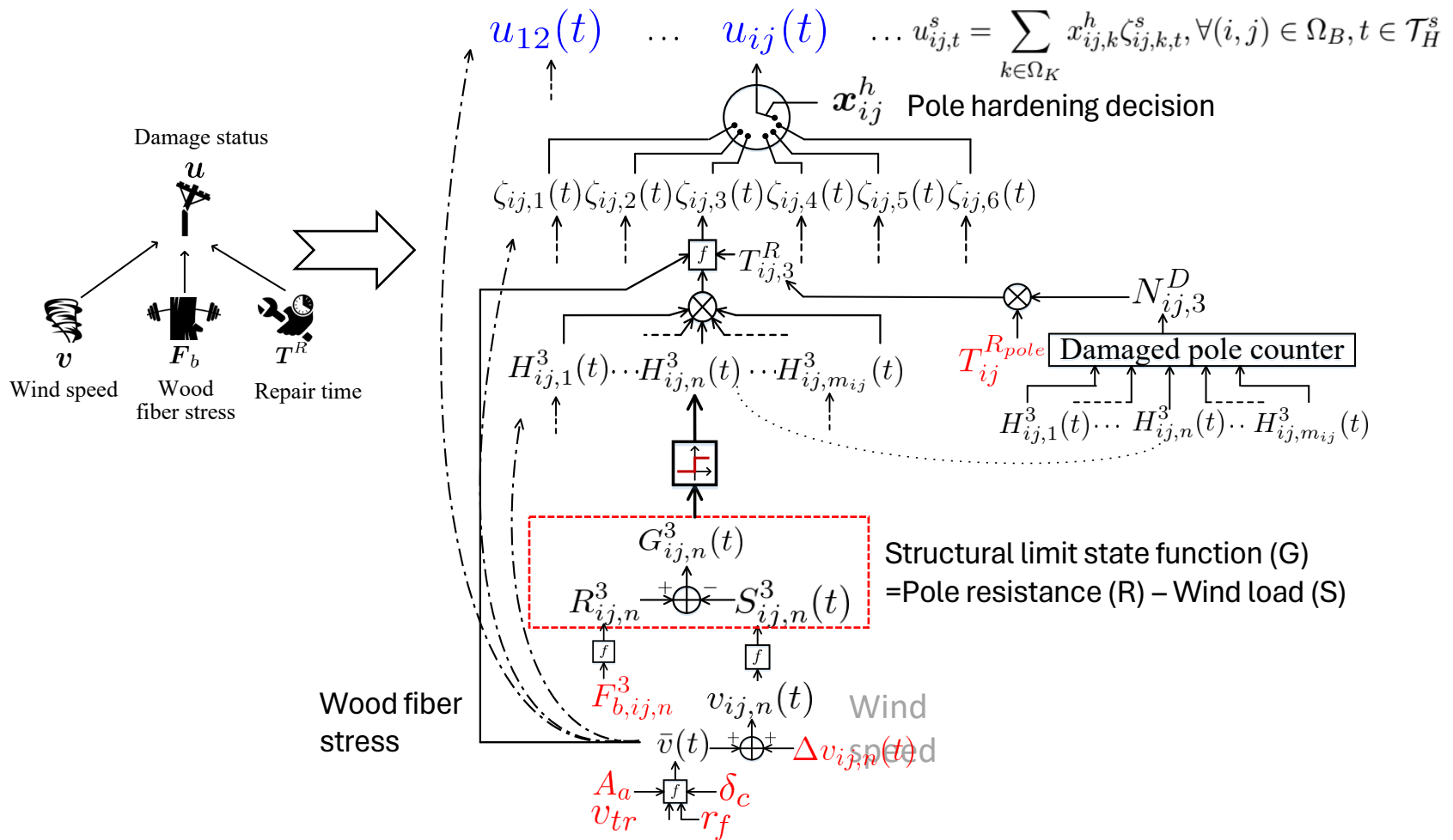
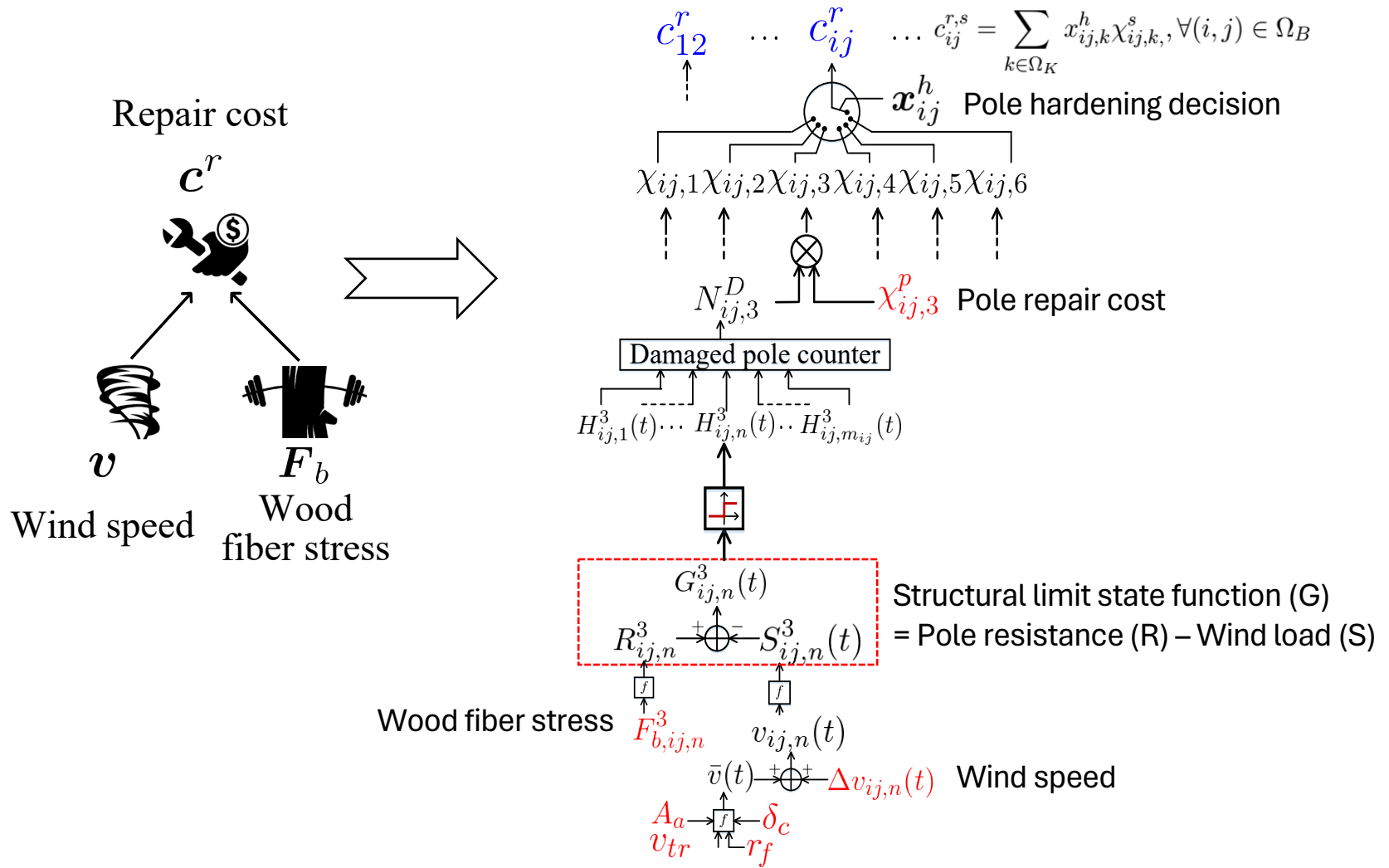


Fig.2. The structure of uncertainty space:
independent observable random variables/processes (highlighted in red) +
deterministic causal connections (parameterized by the first-stage decision)

(a) Line Damage Status Uncertainty



(b) Repair Cost Uncertainty



(c) Load Demand Uncertainty

$$P_i^L(t) = \tau_i^P \cdot M^p(t + t_0^L), \forall i \in \Omega_L, t \in \mathcal{T}_H$$

$$Q_i^L(t) = \tau_i^Q \cdot M^q(t + t_0^L), \forall i \in \Omega_L, t \in \mathcal{T}_H.$$

$$\tau_i^P \sim N(\bar{P}_i, (0.02\bar{P}_i)^2), \forall i \in \Omega_L$$

$$\tau_i^Q \sim N(\bar{Q}_i, (0.02\bar{Q}_i)^2), \forall i \in \Omega_L$$

$$P_1^L(t), Q_1^L(t) P_2^L(t), Q_2^L(t) \dots$$

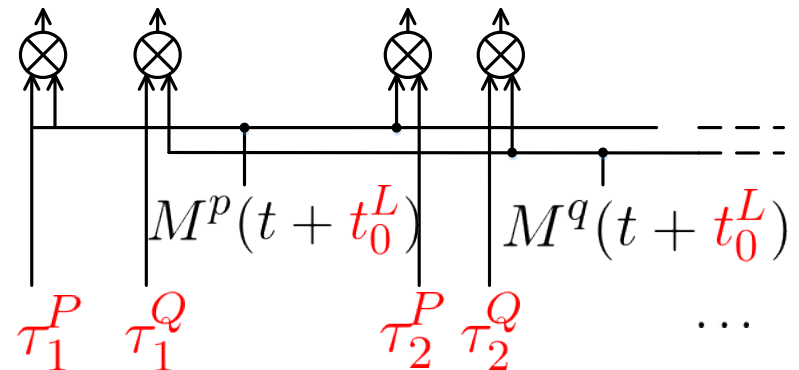


Fig.1. load demand uncertainty

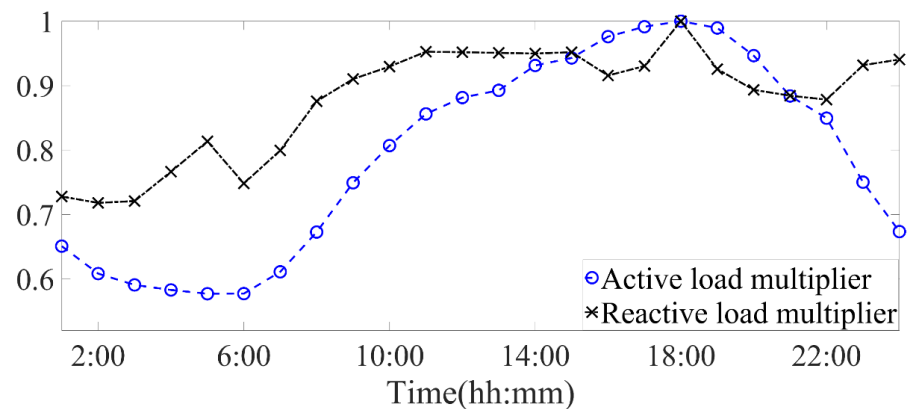
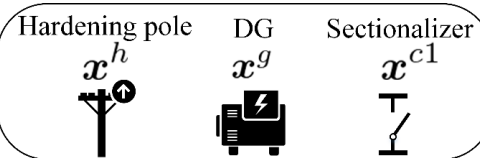


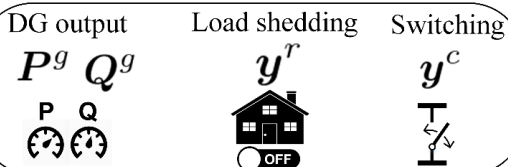
Fig.2. load profile shape at the substation (root node)

Mathematical Representation: Overview

Minimize: Investment Cost
Determine:



Minimize: The costs of the loss of load, DG operation and damage repair
Determine:



- **Investment Stage:** identify the optimal ROD decisions
- **Operation Stage:** achieve self-healing operation
 - need a mathematic formulation to fully model power outage propagation
 - need an analytic optimization to sectionalize a distribution network into multiple self-supplied MGs while maintaining their radial network typologies

Mathematical Representation: First-Stage Formulation

$$\min C_1^I(x^h) + C_1^I(x^g) + C_1^I(x^{c_1}) + w_H \mathbb{E}_{\xi} \phi(x, \xi)$$

s.t.:

Objective:

Minimize the ROD investment cost and the expected cost of the loss of load, DG operation, and damage repair in realized extreme weather events

First stage ROD variables:

x_{ij}^h whether hardening line (i, j) (1) or not (0)
 x_i^g whether installing DG at node i (1) or not (0)

$x_{ij,i}^{c_1}$ whether adding a sectionalizer at the end i of line (i, j) (1) or not (0)

First stage constraints:

$$\sum_{k \in \Omega_K} x_{ij,k}^h = 1, \forall (i, j) \in \Omega_B \quad \text{Hardening strategy limit} \quad \sum_{i \in \Omega_N} x_i^g \leq N_G \quad \text{DG number limit}$$

$$x_{ij,n}^{c_0} + x_{ij,n}^{c_1} = x_{ij,n}^c, \forall (i, j) \in \Omega_B, n \in \{i, j\} \quad \text{Switch installation constraint}$$

$$\mathbb{E}_{\xi} \phi(x, \xi) \cong \sum_{s \in \mathcal{S}} p_r(s) \phi(x, s) \quad \text{The expected cost of the second stage}$$

Second-Stage Problem: Technique Outline (1)

Model the power outage propagation (expressed by a set of constraints)

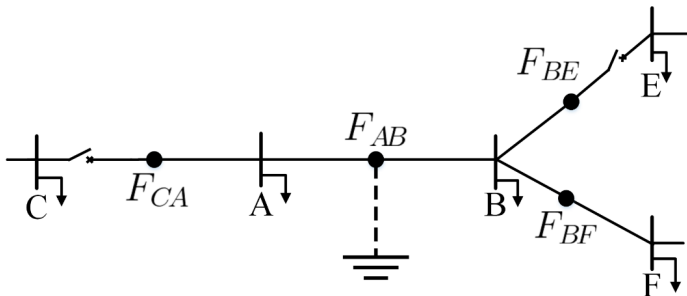


Fig.1. The illustrative example for isolating a fault

- Add a virtual node in the middle of each branch
- Apply a symmetric fault to the virtual node if the line is damaged
- Set the voltage feasible region: $\{0\} \cup [V^{\min}, V^{\max}]$
- Fully curtail a load when its voltage magnitude is zero
- Set loading limits to all branches and penalize load shedding amount in the objective

- Radiality Constraints for each energized networks
 - Graph Theorem [14]: A forest of N nodes has exactly $N - N_C$ edges, where N_C is the number of connected network components.
 - How to obtain N_C in the distribution system
 - Calculate N_C by counting the degree of freedom of voltage angles
 - Formulate a virtual DC optimal power flow (VDCOPF) sub-problem to obtain this degree of freedom
 - the optimal solution of this sub-problem satisfies that the virtual loads in the same energized island are nearly equally distributed at active nodes
 - each energized island has and only has an active node with zero angle
 - The radiality constraint is satisfied *iff* the number of active branches equals the total number of active nodes minus the number of active nodes with zero angles

Second-Stage Formulation

Objective

- Minimize the cost of the loss of load, DG operation, and damage repair in a realized extreme weather event given ROD decisions

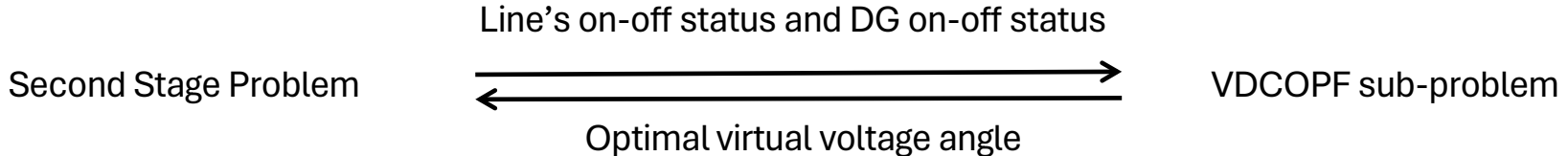
$$\phi(\mathbf{x}, s) = \min \sum_{i \in \Omega_N} \sum_{t \in \mathcal{T}_H^s} c_i^L y_{i,t}^{r,s} P_{i,t}^{L,s} \Delta t + \sum_{i \in \Omega_N} \sum_{t \in \mathcal{T}_H^s} c_i^o P_{i,t}^{g,s} \Delta t + \sum_{(i,j) \in \Omega_B} c_{ij}^{r,s}$$

Constraints

- Distribution system operation
 - Line damage status constraint
 - Line repair cost constraint
 - Line's on-off status constraints (controlled by switch's on-off status)
 - Line flow limits (controlled by line's on-off status)
 - Linearized DistFlow equations (calculate power flow and voltage profile)
 - DG capacity limits
- Fictitious faulting logic constraints (model outage propagation)
 - Virtual node power injection constraints
 - Voltage magnitude limits
 - Load shedding ratio limit
- The minimality condition of VDCOPF sub-problem (obtain the degree of freedom of voltage angle)
- Zero Angle indicator constraint (indicating a node with zero angle)

Key Points

Information passing:



Fictitious faulting logic constraints + Distribution system operation constraints in 1)-3) + Penalty cost of load shedding in objective :

- isolate damaged lines while minimizing the de-energized network parts
- make network constraints such as power flow automatically adapt to the topology after reconfiguration

Radiality Constraints + Zero angle indicator constraint + VDCOPF sub-problem

- can keep each energized network radial

Distribution System Operation Constraints

- 1) Line damage status constraint
- 2) Line repair cost constraint
- 3) Line's on-off status constraints
- 4) Line flow limits
- 5) Linearized DistFlow equations
- 6) DG capacity limits

Binary variables:

$u_{ij,t}^s$ Line damage status

$y_{ij,t}^{c,s}$ Sectionlizer on-off status

$w_{ij,t}^{o,s}$ Line on-off status

- 1
$$u_{ij,t}^s = \sum_{k \in \Omega_K} x_{ij,k}^h \zeta_{ij,k,t}^s, \forall (i, j) \in \Omega_B, t \in \mathcal{T}_H^s$$
- 2
$$c_{ij}^{r,s} = \sum_{k \in \Omega_K} x_{ij,k}^h \chi_{ij,k,t}^s, \forall (i, j) \in \Omega_B$$
- 3
$$\begin{aligned} y_{ij,t}^{c,s} &\leq x_{ij,t}^c, \forall (i, j) \in \Omega_{B_F}, t \in \mathcal{T}_H^s \\ x_{ij,t}^c + y_{ij,t}^{c,s} + 2w_{ij,t}^{o,s} &\geq 2, \forall (i, j) \in \Omega_{B_F}, t \in \mathcal{T}_H^s \\ w_{ij,t}^{o,s} + y_{ij,t}^{c,s} &\leq 1, \forall (i, j) \in \Omega_{B_F}, t \in \mathcal{T}_H^s \\ y_{ij,t}^{c,s}, w_{ij,t}^{o,s} &\in \{0, 1\}, \forall (i, j) \in \Omega_{B_F}, t \in \mathcal{T}_H^s \end{aligned}$$
- 4
$$\begin{aligned} -w_{ij,t}^{o,s} P_{ij}^{\max} &\leq P_{ij,t}^s \leq w_{ij,t}^{o,s} P_{ij}^{\max}, \forall (i, j) \in \Omega_{B_F}, t \in \mathcal{T}_H^s \\ -w_{ij,t}^{o,s} Q_{ij}^{\max} &\leq Q_{ij,t}^s \leq w_{ij,t}^{o,s} Q_{ij}^{\max}, \forall (i, j) \in \Omega_{B_F}, t \in \mathcal{T}_H^s \end{aligned}$$
- 5
$$\begin{aligned} \sum_{\{j | (i,j) \in \Omega_{B_F}\}} P_{ij,t}^s &= P_{i,t}^{g,s} - (1 - y_{i,t}^{r,s}) P_{i,t}^L - \varepsilon_1 V_{i,t}^s, \forall i \in \Omega_N, t \in \mathcal{T}_H^s \\ \sum_{\{j | (i,j) \in \Omega_{B_F}\}} Q_{ij,t}^s &= Q_{i,t}^{g,s} - (1 - y_{i,t}^{r,s}) Q_{i,t}^L, \forall i \in \Omega_N, t \in \mathcal{T}_H^s \\ V_{i,t}^s - \frac{R_{ij}^e P_{ij,t}^s + X_{ij}^e Q_{ij,t}^s}{V_0} - (1 - w_{ij,t}^{o,s}) M_1 &\leq V_{j,t}^s \leq V_{i,t}^s - \\ \frac{R_{ij}^e P_{ij,t}^s + X_{ij}^e Q_{ij,t}^s}{V_0} + (1 - w_{ij,t}^{o,s}) M_1, \forall i &\in \Omega_{N_F}, t \in \mathcal{T}_H^s \end{aligned}$$
- 6
$$\begin{aligned} 0 &\leq P_{i,t}^{g,s} \leq x_i^g P_i^{g,\max}, \forall i \in \Omega_N, t \in \mathcal{T}_H^s \\ 0 &\leq Q_{i,t}^{g,s} \leq x_i^g Q_i^{g,\max}, \forall i \in \Omega_N, t \in \mathcal{T}_H^s \end{aligned}$$

Distribution System Operation Constraints

Fictitious Faulting Logic Constraints

- 1) Virtual node power injection constraints

$$1 \left[\begin{array}{l} -u_{ij,t}^s M_2 \leq \sum_{k \in \{i,j\}} P_{kf_{ij},t}^s + \varepsilon_1 \cdot V_{i,t}^s \leq u_{ij,t}^s M_2, \forall (i,j) \in \Omega_B, f_{ij} \in \Omega_{NF}, t \in \mathcal{T}_H^s \\ -u_{ij,t}^s M_2 \leq \sum_{k \in \{i,j\}} Q_{kf_{ij},t}^s \leq u_{ij,t}^s M_2, \forall (i,j) \in \Omega_B, f_{ij} \in \Omega_{NF}, t \in \mathcal{T}_H^s \end{array} \right]$$

- 2) Voltage magnitude limits

$$2 \left[\begin{array}{l} w_{i,t}^{m,s} V_i^{\min} \leq V_{i,t}^s \leq w_{i,t}^{m,s} V_i^{\max}, \forall i \in \Omega_{NF}, t \in \mathcal{T}_H^s \\ u_{ij,t}^s + w_{f_{ij},t}^{m,s} \leq 1, \forall (i,j) \in \Omega_B, f_{ij} \in \Omega_F, t \in \mathcal{T}_H^s \\ w_{i,t}^{m,s} \in \{0, 1\}, \forall i \in \Omega_{NF}, t \in \mathcal{T}_H^s \end{array} \right]$$

- 3) Load shedding ratio limit

$$3 \left[1 - w_{i,t}^{m,s} \leq y_{i,t}^{r,s} \leq 1, \forall i \in \Omega_N, t \in \mathcal{T}_H^s \right]$$

Radiality constraints

- 1) Radiality constraint

$$1 \left[\sum_{(i,j) \in \Omega_{BF}} w_{ij,t}^{b,s} = \sum_{i \in \Omega_{NF}} w_{i,t}^{m,s} - \sum_{i \in \Omega_{NF}} w_{i,t}^{a,s} \right]$$

- 2) Active branch identification constraint

$$2 \left[\begin{array}{l} w_{ij,t}^{o,s} + w_{i,t}^{m,s} - 1 \leq w_{ij,t}^{b,s} \leq 0.5w_{ij,t}^{o,s} + 0.5w_{i,t}^{m,s}, \forall i \in \Omega_{NF}, (i,j) \in \Omega_{BF}, t \in \mathcal{T}_H^s \\ w_{i,t}^{a,s}, w_{ij,t}^{b,s} \in \{0, 1\}, \forall i \in \Omega_{NF}, (i,j) \in \Omega_{BF}, t \in \mathcal{T}_H^s \end{array} \right]$$

Zero angle indicator constraint

$$w_{i,t}^{a,s} - 1 \leq \frac{1}{2|\Omega_{NF}|} (\mu_{d,i,t}^s - 1 + \varepsilon_3) \leq w_{i,t}^{a,s}, \forall i \in \Omega_N, t \in \mathcal{T}_H^s$$

Binary variables:

$w_{i,t}^{m,s}$	active node	$w_{i,t}^{b,s}$	active branch
$w_{i,t}^{a,s}$	node with zero voltage angle		

The Minimality Condition of VDCOPF Sub-problem

To realize that a connected network component (healthy MG) has one and only one degree of freedom of voltage angle under the condition of full DC power flow equations

$$\begin{aligned} \left(\mathcal{P}_{L,t}^{s,*}, \mathcal{P}_{l,t}^{s,*}, \theta_t^{s,*} \right) = \arg \min_{\mathcal{P}_{L,t}^s, \mathcal{P}_{l,t}^s, \theta_t^s} & \left\{ \sum_{i \in \Omega_{N_F}} (\theta_{i,t}^s + \frac{\alpha_L}{2} (\mathcal{P}_{L,i,t}^s)^2) \right. \\ a : & -(1 - w_{ij,t}^{o,s}) M_3 \leq \mathcal{P}_{ij,t}^s - S_0 B'_{ij} (\theta_{i,t}^s - \theta_{j,t}^s) \\ & \leq (1 - w_{ij,t}^{o,s}) M_3, \forall (i,j) \in \Omega_{B_F} \\ \text{s.t. } b : & -w_{ij,t}^{o,s} M_3 \leq \mathcal{P}_{ij,t}^s \leq w_{ij,t}^{o,s} M_3, \forall (i,j) \in \Omega_{B_F} \\ c : & \sum_{\{j | (i,j) \in \Omega_{B_F}\}} \mathcal{P}_{ij,t}^s - P_{i,t}^{g,s} + \mathcal{P}_{L,i,t}^s = 0, \forall i \in \Omega_{N_F} \\ d : & -\theta_{i,t}^s \leq 0, \quad \forall i \in \Omega_{N_F} \\ e : & -\mathcal{P}_{L,i,t}^s \leq 0, \quad \forall i \in \Omega_{N_F} \\ & \left. \forall t \in \mathcal{T}_H^s \right\}, \end{aligned}$$

KKT Optimality Condition:

Primal feasibility

$$\begin{aligned} -(1 - w_{ij,t}^{o,s}) M_3 \leq \mathcal{P}_{ij,t}^{s,*} - S_0 B'_{ij} (\theta_{i,t}^{s,*} - \theta_{j,t}^{s,*}) \leq (1 - w_{ij,t}^{o,s}) M_3, \\ \forall (i,j) \in \Omega_{B_F}, t \in \mathcal{T}_H^s \\ -w_{ij,t}^{o,s} M_3 \leq \mathcal{P}_{ij,t}^{s,*} \leq w_{ij,t}^{o,s} M_3, \forall (i,j) \in \Omega_{B_F}, t \in \mathcal{T}_H^s \\ \sum_{\{j | (i,j) \in \Omega_{B_F}\}} \mathcal{P}_{ij,t}^{s,*} - P_{i,t}^{g,s} + \mathcal{P}_{L,i,t}^{s,*} = 0, \forall i \in \Omega_{N_F}, t \in \mathcal{T}_H^s \end{aligned}$$

On-off line status

$$\begin{aligned} -(1 - w_{ij,t}^{o,s}) M_4 \leq \lambda_{a,ij,t}^s \leq (1 - w_{ij,t}^{o,s}) M_4, \forall i \in \Omega_{N_F}, t \in \mathcal{T}_H^s \\ -w_{ij,t}^{o,s} M_4 \leq \lambda_{b,ij,t}^s \leq w_{ij,t}^{o,s} M_4, \quad \forall i \in \Omega_{N_F}, t \in \mathcal{T}_H^s \end{aligned}$$

Complementary slackness and dual feasibility

$$\begin{aligned} 0 \leq \mu_{d,i,t}^s \perp \theta_{i,t}^{s,*} \geq 0, & \quad \forall i \in \Omega_{N_F}, t \in \mathcal{T}_H^s \\ 0 \leq \mu_{e,i,t}^s \perp \mathcal{P}_{L,i,t}^{s,*} \geq 0, & \quad \forall (i,j) \in \Omega_{N_F}, t \in \mathcal{T}_H^s \end{aligned}$$

Stationarity

$$\begin{aligned} \partial \mathcal{L} / \partial \mathcal{P}_{L,i,t}^{s,*} : \alpha_L \mathcal{P}_{L,i,t}^{s,*} + \lambda_{c,i,t}^s - \mu_{e,i,t}^s = 0, \forall i \in \Omega_{N_F}, t \in \mathcal{T}_H^s \\ \partial \mathcal{L} / \partial \mathcal{P}_{ij,t}^{s,*} : -\lambda_{a,ij,t}^s + \lambda_{b,ij,t}^s + \lambda_{c,i,t}^s - \lambda_{c,j,t}^s = 0, \\ \forall (i,j) \in \Omega_{B_F}, t \in \mathcal{T}_H^s \\ \partial \mathcal{L} / \partial \theta_{i,t}^{s,*} : \sum_{\{j | (i,j) \in \Omega_{B_F}\}} \lambda_{a,ij,t}^s B_{ij} S_0 + 1 - \mu_{d,i,t}^s = 0, \\ \forall i \in \Omega_{N_F}, t \in \mathcal{T}_H^s \end{aligned}$$

Dual Decomposition Algorithm

- A Compact Notation Form of ROD Model

$$z = \min \left\{ \mathbf{c}^\top \mathbf{x} + \sum_{s \in S} p_r(s) \mathbf{q}^\top \mathbf{y}^{R,s} : (\mathbf{x}, \mathbf{y}^{R,s}) \in \mathbf{K}^s, \forall s \in S \right\}$$

where $\mathbf{K}^s = \left\{ (\mathbf{x}, \mathbf{y}^{R,s}) : \mathbf{A}\mathbf{x} = \mathbf{b}, \mathbf{T}(s)\mathbf{x} + \mathbf{W}(s)\mathbf{y}^{R,s} = \mathbf{h}(s), \mathbf{x} \in \{0, 1\}, \mathbf{y}^{R,s} = (\mathbf{y}_B^s, \mathbf{y}_C^s), \mathbf{y}_B^s \in \{0, 1\}, \mathbf{y}_C^s \geq 0 \right\}, \forall s \in S$

- To induce a scenario-based decomposable structure, the copies of the first-stage variables \mathbf{x} are introduced to create the following reformulation

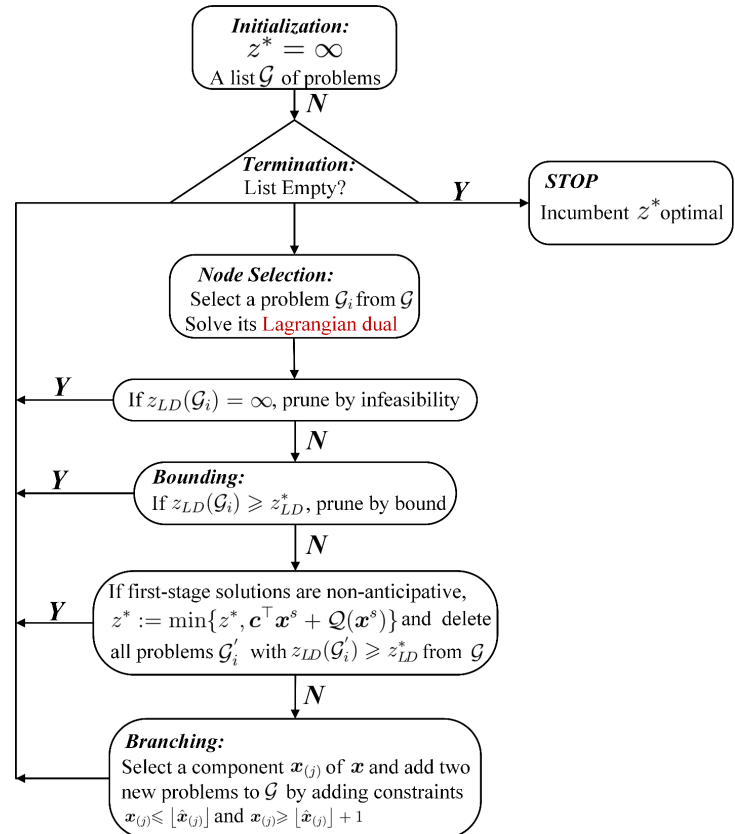
$$z = \min \left\{ \sum_{s \in S} p_r(s) (\mathbf{c}^\top \mathbf{x}^s + \mathbf{q}^\top \mathbf{y}^{R,s}) : \mathbf{x}^1 = \dots = \mathbf{x}^{|S|}, (\mathbf{x}^s, \mathbf{y}^{R,s}) \in \mathbf{K}^s, \forall s \in S \right\}$$

- The Lagrangian relaxation with respect to the nonanticipativity constraint

$$L(\boldsymbol{\mu}) = \sum_{s \in S} L_s(\boldsymbol{\mu}^s) = \sum_{s \in S} \min_{\mathbf{x}^s, \mathbf{y}^{R,s}} \left\{ p_r(s) (\mathbf{c}^\top \mathbf{x}^s + \mathbf{q}^\top \mathbf{y}^{R,s}) + \boldsymbol{\mu}^s \mathbf{x}^s : (\mathbf{x}^s, \mathbf{y}^{R,s}) \in \mathbf{K}^s \right\}$$

- The lower bound of the Lagrangian relaxation:

$$z_{LD} = \max_{\boldsymbol{\mu}} \left\{ \sum_{s \in S} L_s(\boldsymbol{\mu}^s) : \sum_{s \in S} \boldsymbol{\mu}^s = 0 \right\}$$



Case Study

TABLE II
THE INVESTMENT COST OF DIFFERENT ROD METHODS

#No.	Methods	Cost(\$)
1	Upgrading pole class	6,000/pole
2	Adding transverse guys to pole	4,000/pole
3	The combination of upgrading and guying pole	10,000/pole
3	Installing a natural gas-fired CHPs as DG with 400kW capacity	1,000/kW
4	Adding an automatic sectionlizer	15,000

*Assume the span of two consecutive poles is 150 ft.

- The IEEE 123-bus system is mapped into a coastal city in Texas.
- The repair cost of a single pole for 6 pole types is assumed to be the same $\chi_{ij,1}^p = \dots = \chi_{ij,6}^p = \4000
- Consider the budget limitation, the total number of backup DGs is limited to be 5
- The total investment cost is \$5,048,000

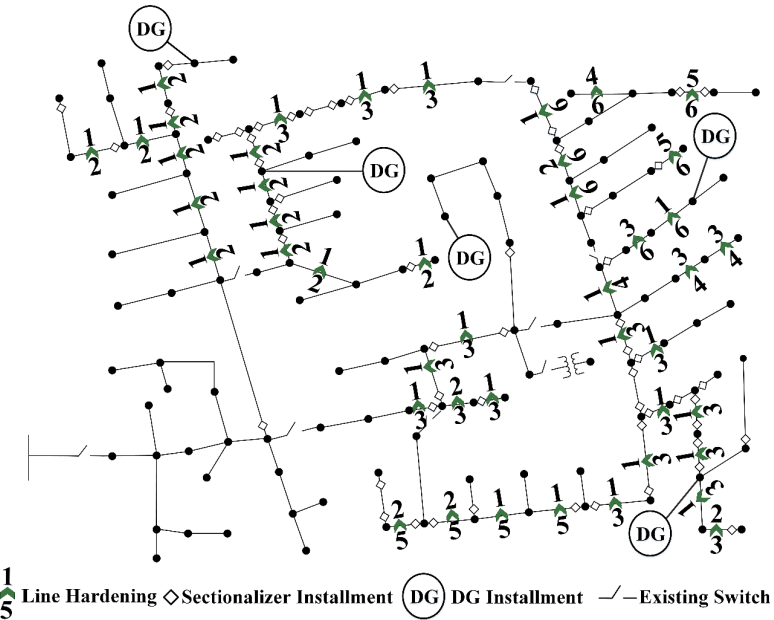
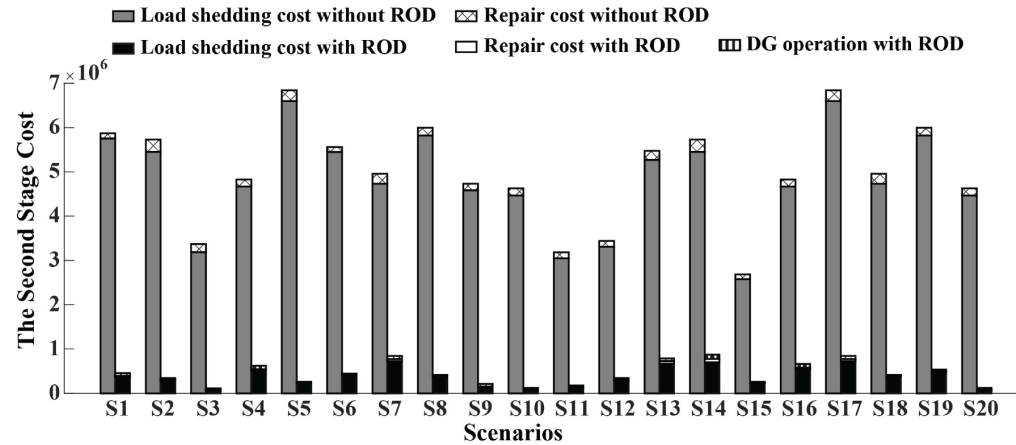


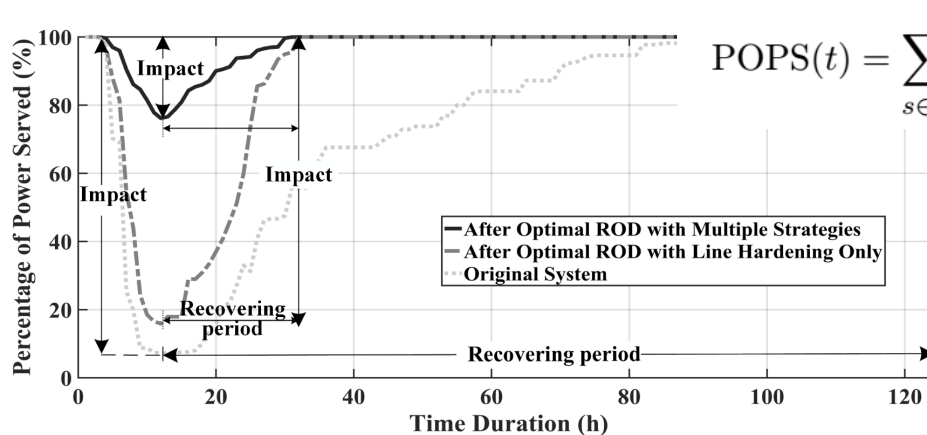
Fig.1. The optimal ROD methods implementation

Case 1: Comparison with and without ROD

- Compare the second stage cost from the hurricane hits the system to the point when all damaged lines are repaired



- The expected second-stage cost with optimal ROD is 8.93% of that without ROD
- Compare the system resilience by the resilience curve, which can be expressed by the percentage of power-served (POPS(t)):



$$\text{POPS}(t) = \sum_{s \in \mathcal{S}} p_r(s) \frac{\sum_{i \in \Omega_N} (1 - y_{i,t}^{r,s}) P_{i,t}^{L,s}}{\sum_{i \in \Omega_N} P_{i,t}^{L,s}}, \forall t \in \mathcal{T}_H$$

Case 2: The Self-healing Operation Case

- To validate the novelty of our MILP formulation strategy to solve the challenges of self-healing operation

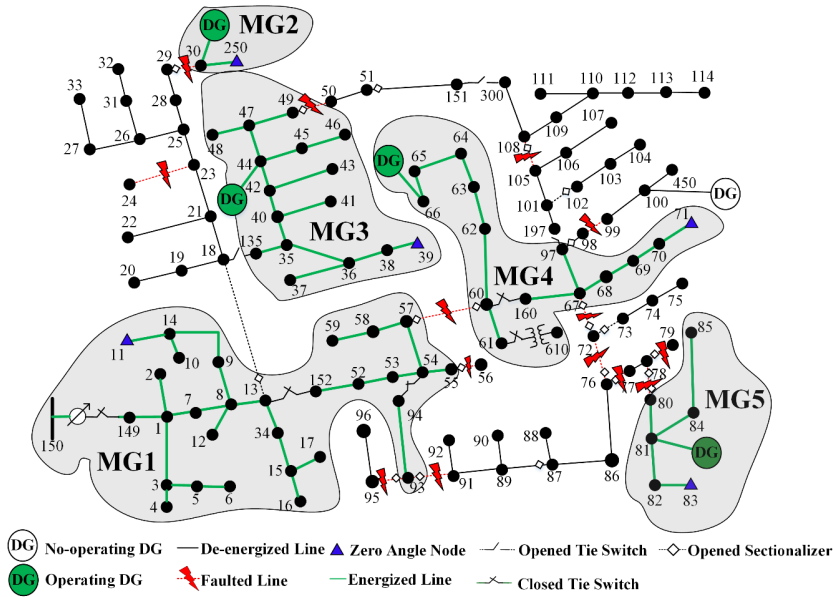


Fig.1. System's self-healing operation at $t = 10$

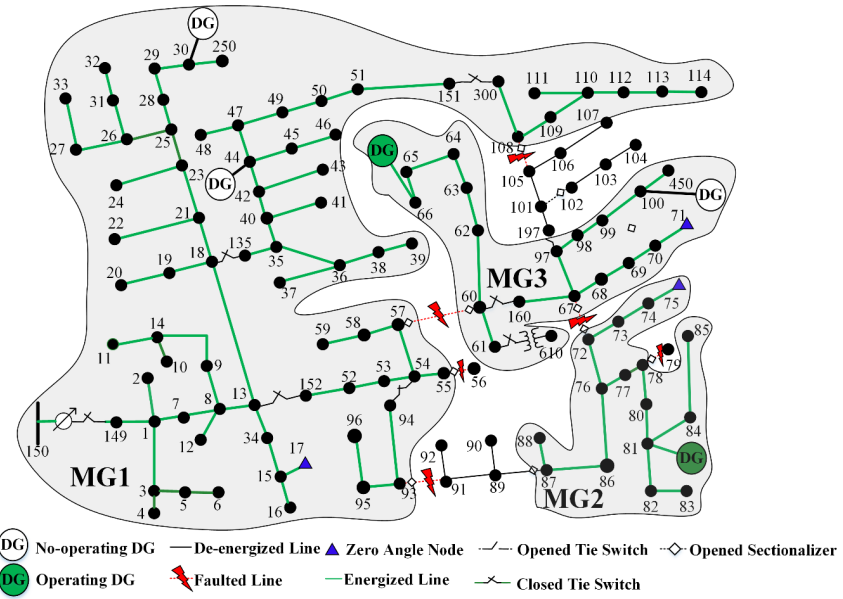


Fig.2. System's self-healing operation at $t = 21$

Conclusions

A new modeling and solution methodology for resilience-oriented design (ROD) of power distribution systems against wind-induced climatic hazards is proposed

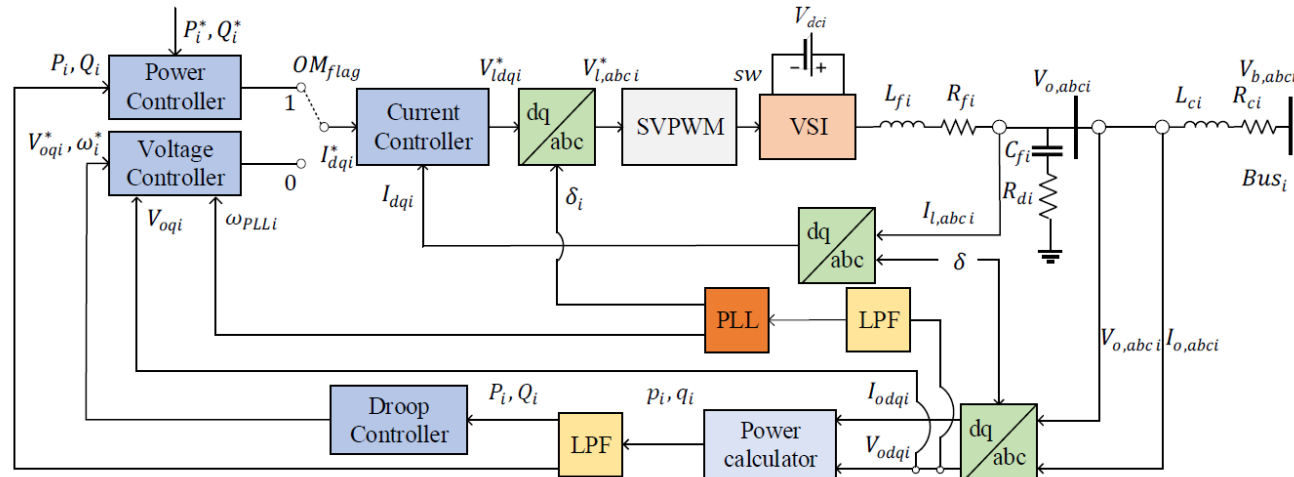
- The spatial-temporal correlations among ROD decisions, uncertainty space, and system operations during and after extreme weather events are well explored and established
- A two-stage stochastic mixed-integer model is proposed with the objective to minimize the investment cost in the first-stage and the expected costs of the loss of loads, repairs and DG operations in the second stage.
- A scenario-based dual composition algorithm is developed to solve the proposed model
- Numerical studies on the 123-bus distribution system demonstrate the effectiveness of optimal ROD on enhancing the system resilience

Advanced Topics in Distribution System Modelling

- Conservative Voltage Reduction (CVR) and Volt- Var Optimization
- Distribution System Resilience
- Microgrid – Dynamic Modelling and Control
 - Background of Microgrids Modeling
 - Mathematical Modeling of Inverter-Dominated Microgrids
 - Reduced-Order Small-Signal Model of Inverter-Dominated Microgrids

Background of Microgrids Modeling

- Microgrids as the main building blocks of smart grids are small scale power systems that facilitate the effective integration of distributed energy resources (DERs).
- In normal operation, the microgrid is connected to the main grid. In the event of disturbances, the microgrid disconnects from the main grid and goes to the islanded operation.
- In the islanded mode operation of a microgrid, a part of the distributed network becomes electrically separated from the main grid, while loads are supported by local DERs. Such DERs are typically power electronic based, making the full system complex to study.
- A detailed mathematical model of microgrids is important for stability analysis, optimization, simulation studies and controller design.



- $OM_{flag} = 1$: the microgrid is operated in grid-tied mode
- $OM_{flag} = 0$: the microgrid is operated in islanded mode

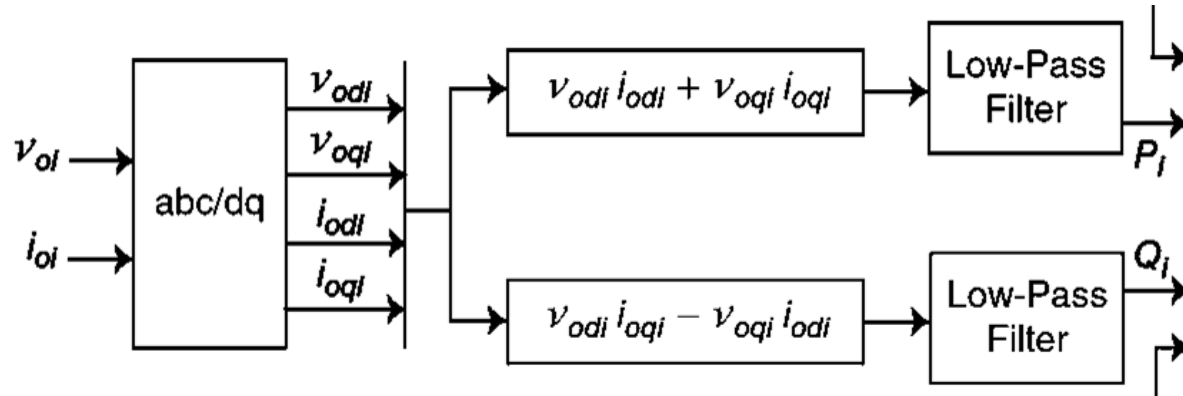
Mathematical Model of Microgrid

- a) Average Power Calculation: The generated active and reactive power can be calculated using the transformed output voltage V_{odq} and current I_{odq} . The average power generated by the inverter is

$$p = (v_{odi} i_{odi} + v_{oqi} i_{oqi}),$$
$$q = (v_{oqi} i_{odi} - v_{odi} i_{oqi}).$$

Using a low-pass filter (LPF) with the corner frequency ω_c , we can obtain the filtered instantaneous powers as follows,

$$\dot{P} = -P\omega_c + \omega_c(v_{odi} i_{odi} + v_{oqi} i_{oqi}),$$
$$\dot{Q} = -Q\omega_c + \omega_c(v_{oqi} i_{odi} - v_{odi} i_{oqi}).$$



Mathematical Model of Microgrid

- b) Phase Locked Loop: The phase lock loop (PLL) is used to measure the actual frequency of the system. According to [1], the PLL input is the d-axis component of the voltage measured across the filter capacitor (Fig. 4).

The mathematical model of PLL is represented as follows,

$$\dot{v}_{odf} = \omega_{cPLL} v_{od} - \omega_{cPLL} v_{odf}, \quad (3a)$$

$$\dot{\phi}_{PLL} = -v_{odf}. \quad (3b)$$

In grid-tied mode, the inverter output phase is synchronized to the main grid using PLL, therefore the derivative of phase angle δ is set to ω_{PLL} :

$$\dot{\delta} = \omega_{PLL} = 377 - k_{p,PLL} v_{odf} + k_{i,PLL} \varphi_{PLL}. \quad (4)$$

In islanded mode, the phase angle of the first inverter can be arbitrarily set as the reference for the other inverters:

$$\dot{\delta}_i = \omega_{PLL1} - \omega_{PLLi} \quad i = 1, \dots, n. \quad (5)$$

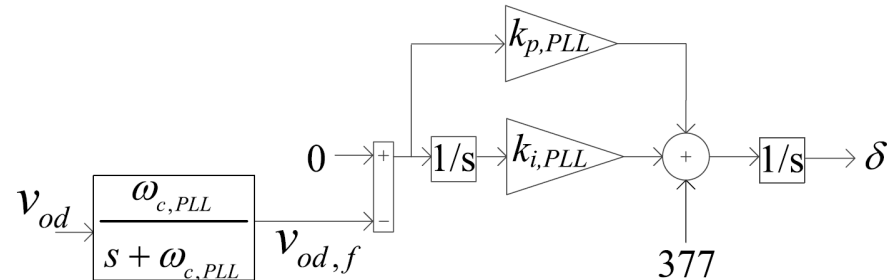


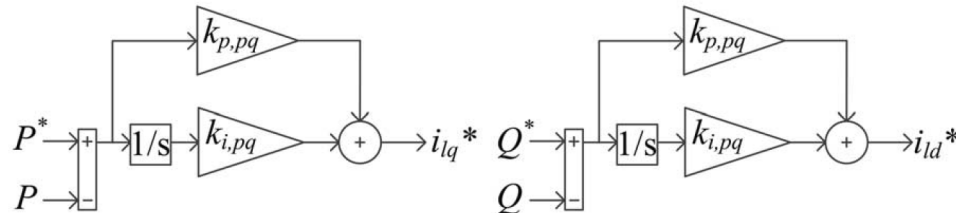
Fig. 3. The diagram of PLL used for DER.

[1] M. Rasheduzzaman, J. A. Mueller, and J. W. Kimball, "An accurate small-signal model of inverter-dominated islanded microgrids using dq reference frame," IEEE J. Emerg. Sel. Topics Power Electron., vol. 2, no. 4, pp. 1070–1080, Dec. 2014.

Mathematical Model of Microgrid

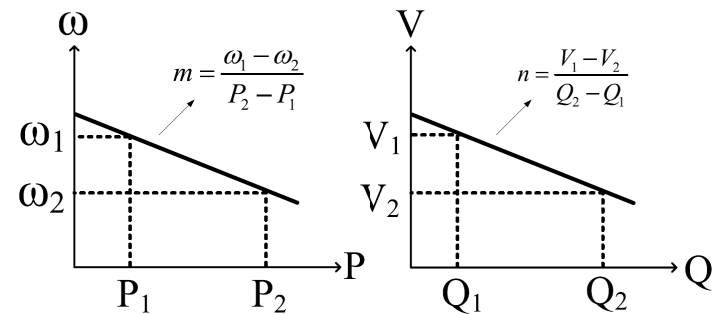
- c) Power Controller: In grid-tied mode, the output power of DER is regulated by the power controller using PI control method. The input references are the commanded real and reactive powers:

$$\begin{aligned}\dot{\phi}_P &= P - P^* & i_{lq}^* &= k_{i,pq}\varphi_P + K_{p,pq}\dot{\phi}_P \\ \dot{\phi}_Q &= Q - Q^* & i_{ld}^* &= k_{i,pq}\varphi_Q + K_{p,pq}\dot{\phi}_Q\end{aligned}$$



- d) Droop Controllers: In grid-connected mode, the inverter's output voltage is set by the grid voltage magnitude. The PLL ensures proper tracking of grid phase so that inverter output remains synchronized to the grid. In islanded mode, a DER has no reference inputs from the main grid. Therefore, it must generate its own voltage and frequency references using droop controllers as follows,

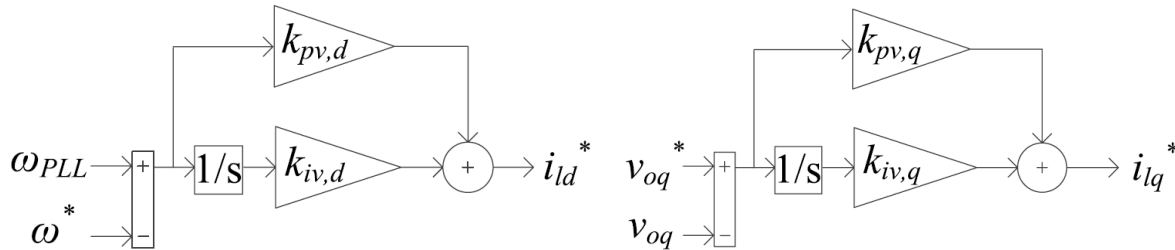
$$\begin{aligned}\omega^* &= \omega_n - mP, \\ v_{oq}^* &= v_{oq,n} - nQ.\end{aligned}$$



Mathematical Model of Microgrid

- e) Voltage Controllers: The reference frequency and voltage magnitude generated by the droop equations are used as set point values for the voltage controllers. Standard PI controllers are used for this purpose, as shown in Fig. 6. The process variables are the angular frequency ω from the PLL and the measured q-axis voltage (v_{oq})

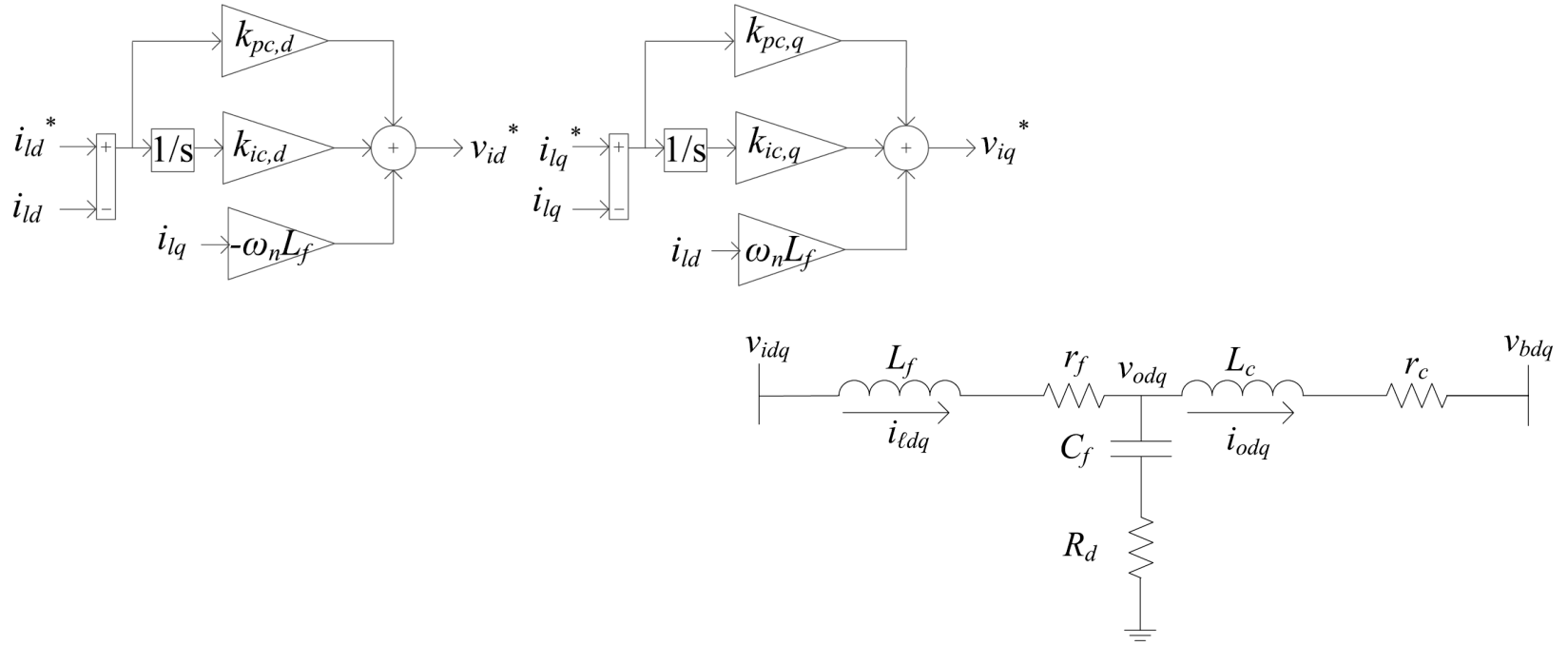
$$\begin{aligned}\dot{\varphi}_d &= \omega_{PLL} - \omega^* \\ i_{ld}^* &= k_{iv,d}\varphi_d + K_{pv,d}\dot{\varphi}_d \\ \dot{\varphi}_q &= v_{oq}^* - v_{oq} \\ i_{lq}^* &= k_{iv,q}\varphi_q + k_{pv,q}\dot{\varphi}_q\end{aligned}$$



- f) Current Controllers: Another set of PI controllers are used for current controllers as shown in Fig.7. These controllers take the difference between the commanded filter inductor currents (i_{ldq}^*), the measured filter inductor currents (i_{ldq}), and produce commanded voltage values (v_{ldq}^*). The values of correspond to the inverter output voltages before the LCL filter. Cross-coupling component terms are eliminated in these controllers as well

$$\begin{aligned}\dot{\gamma}_d &= i_{ld}^* - i_{ld}, \\ v_{ld}^* &= -\omega_n L_f i_{lq} + k_{ic,d}\gamma_d + k_{pc,d}\dot{\gamma}_d, \\ \dot{\gamma}_q &= i_{lq}^* - i_{lq}, \\ v_{lq}^* &= -\omega_n L_f i_{ld} + k_{ic,q}\gamma_q + k_{pc,q}\dot{\gamma}_q.\end{aligned}$$

Mathematical Model of Microgrid



g) LC Filters and Coupling Inductors: The filter in DER is shown in Fig. 8. Without any major inaccuracies, we can assume that the commanded voltage (v_{idq}^*) appears at the input of the filter inductor, i.e., $v_{idq}^* = v_{idq}$. This approach neglects only the losses in the IGBT and diodes. The state equations governing the filter dynamics are presented,

$$\begin{aligned}
 \dot{i}_{ld} &= (-r_f i_{ld} + v_{ld} - v_{od})/L_f + \omega_n i_{lq}, \\
 \dot{i}_{lq} &= (-r_f i_{lq} + v_{lq} - v_{oq})/L_f - \omega_n i_{ld}, \\
 \dot{i}_{od} &= (-r_c i_{od} + v_{od} - v_{bd})/L_c + \omega_n i_{oq}, \\
 \dot{i}_{oq} &= (-r_c i_{oq} + v_{oq} - v_{bq})/L_c - \omega_n i_{od}, \\
 \dot{v}_{od} &= (i_{ld} - i_{od})/C_f + \omega_n v_{oq} + R_d(i_{ld} - i_{od}), \\
 \dot{v}_{oq} &= (i_{lq} - i_{oq})/C_f - \omega_n v_{od} + R_d(i_{lq} - i_{oq}).
 \end{aligned}$$

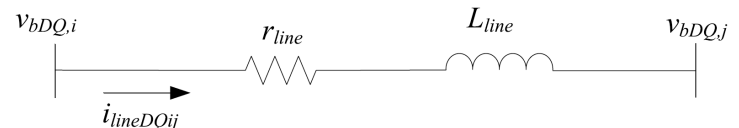
Mathematical Model of Microgrid

- h) Load models: The loads for this system are chosen as combination of resistors and inductors (RL loads). A typical RL load connected to an inverter bus. Line ‘a’ connected to the bus represents the base load and line ‘b’ works as a variable load for that bus. To check the system’s dynamic behavior, a load perturbation is done on ‘b’. Line ‘b’ appears in parallel to ‘a’ when the breaker closes the contact. State equations describing the load dynamics are,

$$\begin{aligned}\dot{i}_{loadD} &= (-R_{load}i_{loadD} + v_{bD})/L_{load} + \omega_{PLL}i_{loadQ}, \\ \dot{i}_{loadQ} &= (-R_{load}i_{loadQ} + v_{bQ})/L_{load} - \omega_{PLL}i_{loadD},\end{aligned}$$

- i) Distribution line: Similar to loads, the distribution line parameters consist of resistance and inductance. In Fig. 10, resistor r_{line} represents the copper loss component of the line. Inductor L_{line} is considered as the lumped inductance resulting from long line cables. Assuming that the line is connected between i th and j th bus of the system, the line dynamics are represented as follows:

$$\begin{aligned}\dot{i}_{lineDij} &= (-r_{line}i_{lineD} + v_{bD,i} - v_{bD,j})/L_{line} + \omega_{PLL}i_{lineQ}, \\ i_{lineQij} &= (-r_{line}i_{lineQ} + v_{bQ,i} - v_{bQ,j})/L_{line} - \omega_{PLL}i_{lineD},\end{aligned}$$



- The frequency is constant throughout the system.
- The variable subscript with upper case DQ denotes measurements from the global reference frame.
- First inverter’s phase angle can be arbitrarily set as the reference for the entire system.

Reference Frame Transformation

Inverter bus 1 serves as the system's reference and consequently is labeled as the global reference frame. Each inverter operates in its own local reference frame. A transformation is necessary to translate between values defined in the local reference frame to the global reference frame. An application of this transformation is shown graphically in Fig. 11.

$$\begin{bmatrix} f_D \\ f_Q \end{bmatrix}_{global} = \begin{bmatrix} \cos \theta & \sin \theta \\ -\sin \theta & \cos \theta \end{bmatrix} \begin{bmatrix} f_D \\ f_Q \end{bmatrix}_{local},$$

$$\begin{bmatrix} f_D \\ f_Q \end{bmatrix}_{local} = \begin{bmatrix} \cos \theta & \sin \theta \\ -\sin \theta & \cos \theta \end{bmatrix} \begin{bmatrix} f_D \\ f_Q \end{bmatrix}_{global},$$

where θ is the difference between the global reference phase and the local reference phase, as shown in Fig. 12.

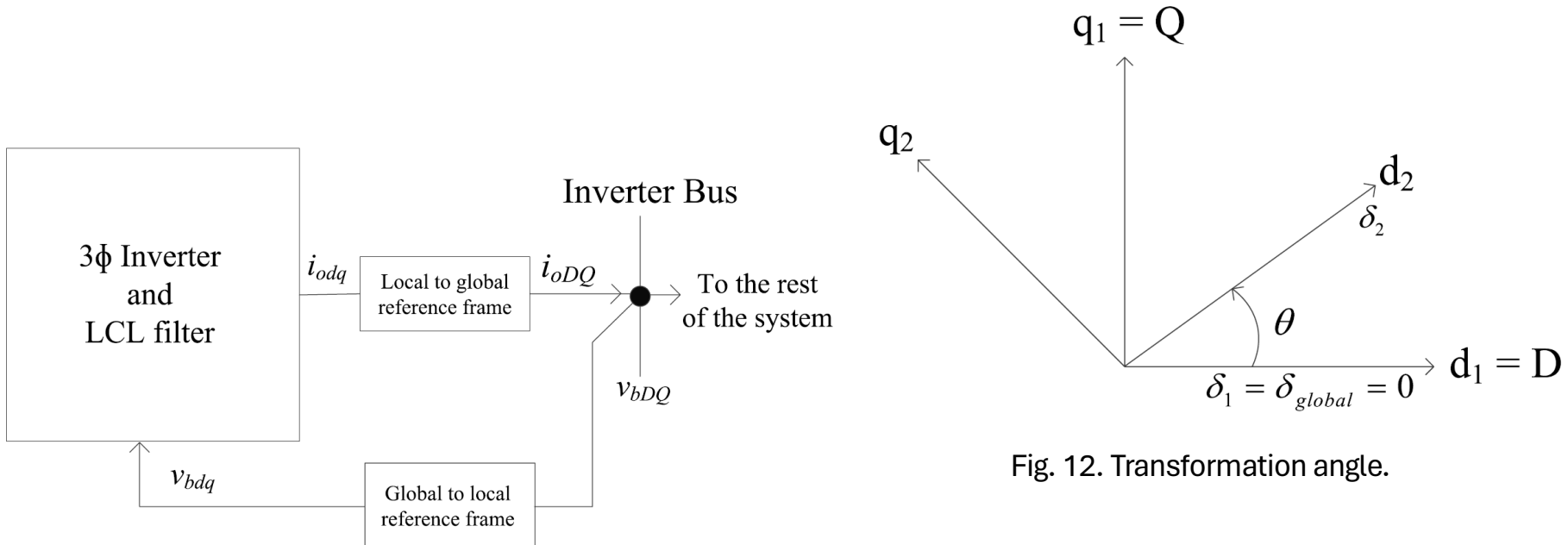


Fig. 11. Reference frame transformation.

Fig. 12. Transformation angle.

State Space Model of Microgrid

The mathematical model of microgrid has been established.

We can represent this model in general state space equations as follows,

$$\dot{x} = f(x, u).$$

When the operation mode changes, the model structure switches as well. Therefore, we can define the state vectors in grid-tied (x_G) and islanded (x_I) modes, respectively.

$$x_G = [\delta_i, P_i, Q_i, \varphi_{Pi}, \varphi_{Qi}, \gamma_{di}, \gamma_{qi}, i_{ldi}, i_{lqi}, v_{odi}, v_{oqi}, i_{odi} \\ i_{oqi}, \varphi_{PLLi}, v_{od,fi}]^T,$$

$$x_I = [\delta_i, P_i, Q_i, \varphi_{di}, \varphi_{qi}, \gamma_{di}, \gamma_{qi}, i_{ldi}, i_{lqi}, v_{odi}, v_{oqi}, i_{odi} \\ i_{oqi}, \varphi_{PLLi}, v_{od,fi}, i_{loadDi}, i_{loadQi}, i_{lineDij}, i_{lindQij}]^T.$$

The inputs are defined as

$$u_G = [P^*, Q^*]^T.$$

$$u_I = [v_{bDi}, v_{bQi}, \omega^*, v_{oq}^*]^T.$$

where $i, j = 1, \dots, m$, m is the number of inverters in microgrid.

Linearization of microgrid model

The above model is a nonlinear model. To simplify the problem, sometimes we need to obtain the small-signal model of microgrids. Let (x_e, u_e) be an equilibrium of system (14), then we can take the Taylor Series expansion of $f(x, u)$ around (x_e, u_e) as follows

$$f(x, u) = f(x_e, u_e) + A(x - x_e) + B(u - u_e) + \text{H. O. T}$$

$$A = \begin{bmatrix} \frac{\partial f_1}{\partial x_1} & \dots & \frac{\partial f_1}{\partial x_n} \\ \vdots & \ddots & \vdots \\ \frac{\partial f_n}{\partial x_1} & \dots & \frac{\partial f_n}{\partial x_n} \end{bmatrix}_{x=x_e}, B = \begin{bmatrix} \frac{\partial f_1}{\partial u_1} & \dots & \frac{\partial f_1}{\partial u_{2m}} \\ \vdots & \ddots & \vdots \\ \frac{\partial f_n}{\partial u_1} & \dots & \frac{\partial f_n}{\partial u_{2m}} \end{bmatrix}_{u=u_e}$$

where n is the total order of microgrid, and m is the number of inverters in the microgrid. Define the perturbation of states and inputs as $\partial x = x - x_e$, and $\partial u = u - u_e$.

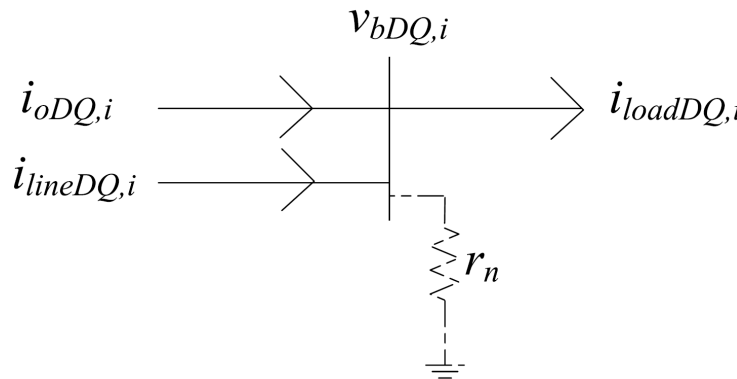
- Since (x_e, u_e) is an equilibrium, $f(x_e, u_e) = 0$.
- When the perturbation is small enough, we can neglect the high order terms.

Then we have

$$\partial \dot{x} = A \partial x + B \partial u$$

Virtual Resistor Method

- In the above model, bus voltages were used as an input to the system, thus, effects of load perturbation could not be accurately predicted.
- However, in practice, the only perturbation that occurs in the system comes from the step change in load. A method is needed to include the terms relating to the bus voltages in the system matrix A .
- To do this, a virtual resistor with high resistance can be assumed connected at the inverter bus. This resistor (r_n), shown in Fig. 13, has a negligible impact on system dynamics.
- Using Kirchhoff's voltage law (KVL), the equations describing the bus voltage in terms of the inverter, load currents and line currents can be expressed. This is shown in



$$v_{bD} = r_n(i_{oD} + i_{lineD} - i_{loadD}),$$

$$v_{bQ} = r_n(i_{oQ} + i_{lineQ} - i_{loadQ}).$$



$$\partial \dot{x}_I = A_{sys} \partial x_I + B_{sys} \partial \tilde{u}_I$$

$$\tilde{u}_I = [\omega^*, v_{oq}^*]$$

Fig. 13. Virtual resistor at a DER bus.

Model Order Reduction Method using Singular Perturbation

- Existing microgrid models have many state variables, thus increasing the computational burden and difficulty of stability analysis.
- The dynamical model exhibits behaviors at two time-scales: faster dynamics for converters and PI controllers; and slower dynamics for power calculator and droop controller.
- The reduced-order model is developed based on the singular perturbation theory that separates the system states into fast and slow dynamics.

Consider a singular perturbation model of a dynamical system whose derivatives of some of the states are multiplied by a small positive parameter ε (perturbation coefficient) as follows

$$\dot{x} = F(x, z, u, t, \varepsilon)$$

$$\varepsilon \dot{z} = G(x, z, u, t, \varepsilon)$$

where $x \in R^N$ representing slower dynamics, $z \in R^M$ representing faster dynamics. Let $\varepsilon = 0$, we have

$$0 = G(x, z, u, t)$$

If G has at least one isolated real roots

$$z = h_i(x, u, t), i=1,2,\dots,k$$

Substitute z into the system dynamics, we obtain the reduced order model as follows

$$\dot{x} = F(x, h_i(x, u, t), u, t).$$

Note that the dimension is reduced from $n+m$ to n .

Model Order Reduction Method using Singular Perturbation

- Compared to conventional order reduction that simply ignores some dynamic states, our method uses slower dynamics to represent faster ones, thus reducing order while maintaining all dynamic characteristics.
- Even though we can get the reduced-order model using the above method, the accuracy of the reduced model is not guaranteed. Define a new time variable $\tau = (t - t_0)/\varepsilon$, and introduce the boundary-layer model as follows,

$$\frac{dy}{d\tau} = g(t, x, y + h(t, x), 0).$$

where $y = z - h(t, x)$ is the change of state variables.

- Then we can specify the singular perturbation theory for small-signal (linear) systems. First, we need to identify the slow and fast dynamics. For linear system, we can use the modal analysis by calculating the participation factor:

$$P_{ij} = \frac{|u_{ij}^T| |v_{ij}|}{\sum_{k=1}^N |u_{kj}^T| |v_{jk}|}$$

- where u_{ij} and v_{ij} are left and right eigenvectors, respectively. Using the participation factor we can know that which eigenvalue participates mostly in which state. Then based on the magnitudes of their corresponding eigenvalues, we can determine the states with larger eigenvalues as fast states, while the others as slow states. For example,

Index	Eigenvalues	Major participants
3	-7853.98	$v_{od,f}$
14, 15	$-2280.14 \pm j35916.37$	v_{od}, v_{og}
12, 13	$-2241.42 \pm j35209.50$	i_{od}, i_{og}
10, 11	$-301.94 \pm j65.61$	i_{id}, i_{iq}

fast

1, 2	$-70.27 \pm j52.26$	P, Q
6, 7, 8, 9	$-73.08 \pm j33.67$	$\gamma_d, \gamma_q, \varphi_P, \varphi_Q$
4	$-6.01 \pm j0.09$	φ_{PLL}
5	0	δ

slow

Order Reduction Method for Small-Signal Microgrid Model

The order reduction algorithm for small-signal microgrid model is given in the following steps [2]:

1. Discard $\dot{\delta}_1$ (corresponding to the reference angle) by removing the corresponding row and column.
2. Rearrange the states of the original state vector x_{sys} such that the slow states (x) are placed at the upper rows and fast states (z) are placed at the lower rows. Use a transformation matrix T_r for reordering. For example, $[x_1 \ x_2 \ x_3]^T$ needs to be reordered as $[x_1 \ x_3 \ x_2]^T$. Use the transformation matrix T_r to multiply the original vector. The new state vector and steady-state operating point vectors become $x_{new} = T_r x_{sys}$ and $X_{new} = T_r X_{sys}$, respectively,

$$T_r = \begin{bmatrix} 1 & 0 & 0 \\ 0 & 0 & 1 \\ 0 & 1 & 0 \end{bmatrix}$$

3. Find the new state matrix A_{new} using T_r : $A_{new} = T_r A_{sys} T_r^{-1}$.
4. Separate the new state matrix and the new states as follows:

$$\begin{bmatrix} \dot{x} \\ \dot{z} \end{bmatrix} = \begin{bmatrix} A_{11} & A_{12} \\ A_{21} & A_{22} \end{bmatrix} \begin{bmatrix} x \\ z \end{bmatrix}, \quad x_{new} = \begin{bmatrix} x \\ z \end{bmatrix}, \quad X_{new} = \begin{bmatrix} X \\ Z \end{bmatrix}.$$

where $A_{11} \in \mathbb{R}^{N \times N}$, $A_{12} \in \mathbb{R}^{N \times M}$, $A_{21} \in \mathbb{R}^{M \times N}$, $A_{22} \in \mathbb{R}^{M \times M}$. Also, x is the representative of the slow states and z is the representative of the fast states.

Order Reduction Method for Small-Signal Microgrid Model

5. Perform the following iteration to find the value of L for a linear system composed of two subsystems [3]:

$$L_{i+1} = A_{22}^{-1}(A_{21} + L_i A_{11} - L_i A_{12} L_i); i = 1, 2, \dots$$

- Start with the initial value $L_0 = A_{22}^{-1}A_{21}$ and iterate 100 times. This will ensure that the eigenvalues of the reduced-order system are as close as possible to that of the slow eigenvalues of the full-order system. For this system, 100 iterations achieved excellent accuracy with minimal computational time.

6. Transform the system into the following using the slow manifold condition $z_f = z + Lx$:

$$\begin{bmatrix} \dot{x} \\ \dot{z}_f \end{bmatrix} = \begin{bmatrix} A_s & A_{12} \\ 0 & A_f \end{bmatrix} \begin{bmatrix} x \\ z_f \end{bmatrix},$$

where $A_s = A_{11} - A_{12}L$; $A_f = A_{22} - LA_{12}$.

7. Perform the following iteration to find the value of M :

$$M_{i+1} = [(A_{11} - A_{12}L)M_i - M_i L A_{12}]A_{22}^{-1} + A_{12}A_{22}^{-1}; i = 1, 2, \dots$$

Start with the initial value $M_0 = A_{12}A_{22}^{-1}$ and iterate 100 times as before for L .

8. Decouple the system into slow and fast time-scale using the fast manifold condition $x_s = x + Mz_f$:

$$\begin{bmatrix} \dot{x} \\ \dot{z}_f \end{bmatrix} = \begin{bmatrix} A_s & 0 \\ 0 & A_f \end{bmatrix} \begin{bmatrix} x_s \\ z_f \end{bmatrix}.$$

[3] P. V. Kokotovic, "A Riccati equation for block-diagonalization of ill-conditioned systems," IEEE Trans. Autom. Control, vol. 20, no. 6, pp. 812–814, Dec. 1975.

Order Reduction Method for Small-Signal Microgrid Model

9. The operating points corresponding to the slow states become

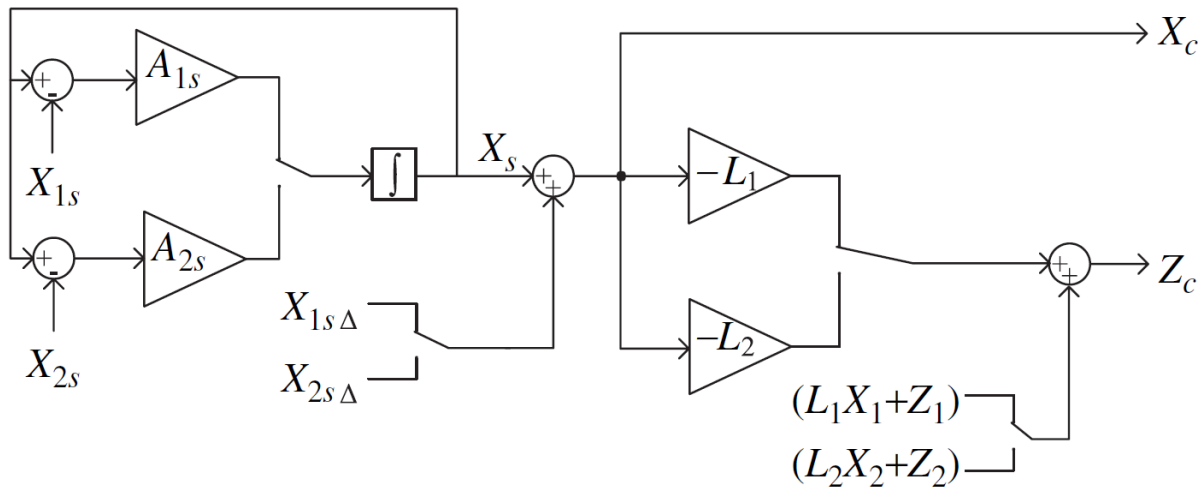
$$X_s = (I - ML)X - MZ.$$

10. To get the corrected response x_s , add $X_{s\Delta}$ to the output of X_s , where $X_{s\Delta} = MLX + MZ$. New outputs are similar to that of the dynamics obtained from the slow states of the original system.

11. Predict the fast states using algebraic solutions

$$z_f = Lx_c + z_c \Rightarrow z_c = -Lx_c + z_f = -Lx_c + (LX + Z).$$

12. The reduced-order system is now ready for simulation. The figure below shows the final arrangement for obtaining the dynamic response considering both the slow and the fast states.



Simulation Validation of Small-Signal Order Reduction

Simulation setup:

- For the grid-tied system, a set of linearization points is obtained with $u = [0 \ 0]^T$ to evaluate the initial higher order matrices A, B . The parameter setting is given in TABLE I. Using modal analysis we can identify the slow/fast states as follows,

$$x = [P, Q, \delta, \varphi_P, \varphi_Q, \gamma_d, \gamma_q, \varphi_{PLL}],$$

$$z = [i_{ld}, i_{lq}, v_{od}, v_{oq}, i_{od}, i_{oq}, v_{od,f}].$$

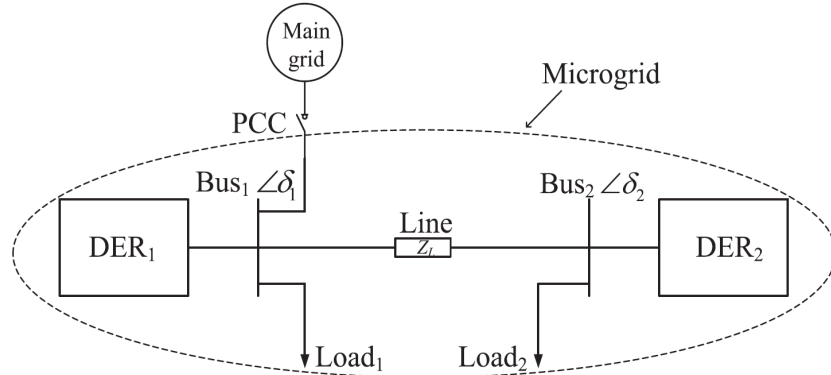


TABLE I
PARAMETERS OF MICROGRID SYSTEM

Parameter	Value	Parameter	Value
L_f	3.90 mH	R_f	0.50Ω
C_f	$16 \mu\text{f}$	R_d	2.05Ω
$K_{P,P}$	0.01	$K_{I,P}$	0.10
$K_{P,C}$	1.00	$K_{I,C}$	100
$K_{P,PLL}$	0.25	$K_{I,PLL}$	2.00
ω_c	50.26 rad/s	ω_n	377 rad/s
ω_{cPLL}	7853.98 rad/s	V_{bD}	0.61 V
V_{bQ}	84.52 V		

- [1] M. Rasheduzzaman, J. A. Mueller, and J. W. Kimball, "An accurate small-signal model of inverter-dominated islanded microgrids using dq reference frame," *IEEE J. Emerg. Sel. Topics Power Electron.*, vol. 2, no. 4, pp. 1070–1080, Dec. 2014.
[2] M. Rasheduzzaman, J. A. Mueller, and J. W. Kimball, Rasheduzzaman. "Reduced-order small-signal model of microgrid systems." *IEEE Transactions on Sustainable Energy* 6.4 (2015): 1292-1305.

Simulation Validation of Small-Signal Order Reduction

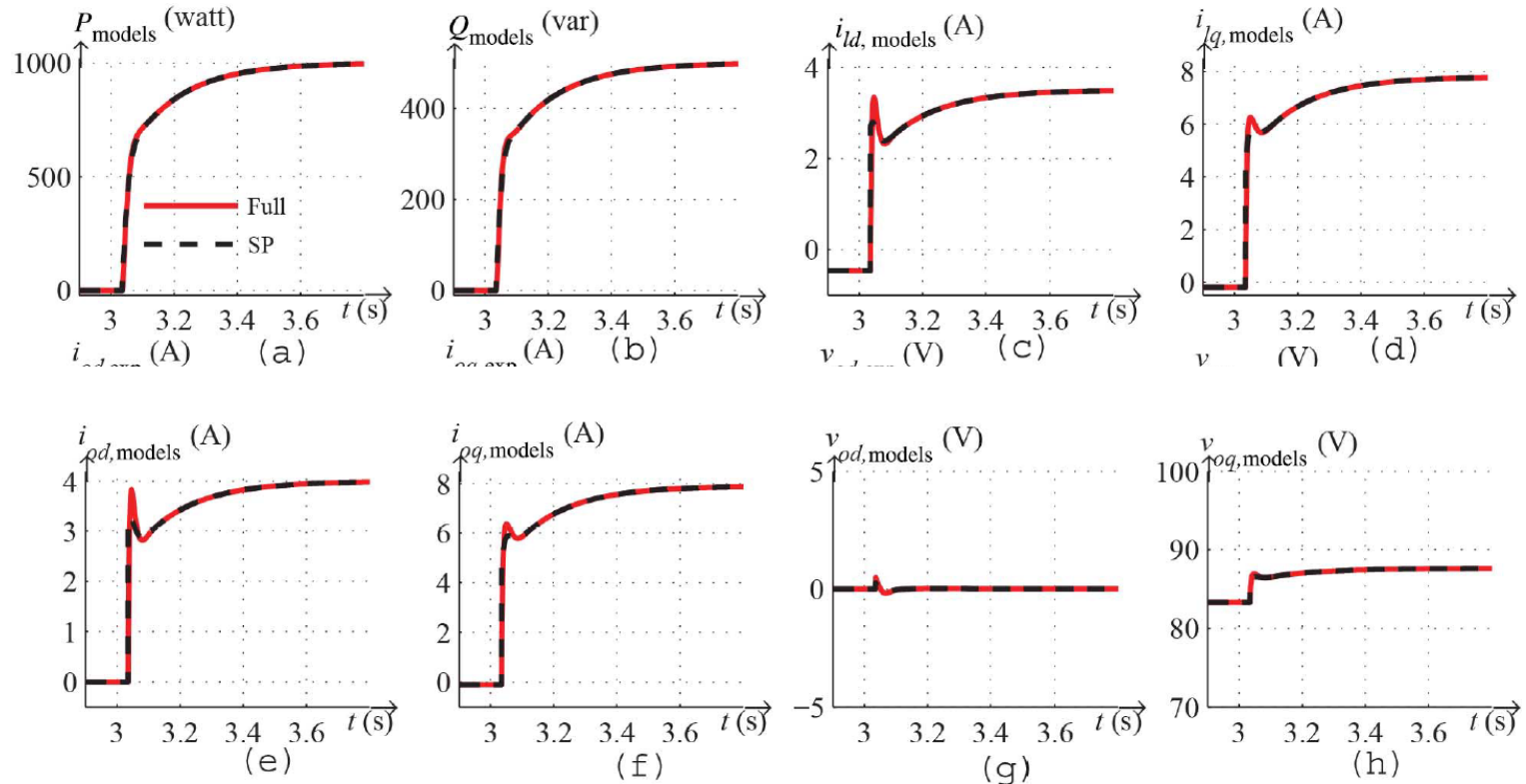


Fig. 16. Verification of the system dynamics of interests. (a) Active power. (b) Reactive power. (c) d-axis inductor current. (d) q-axis inductor current. (e) d-axis output current. (f) q-axis output current. (g) d-axis output voltage. (h) q-axis output voltage [2].

Simulation Validation of Small-Signal Order Reduction

Simulation setup

For the islanded system, the equilibrium point and parameter setting is defined as [2]. The modal analysis result is shown in TABLE II.

TABLE II
EIGENVALUES OF SYSTEM MATRIX A

Index	Eigenvalues	Major participants
1,2	$-7.10 \times 10^8 \pm j376.57$	i_{lineDQ}
3,4	$-2.09 \times 10^8 \pm j376.58$	i_{odq1}, i_{odq2}
5,6	$-1951.65 \pm j10980.03$	v_{oq1}, v_{oq2}
7,8	$-1781.19 \pm j10234.93$	v_{od1}, v_{od2}
9	-7981.28	$v_{od1,f}, v_{od2,f}$
10	-7915.62	$v_{od1,f}, v_{od2,f}$
11,12	$-822.46 \pm j5415.18$	v_{oq1}, v_{oq2}
13,14	$-674.16 \pm j4643.15$	v_{od1}, v_{od2}
15,16	$-2889.85 \pm j351.71$	$i_{loadDQ1}, i_{loadDQ2}$
17,18	$-1500.35 \pm j336.76$	$i_{loadDQ1}, i_{loadDQ2}$
19,20	$-267.94 \pm j82.01$	i_{ldq1}, i_{ldq2}
21,22	$-69.76 \pm j21.47$	$\gamma_{dq1}, \gamma_{dq2}$
27,28	$-25.38 \pm j31.18$	$\varphi_{q1}, \gamma_{q1}, \varphi_{q2}, \gamma_{q2}$
29,30	$-6.16 \pm j22.90$	$\varphi_{d1}, \gamma_{d1}, \varphi_{d2}, \gamma_{d2}$
34,35	$-2.24 \pm j4.68$	$\varphi_{dq1}, \varphi_{dq2}$
31,32	$-10.65 \pm j8.14$	$\delta_2, \varphi_{PLL1}, \varphi_{PLL2}$
33	-7.53	$\delta_2, \varphi_{PLL1}, \varphi_{PLL2}$
23,24	$-50.25 \pm j0.02$	P_1, Q_1, P_2, Q_2
25	-50.27	P_1, Q_1, P_2, Q_2
26	-50.27	P_1, Q_1, P_2, Q_2
36	0	δ_1

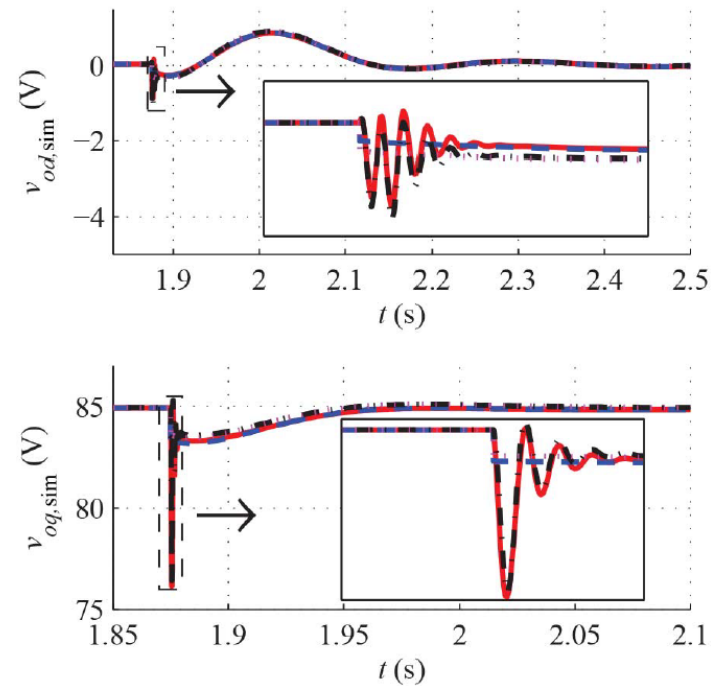


Fig. 17. Fast states marked with rectangles, are oscillatory in the full-order model but disappear in the reduced-order model and become straight lines.

Simulation Validation of Small-Signal Order Reduction

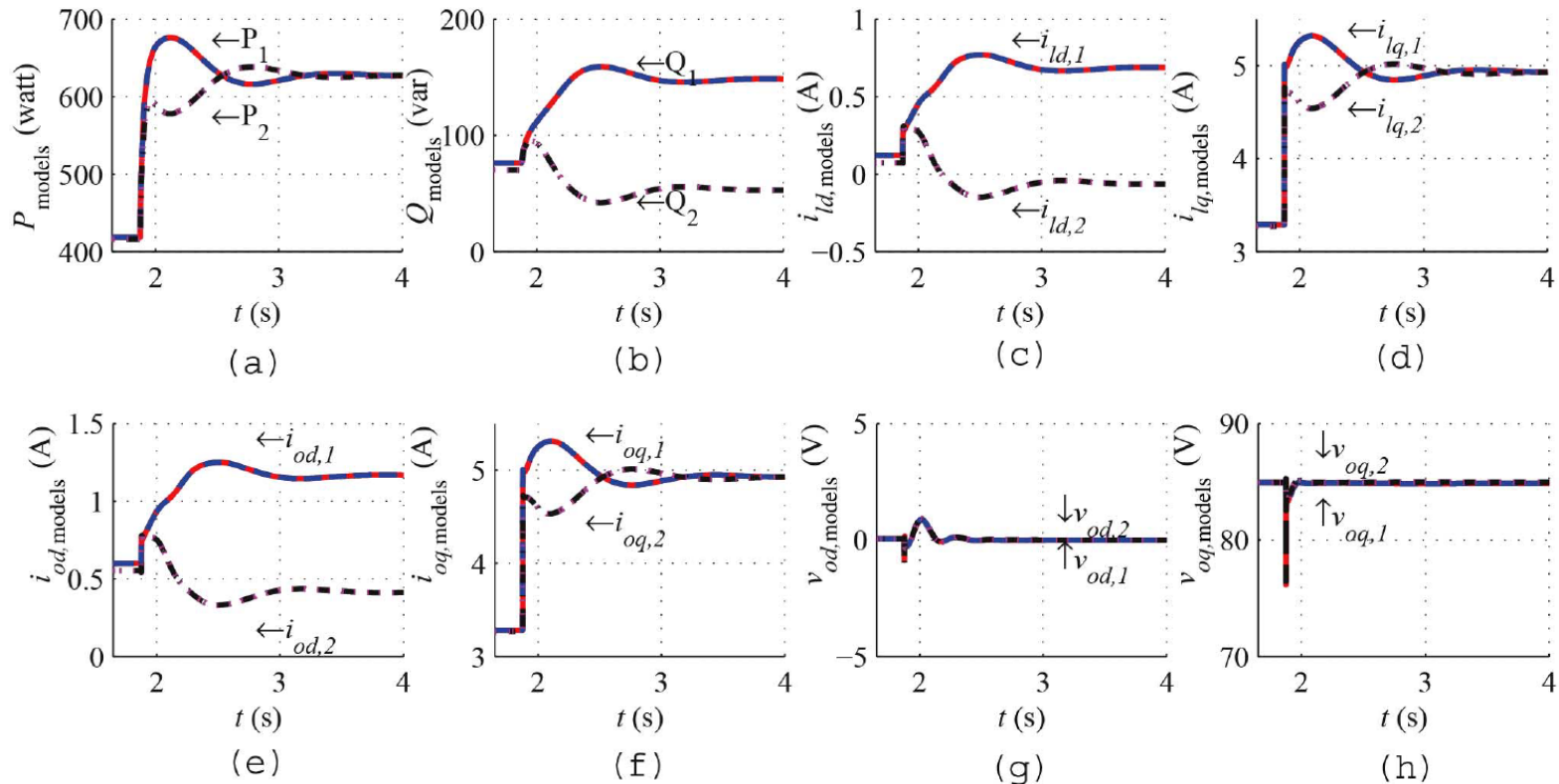


Fig. 18 Verification of system dynamics using results from experiment, full-order model simulation, and reduced-order model simulation. (a) Active power. (b) Reactive power. (c) d-axis inductor current. (d) q-axis inductor current. (e) d-axis output current. (f) q-axis output current. (g) d-axis output voltage. (h) q-axis output voltage. [2].